Stochastic Gene Alterations for the Study of Intestinal Homeostasis and Cancer

By

Ashleigh J. Miller

A DISSERTATION

Presented to

the Department of Molecular and Medical Genetics

and the Oregon Health & Science University

School of Medicine

in partial fulfillment of the requirements for the degree of

Doctor of Philosophy

July 2009

School of Medicine

Oregon Health and Science University

_____

CERTIFICATE OF APPROVAL

_____

This is to certify that the Ph.D. thesis of

Ashleigh Miller

has been approved

_____
Mentor/Advisor

_____
Member

_____
Member

_____
Member

Table of Contents

Acknowledgements

The work discussed in this document was the result of many people providing guidance, instruction, and support these last six years. First and foremost, I thank my graduate thesis advisor, Dr. R. Michael Liskay. Mike is a mentor who always maintains a fine balance between giving me experimental freedom to explore new ideas and providing gentle guidance to help me maintain focus. He encouraged me to try new techniques and helped locate the resources necessary to pursue them. He has helped me to develop critical thinking sills, and to improve my oral and written communication. Mike has also encouraged me to apply for conferences and awards, strengthening my connections to the larger scientific community. Mike has provided an excellent foundation for a successful scientific career, and for that I'm deeply grateful.

Additionally, I thank the many members of the Liskay lab for their support throughout my time here. Jennifer Johnson, the other student in the lab, provided camaraderie through the graduate school experience. Through daily discussions, Naz Erdinez gave me much scientific insight and guidance. Sandra Dudley not only was critical in making the *Pms2^{cre}* mouse, but also taught me most of the animal techniques I used in my thesis work. Odessa Reilly and Kalyn MacDonald both provided much assistance with organizing and maintaining the mouse colonies.

I would also like to thank the members of my Thesis Advisory Committee, Drs. Rosalie Sears, Melissa Wong, and H. Scott Stadler for their guidance, patience,

encouragement, and insight. The excellent faculty and administrative staff in the

Molecular and Medical Genetics department provided a strong educational foundation

and support. Additionally, I thank Dr. Darryl Shibata at USC, who was critical in making

the *Pms2^{cre}* mouse, as well as monitoring my progress through the years.

I would like to thank my many friends, in Portland and beyond. And no words

can express my appreciation to my parents, Art and Marilyn Miller, who not only are the

best examples of balancing successful careers and happy family life, but also instilled in

me confidence, élan, and a zest for life. And lastly, from the bottom of my heart, I thank

my husband Brian, who constantly encourages me to pursue my dreams. He hears about

every success and challenge daily. He is my biggest cheerleader and his love and support

have allowed me to excel. My graduate education is just one of many adventures we

have taken together, and without a doubt the most challenging. Thank you for always

walking along side of me. Lastly, I thank my daughter Erin. She is the best experiment I

have ever embarked on. I can only hope I provide her with as much love,

encouragement, and support as has been given to me, so that she has the freedom and

confidence to pursue her dreams.

List of Illustrations

List of Abbreviations

APC – Adenomatous Polyposis Coli

APC^{min} – Adenomatous Polyposis Coli, Multiple Intestinal Neoplasia

BMDC – Bone Marrow Derived Cells

BMP – Bone Morphogenic Protein

BMPr1A – Bone Morphogenic Protein Receptor Type 1A

BRAF - V-raf murine sarcoma viral oncogene homolog B1

BrDU – Bromodeoxy Uridine

BSA – Bovine Serum Albumen

c-Myc – cellular - Avian expressed myelocytomatosis virus homolog

CRC – Colorectal Cancer

Cre – Cyclization recombination

DNA – Deoxyribonucleic acid

EMT – Epithelial to Mesenchymal Transition

FAP – Familial Adnomatous Polyposis

GI – gastrointestinal

GDP – Guanosine diphosphate

GTP – Guanosine triphosphate

HNPCC – Hereditary Nonpolyposis Colon Cancer

JPS – Juvenile Polyposis Syndrome

K-ras – Kristen rat sarcoma viral oncogene homolog

LOH – Loss of Heterozygosity

loxP – locus of X-over P1

LSL – Lox-Stop-Lox

MLH1 – MutL Homolog 1

MMR – Mismatch Repair

MSH2 – MutS Homolog 2

MSH6 – MutS Homolog 6

OCT – Optimum Cutting Temperature

PBS – Phosphate Buffered Saline

PCR – Polymerase Chain Reaction

Pms2 – Post Mitotic Segregation Increased 2

PTEN – Posphatase and Tensin Homolog Deleted on Chromosome Ten

RFS – Rosa-Flox-Stop

RNA – Ribonucleic Acid

RT-PCR – Reverse Transcriptast Polymerase Chain Reaction

SMA – Smooth Muscle Actin

Smad4 – Smad family member 4 (Mothers Against Decapentaplegic Homolog 4)

TA - Transient Amplifying Cells

Tgfβ- Transforming Growth Factor Beta

TgfβrI – Transforming Growth Factor Beta Receptor Type 1

TgfβrII – Transforming Growth Factor Beta Receptor Type 2

TUNEL - Terminal deoxynucleotidyl transferase mediated dUTP Nick End

Labeling assay

Abstract

Human colorectal cancer (CRC) accounts for one in three diagnosed cancers and one in two cancer-related deaths. A great deal about the underlying genetics of human CRC has been learned from human and mouse studies. Yet we still have limited understanding of how isolated genetic changes in different tissue types contribute to CRC development and progression. To investigate this elusive question, I have utilized a novel *Pms2^{cre}* system for stochastic alteration of *loxP*-marked cancer genes in mice. With this system, Cre activation is achieved through an unrepaired mutation event, with a frequency modulated by DNA mismatch repair status. The *Pms2^{cre}* system represents a more faithful mouse model of human cancers and can be applied to understand the outcome of random, isolated mutation of target genes. Specifically described within this work, stochastic activation of the oncogenic form of *k-Ras* confers a stem cell advantage as observed through increased area of cells harboring the oncogenic mutation and hyperplasia within the colon. In contrast, experiments with a conditionally inactivated *TgfβrII* allele demonstrate that isolated reduction of *TgfβrII* results in a competitive disadvantage along the crypt/villi axis and is associated with an increase in crypt apoptosis. Further, I note haploinsufficiency for reduced *TgfβrII* along the crypt/villus axis. Finally, I apply the *Pms2^{cre}* system to investigate the effects of activating a stabilized form of *c-Myc* and inactivating an allele of *Smad4* alone, or in combination, in gastrointestinal tumor development. My results demonstrate that *c-Myc* stabilization accelerates *Smad4* tumorigenesis. *Smad4/c-Myc*

gastric/duodenal adenomas are more aggressive and invasive than *Smad4*-only tumors. Additionally, *Smad4/c-Myc* adenomas have an increased number of bone-marrow derived cells, which may be the tumor-initiating cell. Not only what genetic changes underly cancer development but in what tissue type . The *TgfβrII* results suggest that isolated disruption of this gene is disadvantageous in tumor initiation. The *Smad4/c-Myc* results suggest different tumor-initiating capabilities when these genes are altered in the epithelial versus the stroma. Thus, the work described in this thesis provides insight into how genetic changes at the single-cell level affect, in a dynamic way, tumor development.

Chapter 1

Background and Significance

Human Colorectal Cancer

Colorectal cancer (CRC) is the third leading cause of cancer-related deaths in the in the United States (National Cancer Institute, 2008). In 2008, an estimated 108,070 people will be newly diagnosed with colon cancer and more than 49,000 people will die (NCI). Half of the population will be diagnosed with CRC by the 8th decade of life. Rates of new cases of CRC diagnoses have slightly decreased from a peak in 1982. The tumor stage at diagnoses is lowering, mainly due to increased surveillance (Desch et al., 2005). CRC treatment is dictated by the stage at which disease is detected. Adenomas detected during colonoscopies are removed by surgical resection. More advanced CRCs are treated by combinations of surgical resection and chemotherapies.

Colon cancers frequently begin as polyps, or areas of increased cellular proliferation, and progress step-wise with increasing genetic instability, accumulation of mutation, and malignancy with each step (Day and Morson, 1978). Colonic polyps can develop into adenomas, or localized noninvasive tumors (Figure 1.1). Adenomas progress into adenocarcinomas when the underlying basement membrane is breached, and the tumor is locally invasive. Invasive adenocarcinomas allow tumor cells to leave the primary site and travel to distant sites throughout the body, initiating metastatic disease; metastatic disease is the typical cause of colon-cancer related mortality. The most common site of metastatic disease in human colon cancer is the liver. Most colon cancers arise sporadically and thus are genetically diverse in their origins (Adrouny, 2002). Subsets of colon cancers have a hereditary basis and for many familial forms the

underlying genetic lesion contributing to the disease is known. The long-term goal of the

work in this thesis is to define and characterize combinations of genetic mutations

leading to colon cancer development.

Familial Colon Cancer Syndromes

Approximately 10% of human colon cancers are classified as familial syndromes

and can be attributed to an inherited genetic mutation. Each type of familial syndrome is

relatively rare, however investigating these diseases provides insight into the genetics of

all colon cancers.

Hereditary Nonpolyposis Colon Cancer

The most common hereditary form of colon cancer is Hereditary Nonpolyposis

Colon Cancer (HNPCC), also known as Lynch Syndrome, and accounts for 4-6% of all

colon cancers (Vasen, 2007). Tumors typically present in the 3rd to 5th decade of life

(Lynch and de la Chapelle, 1999). HNPCC is defined by diagnostic criteria, including a

strong family history with autosomal dominant inheritance, a lesion typically in the

proximal colon in the absence of multiple polyps, and microsatellite instability in the

tumor (Rodriguez-Bigas et al., 1997; Vasen et al., 1999). Aneuploidy is relatively rare in

HNPCC tumors. In addition to colon tumors, HNPCC patients are at an increased risk

for endometrial cancers (in women), and, rarely, cancers of the pancreas, urinary tract,

and skin tumors (Watson and Riley, 2005).

Several genes have been linked to HNPCC, nearly all involved in DNA mismatch repair (MMR). *MSH2* was the first gene linked to HNPCC and mutations in *MSH2* account for up to 60% of HNPCC cases (Fishel et al., 1993). *MLH1* was subsequently identified and accounts for approximately 30% of cases (Bronner et al., 1994). Other genes later identified include *MSH6*, *PMS2*, *PMS1*, and *TGFβRII* (Lu et al., 1998; Miyaki et al., 1997; Nicolaides et al., 1994). Typically, one mutated MMR allele is inherited, followed by complete loss of MMR through loss of heterozygosity (LOH). For *MLH1*, LOH frequently occurs through epigenetic silencing via promoter methylation (Simpkins et al., 1999) whereas LOH mainly occurs through mutation in the remaining MMR genes. A small percentage of patients are classified as having HNPCC based on family history and microsatellite instability, but no mutations in these genes are found. While HNPCC accounts for a relatively small percentage of CRC, a significant percentage (15%) of CRCs can be classified as microsatellite-high (Lindor et al., 2005), suggesting alterations to MMR is a common underlying mechanism of colon cancer progression.

Targeted gene deletions in mice have been constructed for many of the DNA mismatch repair genes implicated in HNPCC. Mice with targeted deletions of *Msh2* (Reitmair et al., 1996)*, or *Mlh1* (Baker et al., 1996) develop adenomas and adenocarcinomas in the small intestine with microsatellite instability, partially recapitulating the human disease. Mice with *Msh6* deletions develop intestinal tumors, however, show little to no microsatellite instability (Edelmann et al., 1997). Interestingly, mice null for *Pms2* show microsatellite instability but primarily develop

lymphomas and sarcomas; they do not develop intestinal adenomas (Prolla et al., 1998). Collectively, the mouse models of HNPCC highlight the central importance of DNA mismatch repair in tumor suppression, particularly within the gastrointestinal tract.

Familial Adenomatous Polyposis

A second inherited form of colon cancer, Familial Adenomatous Polyposis (FAP), is a rare, autosomal dominant cancer syndrome characterized by hundreds to thousands of polyps developing in the colon within the first few decades of life. The average age of colorectal cancer onset in FAP patients, if unidentified is within the 4th decade of life (de Silva and Fernando, 1998). Treatment typically involves surgical removal of the entire colon and heightened surveillance. FAP is relatively rare, accounting for only 1% of all colon cancers. The inherited mutant gene underlying FAP is *APC* (Kinzler et al., 1991; Nishisho et al., 1991), a tumor suppressor gene mutated in most FAP patients and up to 90% of sporadic colon cancers (Wood et al., 2007). The *APC* gene encodes a 2,843 amino acid protein (Groden et al., 1991) that interacts with ß-catenin to negatively regulate the Wnt signaling pathway (Korinek et al., 1997; Morin et al., 1997; Rubinfeld et al., 1993). Wnt signaling is a critical regulator of intestinal homeostasis (Pinto et al., 2003; Wong et al., 1998) and represents a key regulatory step in cell proliferation and differentiation (Clevers, 2006). *APC* has more than 800 reported mutations, most being nonsense or frame shift mutations resulting in premature stop codons (Fodde and Khan, 1995).

The gene *Apc*, mutated in FAP as well as most sporadic human CRC, has been extensively studied in the mouse. The first mouse *Apc* mutation resulted from a mutagenesis screen. The Apc^{min} (Multiple Intestinal Neoplasia) mouse, heterozygous for a truncation mutation at codon 850, develops >30 adenomas within the small intestine within 4 months (Moser et al., 1990). Subsequent engineered mice bearing *Apc* truncation mutations produce variable numbers of adenomas. For example, the $Apc^{\Delta716}$ mouse has a truncation at codon 716 and develops ~300 small intestine adenomas (Oshima et al., 1995), whereas the Apc^{1638N}, containing a truncation at codon 1638, develops only 3-10 adenomas (Fodde et al., 1994). Although the number of lesions varies, adenomas from these three models are histologically indistinguishable. These models demonstrate that the region of *Apc* truncation correlate with the pathogenicity in a manner similar to *APC* mutations found in humans (Nagase et al., 1992).

While *Apc* mutant mouse adenomas mimic the initial formation of polyps observed in FAP patients, the mouse tumors rarely progress past the adenoma stage due to tumor-associated morbidity. Many studies have combined *Apc* mutants with other target genes to accelerate the tumor phenotype (reviewed extensively in (Taketo and Edelmann, 2009). For example, combining a *Smad4*-null allele with $Apc^{\Delta716}$ results in adenocarcinomas, tumors more advanced than those in $Apc^{\Delta716}$ alone (Taketo and Takaku, 2000). Similarly, heterozygous deletion of the tumor suppressor gene *PTEN* in an Apc^{min} background results in invasive carcinomas. These results suggest both *PTEN* and *Smad4* signaling pathways, in combination with mutation of *Apc*, accelerate the tumor phenotype. In contrast, ablation of expression of the proto-oncogene *c-Myc* in an

Apc^min background results in fewer adenomas, suggesting *c-Myc* is critical for *Apc-*initiated tumorigenesis (Ignatenko et al., 2006). In this manner, combinations of mutant *Apc* alleles and other candidate genes provide insight into what basic genetic pathways may underlie the adenoma-carcinoma progression.

Juvenile Polyposis Syndrome and PTEN Hamartoma Tumor Syndrome

Juvenile Polyposis Syndrome (JPS), another rare inherited form of colon cancer, is autosomal dominant and predisposes carriers to several tumor types, including hamartomatous polyps that can develop into malignant lesions (Giardiello et al., 2001). Germline mutations in two genes of the Tgfβ signaling family are identified as leading to JPS: the intracellular signaling molecule *SMAD4* (Howe et al., 2002; Woodford-Richens et al., 2000; Woodford-Richens et al., 2001) and the signaling receptor *BMPr1A* (Howe et al., 2001). Both genes are tumor suppressor genes and together, mutations found in *SMAD4* and *BMPr1A* account for 40% of JPS cases.

A fourth familial form of colon cancer is known as PTEN hamartoma tumor syndrome (PTHS) and includes Bannayan-Riley-Ruvalcaba Syndrome and Cowden syndrome (Blumenthal and Dennis, 2008). Patients present with hamartomous tumors, or nonmalignant growths consisting of a disorganized mass of tissue, in the colon. Nearly 85% have mutations in the *PTEN* gene (Liaw et al., 1997), a tumor suppressor gene that normally negatively regulates AKT growth signaling.

Sporadic Colon Cancers

While much has been learned about the genetics of colon cancer development based on familial syndromes, at least 85% of human CRC are sporadic. Microarray studies of 12 sporadic colon cancers show the high degree of variation in gene expression (Sjoblom et al., 2006; Wood et al., 2007), suggesting each cancer is genetically unique. While cancers differ at the level of gene mutation, common signaling pathways are disrupted in sporadic CRC, suggesting that these conserved pathways play important regulatory roles in epithelial homeostasis (Fearon and Vogelstein, 1990). A variety of mutations within a signaling pathway have been indicated in CRC. For example, the Tgfß signaling can harbor mutations in either, but not both, *TgfßrI* or *Smad4* (Seshimo et al., 2006). Likewise, two mutations within the Ras signaling pathway, *KRAS* and *BRAF*, are found to be frequent but mutually exclusive in CRC (Simi et al., 2008). Not surprisingly, genes involved in familial CRCs are also frequently mutated in spontaneous tumors. Nearly all colon cancers have constitutively active Wnt signaling, frequently through mutation or loss of APC (Powell et al., 1992), a key Wnt signaling regulator. Nearly 40% of human GI cancers harbor a mutation in *PTEN* (Parsons et al., 2005). Thus, several signaling pathways critical to tumorigenesis have been identified through studies of spontaneous human colorectal cancers.

Tumors progress through specific stages, from initial hyperplasia to full blown metastatic disease. Tumors accumulate mutations as they progress and, through acquisition of mutations and selection, acquire new capabilities. There are six hallmarks

of tumors: sustained replication, insensitivity to growth-inhibitory signals, self-

sufficiency in growth signals, evading apoptosis or programmed cell death, sustained

angiogenesis, and invasion into surrounding tissue and metastasis (Hanahan and

Weinberg, 2000). Each of these hallmarks can be associated with mutations in specific

genes and pathways (Vogelstein and Kinzler, 2004), see Figure 1.1). In colon cancer,

mutation of APC is frequently the most common event, permitting cells to both be

insensitive to differentiation cues (Sansom et al., 2004).
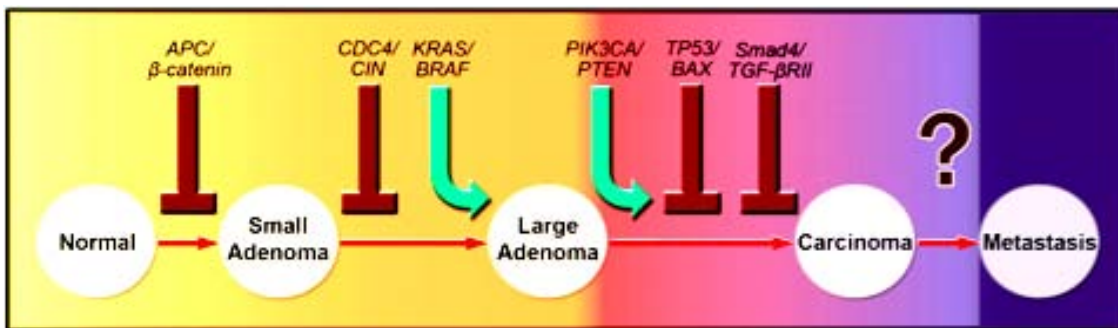
**Figure 1.1 – Stepwise colon cancer progression model and associated genetic
mutations.** Reprinted with permission from PNAS Vol 105, No 11 pg 4283-8, 2008.

Increase in adenoma size is associated with mutations in the Ras GTPase *k-RAS* or a

downstream partner, *BRAF*, which cause cells to proliferate in the absence of growth

signals (Winston et al., 1996). Increased invasiveness and metastasis is associated with

disruptions to the Tgfβ/BMP signaling pathway (Nawshad et al., 2005; Oft et al., 1998).

End stage tumors are often found to have mutations in the p53 pathway, rendering those

tumor cells insensitive to apoptosis (Oren, 2003). Most importantly, human cancers often

harbor mutations in more than one of these pathways (Sjoblom et al., 2006). The set of

mutations found in a particular tumor can indicate how a tumor will respond to treatment

and how aggressive a tumor may become.

Mouse GI cancer models involve disruption of target genes in signaling

pathways controlling growth and differentiation. For example, several mutants of the

gene *Smad4* develop gastric adenomas occluding the duodenum, partially recapitulating

JPS (Hohenstein et al., 2003; Takaku et al., 1999). Mice bearing GI-specific activation of

an oncogenic form of *K-ras* develop hyperplastic growth of epithelia but do not develop

adenomas (Tuveson et al., 2004). Interestingly, GI adenomas are seen in mice bearing

conditional deletion of genes in stromal cell types; conditional deletion of *TgfβrII* within

fibroblasts results in intestinal adenomas (Bhowmick et al., 2004) and conditional

deletion of *Smad4* within the T-cell population promotes gastric/duodenal adenoma

formation (Kim et al., 2006).

Tumor Suppressor and Oncogenes Investigated in this Thesis

TgfβrII and *Smad4*

Tgfβ is a soluble, extracellular signaling molecule controlling cellular

proliferation, differentiation, and motility. In the intestine it is secreted by stromal cells

in a gradient, with increasing concentrations in the crypt and lowering concentrations in

the villi (Koyama and Podolsky, 1989). Conversely, Tgfß receptors are expressed in a

gradient along the crypt/villi axis, with increased levels observed in villi (Avery et al.,

1993). Tgfβ receptors are a super family of single-pass transmembrane receptor

serine/threonine kinases that combine upon binding to Tgfβ, autophosphorylate and

subsequently phosphorylate downstream effectors (Massague, 1996). Three types of

Tgfβ receptors are found in mammals, TgfβrI, TgfβrII and TgfβrIII. The function of

TgfßrIII is not well defined. TgfβrII is the main receptor for Tgfβ ligand, and

homodimerizes upon ligand binding. The TgfβrII/Tgfβ ligand complex binds to a TgfβrI

homodimer, and phosphorylates TgfβrI on intracellular residues (de Caestecker, 2004).

The best characterized target of Tgfβ signaling is the Smad pathway. The activated Tgfβ

receptor complex phosphorylates the receptor Smads, Smad2 and Smad3 (Abdollah et al.,

1997). The activated Smad2/3 dimer binds to Smad4, translocates to the nucleus and acts

on Tgfβ-targets (Moustakas et al., 2001). Signaling response to Tgfβ ligand is halted

through inhibitory Smads, Smad6 and Smad7, inhibiting further kinase activity of

activated TgfβrII/I (Hayashi et al., 1997; Imamura et al., 1997). Activated TgfßrII/I

complex is endocytosed and destroyed, thereby also halting Tgfß signal (Mitchell et al.,

2004; Vilar et al., 2006).

Smad4 is the co-Smad for both TGFβ and BMP signaling. For TGFβ signaling, it

binds to the activated Smad2/3 complex, as discussed above (Lagna et al., 1996). Smad4

also can bind to activated Smad1 and Smad5, the two r-SMADs activated by BMP

signaling receptors (Kretzschmar et al., 1997). Samd4 transcriptional targets are thus

partially specified by the partnering Smads. The r-Smad/Smad4 transcriptional response

is further specified by interaction with transcription factors, including forkhead,

homeobox, zinc-finger, bHLH, and AP1 families of transcription factors (Feng and

Derynck, 2005). Tgfß/BMP signaling response can be modified in a cell-type specific

manner through co-expressing of different transcription partner proteins. To halt

activated r-Smad/Smad4 transcriptional activity, Smad complexes are continuously

exported from the nucleus whereupon they are ubiquinated and degraded (Zhu et al., 1999).

Genes in the TGFß signaling pathway are commonly mutated in advanced human CRC (Grady et al., 1998; Sjoblom et al., 2006). Disruptions to *Tgfß* signaling, such as mutation to *TGFßRII* or *SMAD4* promote tumor growth and invasion, evasion of the immune system, and epithelial to mesenchymal transition and metastasis (Massague, 2008). *TGFßRII* is frequently found to be mutated in HNPCC tumors as there is a mononucleotide run, a sequence highly susceptible to mutation in microsatellite unstable tumors (Samowitz et al., 2002). *SMAD4*, initially identified from deletion mapping in pancreatic cancers (Hahn et al., 1996), is also frequently mutated in human gastrointestinal cancers (Powell et al., 1997). *TGFßRII* and *SMAD4* have overlap in their signaling pathways, but are not entirely epistatic, as *SMAD4* receives input from both TGFß and BMP and *TGFßRII* has non-canonical signaling effects (Kretzschmar et al., 1997; Massague, 1998). Therefore, it is valuable to study mouse models of both *TgfßrII* and *Smad4*, as they may produce different results.

KRAS

KRAS is one of the more than 100 members of the Ras family GTPases (Reviewed extensively in (Colicelli, 2004). KRAS acts at the cell membrane to transduce growth stimulatory mitogenic signals from surface receptors to downstream effector proteins. KRAS functions via transient activation, by binding a GTP, through a guanine nucleotide exchange factor (Lagna et al., 1996). The GTP-bound KRAS remains active,

12

and acts on downstream targets including PI3 kinase and the Raf/Mek/Erk signaling cascade (Zuber et al., 2000). KRAS activity halts when the GTP is hydrolyzed to GDP autocatalytically, and remains inactive until binding a new GTP (Boguski and McCormick, 1993). In this manner, KRAS acts as a molecular on/off switch to mediate cellular proliferation, migration, apoptosis and differentiation.

KRAS was initially identified by its homology to the retroviral Kristen rat sarcoma virus (Der et al., 1982). The two human *KRAS* genes are *KRAS1*, a pseudogene, and *KRAS2,* which produces a 21kD protein with only 6 amino acid changes from the viral protein (Chang et al., 1982). *KRAS* mutations are detected with a high frequency, ranging from 10% to 30%, in a variety of human cancers, including breast, colon, lung, skin, and pancreatic cancer (Bos, 1989). Most oncogenic forms of *KRAS* harbor mutations in one of three codons coding for the amino acid residues Glycine 12, Glycine 13, or Proline 61 (Andreyev et al., 1998). These three residues are critical for the deactivating hydrolysis of GTP to GDP (Milburn et al., 1990). Thus, these mutant forms of KRAS are locked in a constitutively activated GTP-bound state.

KRAS mutations are found to different extents in human tumors. The highest frequency of *KRAS* mutations, up to 90%, are found in pancreatic cancers (Almoguera et al., 1988). *KRAS* mutations are found in 47% of hyperplastic colorectal polyps (Otori et al., 1997), and up to 51% in all stages of colorectal cancers (Rajagopalan et al., 2002), suggesting *KRAS* activation is a hallmark of a premalignant lesion. The tissue specificity for *KRAS* mutation is recapitulated in mouse models. In a "hit-and-run" mouse model of

13

Kras activation, mice preferentially developed adenomas in the lung (Johnson et al., 2001)). Utilizing a conditional allele of oncogenic *Kras* activated by an intestinal epithelial form of Cre recombinase, mice developed hyperplasia in the intestine and colon (Tuveson et al., 2004). The same study noted expression of the oncogenic form of *Kras* in mouse embryonic fibroblasts alone was sufficient to impart an enhanced proliferation and partial transoformation phenotype in the absence of any additional genetic changes.

c-Myc

c-Myc is a transcription factor and is a major regulator of cellular proliferation, cell growth, apoptosis, and stem cell renewal (Jones and Cole, 1987; Luscher and Eisenman, 1990). c-Myc is a 65kD protein located mainly in the nucleus (Persson and Leder, 1984) and contains basic helix-loop-helix and leucine zipper domains characteristic of DNA binding proteins (Landschulz et al., 1988; Murre et al., 1989). c-Myc regulates expression of up to 15% of genes in the human genome, both protein coding and non-coding (Dang et al., 2006; Fernandez et al., 2003; Zeller et al., 2003).   c-Myc protein dimerizes with its partner, MAX, to activate transcription of target genes (Blackwood and Eisenman, 1991; Ma et al., 1993). c-Myc activity has diverse cellular consequences, including activation of the cell cycle, differentiation, increased cell growth, increased cell migration and stem cell renewal (reviewed extensively in (Meyer and Penn, 2008).

As c-Myc is a central protein in normal cellular processes, it is not surprising Myc is tightly regulated at all cellular levels. For example, *c-Myc* expression is regulated, in

part, by mitogenic signals: it is activated by Wnt signaling and is repressed by Tgfß

signaling (He et al., 1998; Yagi et al., 2002). *c-Myc* mRNA is stabilized by the

ribonucleotide binding protein IGF2BP1 and is degraded by Apurinic/apyrimidinic

endonuclease 1 (Barnes et al., 2009; Weidensdorfer et al., 2009). c-Myc protein is

stabilized by phosphorylation at Serine 62 and is targeted for ubiquitin-medited

destruction by phosphorylation of Threonine 58 (Gregory et al., 2003; Pulverer et al.,

1994; Sears et al., 2000). These, and many other factors, result in c-Myc expression

fluctuating in a cell proliferation dependent manner and having rapid turnover rate, with a

normal half-life of 30 minutes or less (Hann and Eisenman, 1984; Jones and Cole, 1987).

c-Myc is a proto-oncogene first identified through its homology to the

transforming gene in the avian myelocytomatosis virus MC29 (Hu et al., 1979;

Vennstrom et al., 1982). Increased levels of c-Myc are found in most human cancers,

and cancer cells employ multiple mechanisms to increase c-Myc levels. For example, in

Burkitt Lymphoma, the *c-Myc* gene is translocated into the immunoglobin heavy chain

region, resulting in increased *c-Myc* transcription (Dalla-Favera et al., 1982; Taub et al.,

1982). Amplification of the *c-Myc* gene increases *c-Myc* expression in some colon

cancer and leukemia cell lines (Alitalo et al., 1983; Collins and Groudine, 1982). Finally,

increased levels of c-Myc in cancers occur through modifications in Myc protein

stability. In response to high Erk activity in Ras transformed cells, c-Myc

phosphorylation is increased at the Serine 62 residue, resulting in prolonged protein

stability (Sears et al., 2000). Additionally, mutations in c-Myc at the destabilizing

Threonine 58 residue are reported in lymphomas, thus preventing phosphorylation and

subsequent ubiquitin-mediated degradation (Gregory and Hann, 2000). In a final

example, the c-Myc ubiquitin ligase, FBW7, is mutated in some T-cell acute

lymphoblastic leukemia cells, impairing destruction of c-Myc (Bahram et al., 2000). All

these, and more, modifications to c-Myc stability have a similar outcome: increased

levels of c-Myc activity, and hence oncogenicity, through increased protein levels or

increased protein half-life.

c-Myc levels are frequently elevated in human gastrointestinal cancers (Erisman

et al., 1988). c-Myc is a transcriptional target of Wnt signaling, and c-Myc protein levels

increase upon Wnt stimulation; inactivating mutations in *APC*, found in upwards of 90%

of human gastrointestinal cancers, result in increased expression of *c-Myc* (He et al.,

1998). c-Myc appears to be the main tumor-promoting target of *Apc*-dependent adenoma

formation in mice (Sansom et al., 2007). Additionally, increased c-Myc activity reduces

expression of two suppressors of Wnt signaling, DKK1 and SFRP1, creating a positive

feedback-loop for increasing *c-Myc* expression (Cowling et al., 2007).   The c-Myc is a

transcriptional target of *Smad4*, and is repressed by TGFß signaling (Yagi et al., 2002).

As discussed above, TGFß signaling components are frequently mutated in advanced

human colorectal cancers (Grady et al., 1998; Sjoblom et al., 2006). Thus increased c-

Myc levels in human gastrointestinal cancers may be achieved in two or more ways: by

increased Wnt signaling through loss of *APC* or by decreased TGFß signaling through

loss of *TGFßRII* or *SMAD4.*

Mouse Models of Development and Disease

Mouse models of human disease has augmented our understanding of human cancer genetics (Clarke, 2007). The mouse as a model system has many advantages, including rapid generation time, have a short lifespan, and a well-characterized genome with a high degree of conservation compared to the human genome. As such, mutations involved in human tumor development are highly conserved in mice. In particular, mice have proven to be an information system for modeling human GI cancers (Letterio, 2005; Taketo and Edelmann, 2009). Not surprisingly, mutations identified in human tumors have similar biological outcomes in mice. Additionally, technologies discussed below have allowed manipulation of the mouse genome in a targeted manner, permitting candidate genes to be modified in a spatial or temporal manner. Ultimately, mouse models of human cancers have the potential to serve as preclinical models to test novel therapeutic approaches.

The main approach to modeling human cancers in mice is to disrupt individual target genes. Over-expression of oncogenes to determine gene function in cancer was first achieved by generation of transgenic mice (Palmiter et al., 1982). This strategy works particularly well for investigating consequences of oncogenes or dominant-negative protein products. However, transgenic approaches have severe limitations, mainly because it is difficult to maintain consistent expression of the introduced transgene: the introduced DNA may integrate at a site that becomes silenced, or where expression is influenced by nearby promoters, resulting in limited expression of the

candidate gene (Henikoff, 1998). Additionally, it is difficult to control the number of copies of the introduced DNA that integrate, and the resultant variations of gene expression may alter tumor phenotypes.

A more powerful approach is to target deletions or changes to endogenous candidate genes within the mouse genome (Mansour et al., 1988). In this manner, individual tumor suppressor genes can be deleted or "knocked-out", or oncogenic mutations can be introduced, or "knocked-in". This strategy capitalizes on rare homologous recombination events in mouse embryonic stem cells between a targeting vector and the cognate chromosomal DNA. Including a drug-selectable marker in the targeting construct permits effective screening for correct incorporation of the mutated DNA into its target (Marten H. Hofker, 2003). One main drawback to targeted gene deletion is that many tumor suppressor genes involved in cancer development are critical regulators of normal cellular function and hence are essential genes. In such cases, homozygous deletion of tumor suppressor genes is embryonic lethal (for examples, see (Oshima et al., 1996) and (Takaku et al., 1999). Therefore, for most tumor suppressor genes targeted knock-out mice can only be utilized when that gene shows haploinsufficiency or frequent loss of heterozygosity. For example, mice homozygous for *Smad4* deletion are embryonic lethal, whereas heterozygous *Smad4* knockout mice develop gastrointestinal tumors. Most of these tumors retain one functional copy of *Smad4*, suggesting haploinsufficiency for *Smad4* (Takaku et al., 1999). However, several issues limit the reach of knock-out technology. First, many genes suspected to be involved in tumor development and progression do not show haploinsufficiency or

infrequently undergo loss of heterozygosity. Secondly, oncogenic mutations are

dominant mutations and are often embryonic lethal, and thus are difficult to study

through traditional knock-out/in technology. Finally, incorporating multiple genetic

mutations within the same animal is difficult, therefore this approach often limits

investigation to single genes.

A system adapted from the bacteriophage P1, Cre/*lox* system, facilitates

conditional alteration of target genes in mice and allows more sophisticated studies

beyond traditional knock-outs (Sauer and Henderson, 1988). As shown in Figure 1.2, the

Cre/*lox* system allows a target gene to be normally expressed until Cre recombinase is

expressed. The system consists of two components: the Cre recombinase enzyme and a

34-bp palindromic *loxP* sequence (Hoess et al., 1984). Cre recombinase catalyzes

recombination between two *loxP* sequences with the nature of the recombinant product

being dependent on the orientation of the *loxP* repeats. For the direct orientation the

intervening DNA is deleted, whereas for inverted repeats the sequences are inverted

(Abremski et al., 1983). Direct-oriented *loxP* sites can be engineered within a target gene

to either activate or inactivate expression. The first example of a tissue specific promoter

was a proof-of-principle experiment utilizing Cre/*lox* regulated *Cre* expression with a T-

cell specific promoter, resulting in a *loxP*-marked reporter gene expressed only in T-cells
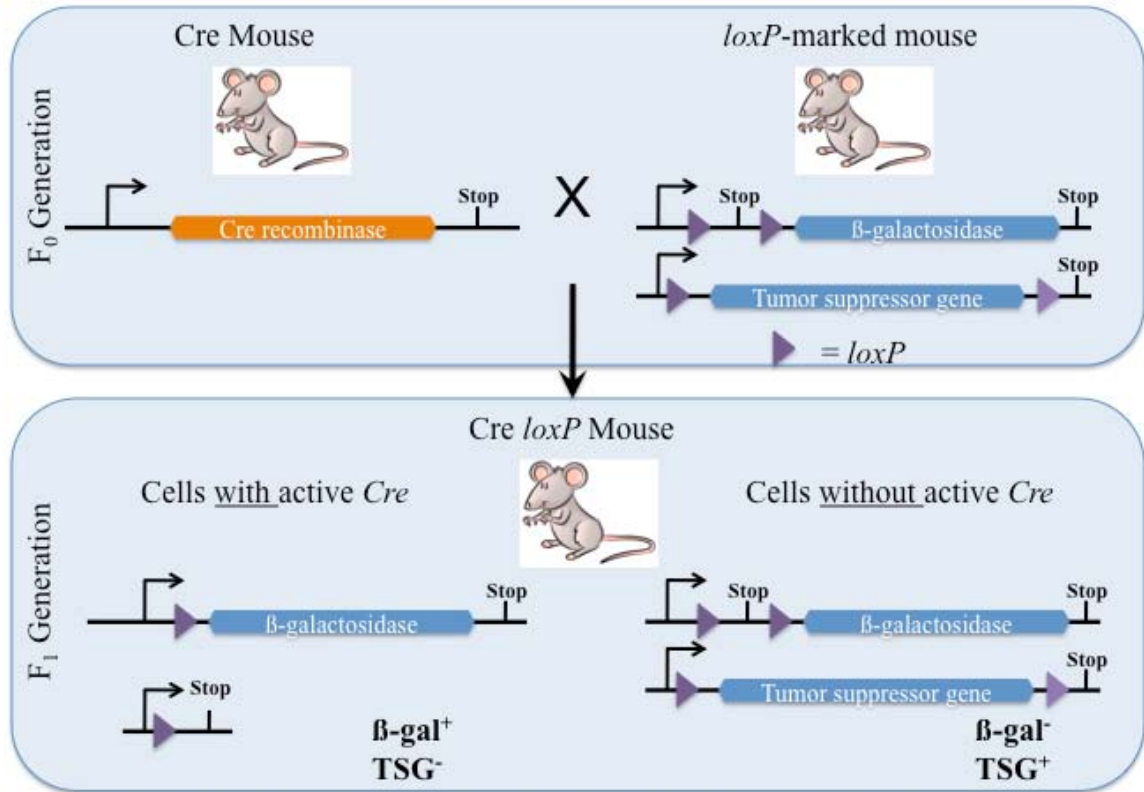
Figure 1.2 – Cre recombinase acts at *loxP* sequences to recombine intervening DNA.
Illustration of a model experiment in which Cre recombinase disrupts function of two
loxP-marked target genes. In this example, the targeted tumor suppressor gene is
expressed normally until Cre recombinase is bred into the mouse, whereas the reporter ß-
galactosidase gene is held transcriptionally inactive due to a *loxP*-flanked upstream
transcriptional stop signal. Upon Cre recombinase expression, the intervening sequence
between *loxP* sequences are removed, thereby activating ß-galactosidase expression and
inactivating expression of the tumor suppressor gene. Cre recombinase expression is
typically regulated under a tissue-specific or inducible promoter. Adapted from Matthias
Zepper, with permission under the terms of the GNU Free Documentation License, V. 1.2

(Orban et al., 1992). To promote conditional modification of the target gene in a

particular tissue, *Cre* expression can be regulated via tissue-specific promoters.

Additionally, Cre expression can be regulated in a temporal manner through use of an

inducible promoter (Kellendonk et al., 1996).   For example, Cre can be activated in a

tissue wide manner at a specific point in time by inducing with an antibiotic or drug (Utomo et al., 1999). One final advantage to the Cre/*lox* system is that Cre can faithfully act upon multiple *loxP*-marked alleles within the same cell (Liu et al., 2002), allowing investigators to combine target genes within the same background.

While the advent of Cre/*lox* technology has facilitated testing one or more genetic alterations in a single animal, there has remained one prime limitation in terms of modeling sporadic tumorigenesis. Experiments in which mutations are induced tissue-wide, or at a designated point in time, within an animal do not accurately model sporadic cancer development. Tumors initiate through mutations in an isolated cell surrounded by otherwise normal tissue. Several thoughtful approaches have arisen to address this issue (Tuveson and Jacks, 2002; Wang et al., 2007b). The Jacks lab created a latent allele system where two copies of the *K-ras* exon 1 were inserted in a tandem manner, the first bearing an activating mutation. This latent allele is silent as an intervening *neo* sequence disrupts translation (Johnson et al., 2001). Upon random, low frequency homologous recombination the *neo* sequence and duplicate exon1 are lost, and the oncogenic *K-ras* is expressed. Although the *K-ras* latent allele system proved valuable in modeling human lung cancer, this approach is limited to single oncogenes.

A second approach, developed by Allan Bradley, utilized an alternative recombination system adapted from *Drosophila*, FLP/FRT, in conjunction with Cre/*loxP* (Wang et al., 2007b). In this system, an *frt* site is located directly upstream of a mutant form of one tumor suppressor gene, *Tp53*. *loxP* sites are engineered on the two

homologous chromosomes, close to the centromere. Expression of FRT and Cre results in rare mitotic recombination during cell division thereby producing one cell that harbors two mutant p53 alleles, and the other with two wild-type copies. This clever approach permits mosaic loss of p53 in a manner more representative of how human mutations occur. However, this approach is not easily adaptable for studying the consequences of mutation of multiple target genes that reside on different chromosomes.

We therefore sought to develop a novel Cre/*lox* system whereby we could cause isolated mutations in multiple target genes in a stochastic manner in the mouse. Designated *Pms2^{cre}*, the system permits isolated Cre activation in a small percentage of cells in most tissues throughout the life of a mouse (Miller et al., 2008). A description of the tractable nature and validation of the *Pms2^{cre}* system will be presented in Chapter 2, and application of this system to facilitate stochastic inactivation of tumor suppressors and oncogenes, alone or in combination, will be described in Chapters 3 and 4.

The Mouse Gastrointestinal Tract as an Experimental System

The mouse gastrointestinal (GI) tract is an ideal system in which to investigate development, homeostasis and cancer. The intestinal epithelium of the GI tract is organized as a complete biological system in a monolayer of tissue (Crosnier et al., 2006). It contains stem cells, actively dividing and differentiating cells, terminally differentiating cells and extruding/apoptotic cells (Figure 1.3) (Cheng and Leblond, 1974a, c). In the small intestine, the epithelial layer projects upwards from the lumen

forming finger-like structures called villi. Villi consist of mainly nutrient-absorbing cells

and secretory cells (Cheng and Leblond, 1974b). Villi greatly increase the absorptive

surface area, allowing for efficient uptake of nutrients.   No villi are present in the colon.

Throughout the intestine, small invaginations of cells create flask-shaped crypts in which

the stem cell and highly proliferative transient amplifying cells reside. In the small

intestine, crypts also contain Paneth cells, a differentiated cell type. Each crypt contains

1-6 stem cells located near the base of small intestine crypts, and at the base of colon

crypts (Bjerknes and Cheng, 2005; Cairnie et al., 1965b). The stem cells divide

approximately once per day, and give rise to a more rapidly dividing population of

transient amplifying (TA) cells (Bjerknes and Cheng, 1999). The TA cells divide and

differentiate as they ascend the crypt, providing cells to the villi for nearly 12 weeks

(Cairnie et al., 1965a). TA cells provide cells to portions of multiple villi, typically to the

4-6 villi adjacent to the crypt. The progeny of the stem cell differentiate as they migrate

toward the crypt-villus junction. The villus has three terminally differentiated cell types:

absorptive epithelia, enteroendocrine cells, and goblet cells (Cheng and Leblond, 1974c).

In the small intestine, TA cells also migrate downwards to give rise to a fourth

differentiated cell type, the Paneth cells (Nichols et al., 1974). Villus epithelium migrate

upwards, with an approximate transit time of 3-5 days (Cheng and Bjerknes, 1985), and

are shed into the lumen or die by apoptosis at the villus tip (Hall et al., 1994). The

longer-lived, crypt-based Paneth cells turnover approximately every 3 weeks (Ireland et

al., 2005).
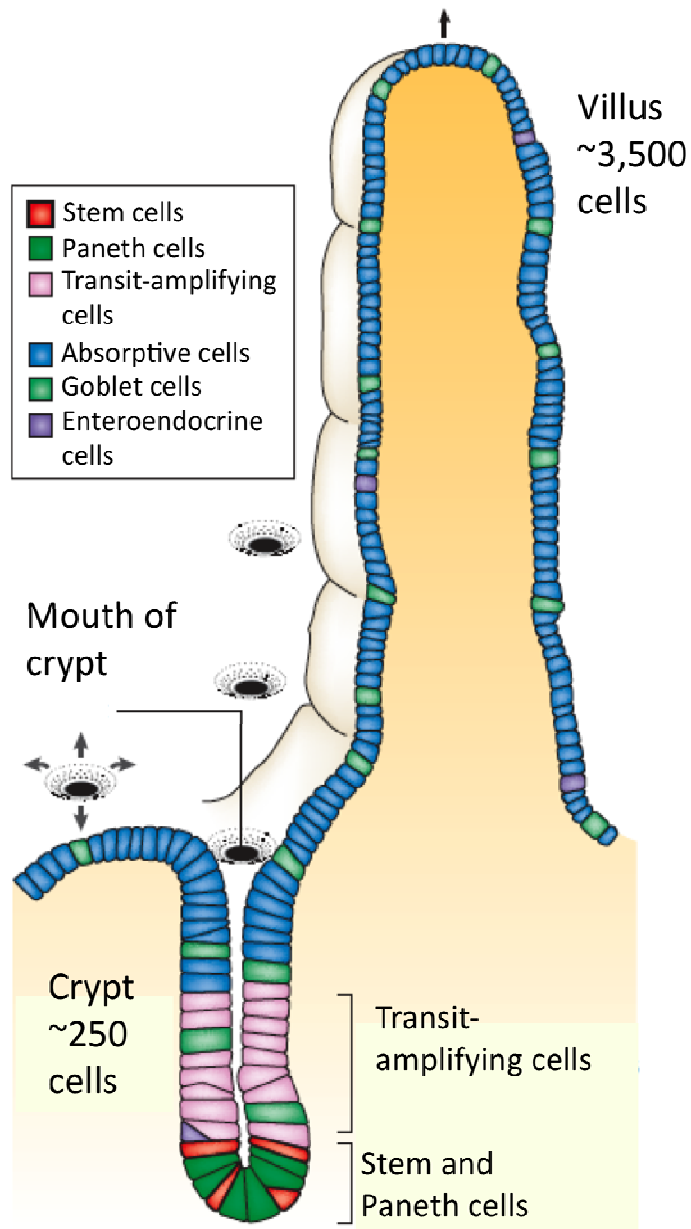
Figure 1.3 Architecture and distribution of cell type in the mammalian small intestine.
Cross section of a single crypt/villi axis. One or more stem cells reside near the base of the crypt and divide asymmetrically to self-renew and give rise to the transient-amplifying cells (TA). The TA cells divide and migrate bi-directionally while undergoing differentiation to populate the crypt base and villi with differentiated cells. Four principal differentiated cell types arise from a common stem cell. Absorptive epithelia cells and the three secretory cells: goblet, enteroendocrine, and Paneth cell. Reprinted with permission from Macmillan Publishers LTD: Nature Reviews Genetics 7, 349-359, copyright 2006.

At birth, the mouse intestine is relatively immature. At postnatal day zero, villi are small and no crypts are present; stem cells reside in the space between the villi (Calvert and Pothier, 1990). Within two weeks, epithelial cells invaginate into the luminal space, creating crypts in which the stem cells reside (Schmidt et al., 1988). The length of the intestine continues to increase until 4 months of age (Cheng and Bjerknes, 1985). During this process, additional crypts form by crypt budding, where the base of the crypt harboring the stem cells cleaves into two, followed by crypt fission (Bjerknes and Cheng, 2005). New crypts formed by crypt budding contain stem cells from a common progenitor. As growth slows, crypt number is maintained through a balance between crypt fission and crypt extinction. Crypt extinction occurs when the crypt stem cell does not self-renew and the crypt is eventually lost (St Clair and Osborne, 1985). The proper number of crypts and villi, as determined by the physiological demands and health of the mouse, are maintained throughout the life of the animal; a homeostasis maintained through balanced growth signals (Crosnier et al., 2006).

Altering individual target genes within the stem cell or transient amplifying population can elucidate the physiologic role a gene plays in maintaining homeostasis or in cancer development. For example, as shown in animals harboring knock-out alleles of *Ephrin B2* and *B3*, correct Paneth cell positioning is dependent on *Ephrin* expression, (Batlle et al., 2002). Particularly exciting is recent work describing tumor outcomes dependent on disruption of the tumor suppressor gene *Apc* in different cell types (Barker et al., 2009). Deleting *Apc* in the putative stem cell resulted in macro-adenoma

formation, whereas deletion of *Apc* in the TA population resulted in micro-adenomas, the majority of which did not progress to macro-adenomas. These studies illustrate the value of mouse models in increasing our understanding of basic biology and genetics of human disease.

Thesis Prospectus

This dissertation utilizes a stochastic Cre/*lox* system to investigate some of the more common genes found disrupted in human CRC. The unique aspect of the Cre/*lox* system used is that it allows target genes to be disrupted in isolated cells, a manner more representative of how human cancers develop. Additionally, the promoter regulating *Cre* expression is expressed in all actively dividing tissue. Thus, these studies are not biased as to which tissue type, when expressing mutant genes, will initiate tumors. Four target genes are explored in this work: the two tumor suppressor genes *TgfβrII* and *Smad4* and the two oncogenes *K-ras* and *c-Myc*.

Contained within this work, I have characterized the *Pms2^{cre}* system, which was developed to permit stochastic alteration of target genes in isolated cell populations: a manner reflective of the natural process of human cancer mutations. Inclusion of a Cre-activated *LSL-k-Ras^{G12D}* with *Pms2^{cre}* validated the system by demonstrating stochastically activated k-Ras within the mouse GI stem cell or proliferating progenitor cell conferred a selective advantage. Conversely, isolated inactivation of *TgfβrII* within stem cells or proliferating progenitor cells placed those cells at a competitive

disadvantage with surrounding epithelia. The reduced number of *TgfβrII* -disrupted cells populating villi suggested *TgfβrII* involvement in maintaining adult intestine homeostasis. Further, an increase in apoptosis was observed in crypts with reduced TgfβrII. Additionally, haploinsufficiency for *TgfβrII* was shown for both reduced competitive fitness along the crypt/villi axis and the apoptotic increases. Finally, I utilized the *Pms2^{cre}* system to investigate the involvement of target genes, a stabilized form of *c-Myc* and inactivated *Smad4*, alone and in combination, in the development and progression of gastric/duodenal tumors in mice. Interestingly, stabilized c-Myc appeared to accelerate Smad4-dependent tumorigenesis as well as impart a more aggressive tumor phenotype. I also found evidence that the tumor initiating cell type was different between the two target gene combinations: epithelial cells likely initiated *Smad4*-only tumors whereas *Smad4/c-Myc* tumors arose from stromal-derived cells. These studies demonstrate the value of the *Pms2^{cre}* system in gaining further insight into the underlying biology governing tumorigenesis, both in gastrointestinal tumors and tumors in other tissues. The work presented here represents a step forward in our ability to investigate the underlying genetics of CRC by more faithfully modeling how tumor-initiating mutations occur: in isolated cells throughout the life of the mouse.

Chapter 2

Characterization of *Pms2^{cre}*

Tractable Cre-*lox* system for stochastic alteration of genes in mice.

Ashleigh J. Miller[1], Sandra D. Dudley[1], Jen-Lan Tsao[2], Darryl Shibata[2], and R. Michael Liskay[1*].

1 Molecular and Medical Genetics, L103, OHSU, 3181 Sam Jackson Park Rd., Portland, OR, 97239.

 2 Department of Pathology, USC Keck School of Medicine, Los Angeles, CA 90033.

*Corresponding author: R. Michael Liskay

                             Dept. of Molecular and Medical Genetics

                             Oregon Health & Science University, L103

                             3181 SW Sam Jackson Park Rd.

                             Portland, OR   97239-3098

                             Phone: (503) 494-3475

                             FAX: (503) 494-6886

                             Email: liskaym@ohsu.edu

I. Abstract

We have developed a cell division-activated "Cre-*lox*" system for stochastic recombination of floxed loci in mice. Cre activation by frameshift reversion is modulated by DNA mismatch repair status, and occurs in individual cells surrounded by normal tissue, mimicking spontaneous cancer causing mutations. This novel system should be particularly useful for delineating pathways of neoplasia, and determining the developmental and ageing consequences of specific gene alterations.

II. Results and Discussion

Valuable mouse cancer models exist that combine conditional expression of the Cre recombinase with various *loxP*-flanked tumor suppressor or oncogene alleles (Jonkers et al., 2001). In these model systems, "cancer" is induced by gene alteration ubiquitously throughout the target tissue or in a selected cell type. This however does not accurately mimic the natural process of sporadic cancer initiation and progression. Two Cre-*lox* models that facilitate stochastic cancer gene alterations in isolated cells rely on homologous recombination to induce activation of an oncogene (Johnson et al., 2001) or inactivation of one or more tumor suppressor genes on the same chromosome (Wang et al., 2007b). One system is restricted in that it is only applicable to activation of an oncogenic *K-ras* allele (Johnson et al., 2001). A second more flexible system utilizes engineered *loxP/FRT* sites to induce mitotic recombination of individual chromosomes bearing modified genes (Wang et al., 2007b). Here we report on a highly versatile system that features Cre-mediated stochastic genetic changes in single cells/cell lineages within normal tissue. The system can be applied to any *flox*-marked allele, is dependent on cell division and can be modulated by DNA mismatch repair status.

To construct an inactive but revertible *Cre* allele, we first engineered an 11 bp A/T run in a modified version of Cre (Lewandoski and Martin, 1997) without altering the nuclear localization signal . We added an extra A/T bp creating a +1 bp out-of-frame *Cre* allele, which we term the "*12A-Cre*". To insure efficient expression at the intended target locus, the *12A-Cre* cassette was further modified to contain a splice acceptor and internal

ribosome entry site (IRES). The *12A-Cre* cassette plus a *neo* module was cloned between

homology arms of the DNA mismatch repair (MMR) gene *Pms2* (Baker et al., 1995) to

generate a *Pms2-Cre* targeting vector. Targeting resulted in an out-of-frame *Cre* gene

under the control of the *Pms2* promoter which is expressed in multiple cell types,

including stem cells of the mouse intestine (Narayanan et al., 1997). Targeting to *Pms2*

removed exon 2, creating a null allele referred to as $Pms2^{cre}$ (Fig. 2.1a). Due to mismatch

repair deficiency, $Pms2^{cre/cre}$ mice should have increased frequency of -1bp frameshifts

(Harfe and Jinks-Robertson, 2000) and hence increased *Cre* reversion relative to

$Pms2^{cre/+}$ mice. Therefore, Cre activation frequency can be modulated appropriately for a

particular study by breeding $Pms2^{cre/+}$ or $Pms2^{cre/cre}$ mice. Importantly, this system

should better mimic sporadic carcinogenesis as Cre-activation is stochastic, limited to

individual cells, and linked to cell division.

Because of our interest in intestinal cancers, we focused on Cre activation in the

gastrointestinal tract. To estimate relative *Cre* reversion in $Pms2^{cre/+}$ and $Pms2^{cre/cre}$

mice, we bred our Cre-activatible to the *ROSA26*r LacZ reporter mouse (Soriano, 1999).

Progeny were examined over a 12-month period and Cre activation in the intestine was

visualized by β-galactocidase staining as "ribbons" of blue staining up villus sides, or "ß-

gal$^+$ foci" (Wong et al., 1996). As expected, *Cre* reversion in $Pms2^{cre/cre}$ (MMR-

deficient) mice (Fig. 2.1d-f,j) was significantly elevated (~100-fold) relative to $Pms2^{cre/+}$

(MMR-proficient) mice (Fig. 2.1b,c,j). The average total numbers of ß-gal$^+$ foci in the

$Pms2^{cre/+}$ and mice $Pms2^{cre/cre}$ were 26 and 3300, respectively. We frequently observed a

ribbon-like pattern of β-gal staining from crypt base to the villus tip (Fig. 2.1c,e,f,g) with

the highest number of ß-gal$^+$ foci in the proximal small intestine trending toward fewer in the distal small intestine (Fig. 2.1j). The total number of ß-gal$^+$ foci appeared to increase with age (Fig. 2.3a), consistent with mutations accumulating with age in the epithelium. ß-gal$^+$ foci size was typically small, consistent with the progeny of a single stem/progenitor cell contributing to one to three villi (Fig. 2.1j). This small size of ß-gal$^+$ foci suggests stem cells with reactivated Cre usually remain confined to a single crypt with a single crypt supplying cells to several adjacent villi (Marshman et al., 2002). Typically, each of the four differentiated cell types in a particular crypt and associated villus appeared to stain positive for β-gal (Figs. 2.1h,i) again consistent with *Cre* reversion having occurred in a stem cell. Micro-dissection of individual villi followed by a PCR assay for Cre-mediated recombination at the *Rosa26r* locus was consistently positive in ß-gal$^+$ villi but negative in ß-gal$^-$ villi (Fig. 2.3b). In addition, patches of β-galactosidase expressing (Cre-activated) cells were observed in all tissues examined: intestine, pancreas, kidney, liver, muscle (data not shown), as expected based on the distribution of *Pms2* expression (Narayanan et al., 1997).

Numbers and sizes of ß-gal$^+$ foci provide a baseline of intestinal stem cell fates following stochastic Cre reactivation. Each crypt contains multiple stem cells within a niche (Marshman et al., 2002), and the co-inactivation/activation of a tumor suppressor or oncogene may change the number of ß-gal$^+$ cells by providing a selective advantage (more or larger patches) or disadvantage (fewer or smaller patches) to that stem cell, even in the absence of visible histological changes. In turn, clonal evolutions, i.e. the replacement of cell populations by the progeny of a single altered cell within a normal

appearing tissue can be visualized. As a next step, we tested the oncogenic allele, *LSL-K-ras^{G12D}* (Jackson et al., 2001) activated by Cre-mediated excision of a stop codon, in our system. *Pms2^{cre/cre},Rosa26r,LSL-K-ras^{G12D}* mice became moribund at 5 weeks due to high lung tumor burden, a phenotype previously associated with activation of *K-ras^{G12D}*(Jackson et al., 2001). Lung tumors were ß-gal$^+$, consistent with Cre activation and subsequent *K-ras^{G12D}* expression (data not shown). Intestines from *Pms2^{cre/cre},Rosa26r,LSL-K-ras^{G12D}* animals were scored for the number and size of blue staining regions (Fig. 2.2a). The numbers of ß-gal$^+$ foci in the *Pms2^{cre/cre},Rosa26r,LSL-K-ras^{G12D}* animals did not change but the number of ß-gal$^+$ villi per patch, or ß-gal$^+$ patch size, clearly increased in the small intestine and cecum (Fig. 2.2a,b). The morphology of most ß-gal$^+$ villi was normal, with a few irregularly sized villi (Fig. 2.2c). The increase in patch size implies that sporadic activation of *K-ras^{G12D}* can confer a selective advantage at some stage, apparently by facilitating dominance of that stem cell over wild type stem cells (Calabrese et al., 2004), including the ability to spread over larger areas presumably through crypt fission (McDonald et al., 2006). This apparent clonal expansion and crypt fission of activated *K-ras* expressing cells would facilitate the subsequent acquisition of the additional alterations needed to confer a visible neoplastic phenotype.

We have described a novel Cre-*lox* system that facilitates monitoring the short and longer term consequences of genetic changes within single cells in normal tissue in the mouse. This system relies on a stochastic reversion event, which activates Cre recombinase expression and can be modulated by MMR status. Visualizing cell lineages

experiencing Cre activation is facilitated by staining for Cre-inducible β-galactosidase, which also allows for monitoring the relative survival and developmental capacity of mutant cells even in the absence of visible neoplasia. In this way, clonal evolution- the replacement of cell populations by the progeny of a single cell - within normal appearing tissues may be visualized. Patterns of ß-gal[+] foci revealed that Cre activation can occur in stem cells and/or proliferating progenitors and increases with age. Normally the progeny of a single stem cell are confined to a single crypt, but sporadic mutations may alter survival or the ability to spread. Some mutations may be initially neutral, whereas others may be lethal or reduce fitness relative to wild-type stem cells within a niche. Alternately some mutations, as illustrated with *LSL-K-ras*[G12D], may confer a selective advantage, leading to expanded ß-gal[+] regions.

We note that because *Pms2*[cre/cre] mice are defective in MMR, random mutations in the genome could complicate interpretations. However, controls can be studied in parallel, e.g. mice that do not harbor tumor suppressor or oncogene Cre targets. Furthermore, although *Pms2*[cre/cre] animals have a reduced life-span with a half-life of 10 months, the animals can be useful for determining "short term" consequences of stochastic knockout of specific tumor suppressor loci individually, or in combination (our unpublished data). Additionally, this system has inherent flexibility because either MMR-proficient, *Pms2*[cre/+] mice, which are not prone to cancer or MMR-deficient *Pms2*[cre/cre] mice can be used to modulate the activation rate of *Cre*. Judicious use of *Pms2*[cre/+] or *Pms2*[cre/cre] mice will be directed by the nature and number of "Cre targets" (*flox*'d alleles) in a particular study.

Because *Pms2* is expressed in multiple tissues and MMR is likely to be active in a variety of stem cell types, the *Pms2^{cre}* system described here offers flexibility in terms of probing both normal and abnormal development in a variety of tissues. In addition, having a widely-expressed promoter driving *Cre* offers the potential for determining for any given tumor whether *Cre*-activation occurring in the tissue/cell type that gave rise to the tumor and/or an underlying/surrounding tissue type was critical. Nevertheless, it may be advantageous in certain situations to use a tissue specific promoter, such as the *villin* promoter, which would target Cre-activation to the epithelium of the mouse gut (Robine et al., 1985).

Acknowledgements

Erratum

This chapter is slightly modified from the text as published in the March 2008 issue of Nature Methods. The published term "blue spots" has been changed to read "ß-gal^{+} foci" or "ß-gal expressing".

III. Methods

Generation of *Pms2^cre* carrying mice. The SV40 NLS within Cre recombinase

(Lewandoski and Martin, 1997) was mutated from CCAAAGAAGAAGGAGAAG to

CCAAAAAAAAAAAAGGAAG by site-directed mutagenesis. The changes preserved

the NLS with the exception that a single additional adenosine nucleotide was added,

inducing a +1bp frameshift. A splice acceptor (SA) and an internal ribosomal entry site

(IRES) cloned 5' to the *cre* ATG and a *neo* cassette was cloned 3' to *cre.* The *IRES-cre-*

neo was inserted between the 5' and 3' *Pms2* homology arms (Baker et al., 1995) using a

5' *Xho*1 adaptamer and a 3' blunt-end adaptamer, to put *Cre* under control of the *Pms2*

promoter. To enrich for targeted clones by "negative selection", this construct was

inserted into pTK1-TK2 using the *Xba*1 and *Bgl*II. The final targeting vector was

linearized with *Sal*1 and electroporated into mouse ES cells G418-gancyclovir resistant

ES cell colonies were screened by Southern for proper targeting at the *Pms2* locus as

previously described (Baker et al., 1995). Targeted ES cells were injected into

blastocysts, implanted into pseudo-pregnant female mice, and chimeric animals were

obtained. F1 offspring from chimera mice were genotyped with the following primers.

The wild-type *Pms2* allele was detected with the primers PMS2A:

TTCGGTGACAGATTTGTAAATG and PMS2W: TCACCATAAAAATAGTTTCCCG,

giving a product of ~350bp. The *Pms2^cre* allele was detected with the primers CreF:

AACATTCTCCCACCGTCAGT and CreR: CATTTGGGCCAGCTAAACAT, giving a

product of ~300bp.   Post-Cre recombination PCR amplification at the *Rosa26r* locus was

detected with the primers PCbGAL1: GCAAGGCGATTAAGTTGGGTAACG and

PCbGAL2: CAGTAGTCCAGGGTTTCCTTGATG, giving a product of ~320bp.

$Pms2^{cre/+}$ mice were mated with *Rosa26* conditional *LacZ* reporter mice

(*Rosa26r*) (Soriano, 1999) to generate $Pms2^{cre/+}$,*Rosa26r*, which were then bred to

obtain $Pms2^{cre/cre}$,*Rosa26r*. $Pms2^{cre/+}$,*Rosa26r* mice were mated with $LSL\text{-}K\text{-}ras^{G12D\backslash+}$

(Jackson et al., 2001) mice to generate $Pms2^{Cre/+}$,$LSL\text{-}K\text{-}ras^{G12D/+}$,*Rosa26r*. These were

subsequently inbred to obtain $Pms2^{cre/cre}$,$LSL\text{-}K\text{-}ras^{G12D/+}$,*Rosa26r*. Animal protocols

were approved by Oregon Health and Science University Department of Comparative

Medicine and were in accordance with The Guide for Care and Use of Laboratory

Animals as outlined by the Office of Laboratory Animal Welfare (OLAW) and the

National Institutes of Health.

Fixation/staining/sectioning. Whole mount β-galactosidase staining of intestines was

performed as previously described (Wong et al., 1996). Briefly, at appropriate time

points mice were sacrificed by cervical dislocation. Intestines were dissected whole

block, flushed with cold PLP (75mM Lysine buffer pH 7.4, 70mM NaPO4, 10mM

NaIO4, 2% PFA), cut open along mesenteric line, pined onto dissection plates and PLP-

fixed for 1 hour. Intestines were treated for 45 minutes with DTT solution (20mM DTT,

20% EtOH, 15mM Tris pH 8.0) followed by x-gal stain (2mM x-gal, 4mM each

$K_3Fe(CN)_6$ $K_4Fe(CN)_6$-H2O, 2mM MgCl in PBS) 12h at 4°C. Blue villi emanating from

a single crypt was designated as one "spot". Total number of spots were scored at 20x

magnification. To determine the number of spots in each region, x-gal stained villi were

counted from three 1-cm segments of each intestinal region, averaged and extrapolated for the entire length of the region. "Spot size" was determined based on number of villi involved: 1 to 3, representing a single crypt, 4 to 10, representing 2-3 crypts, 11 to 50 and greater than 50, representing multiple crypts. Intestines were dehydrated to 70% ethanol, paraffin embedded and sectioned to 5 micron thickness. Sections were stained with hematoxylin and eosin.

Figures
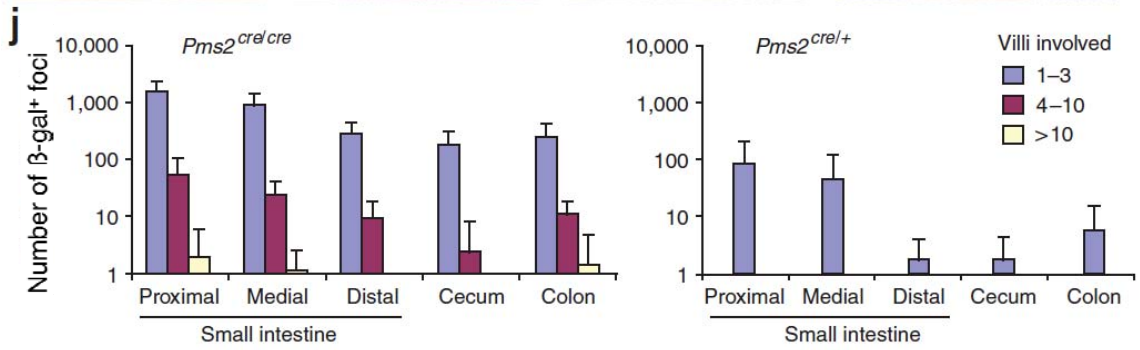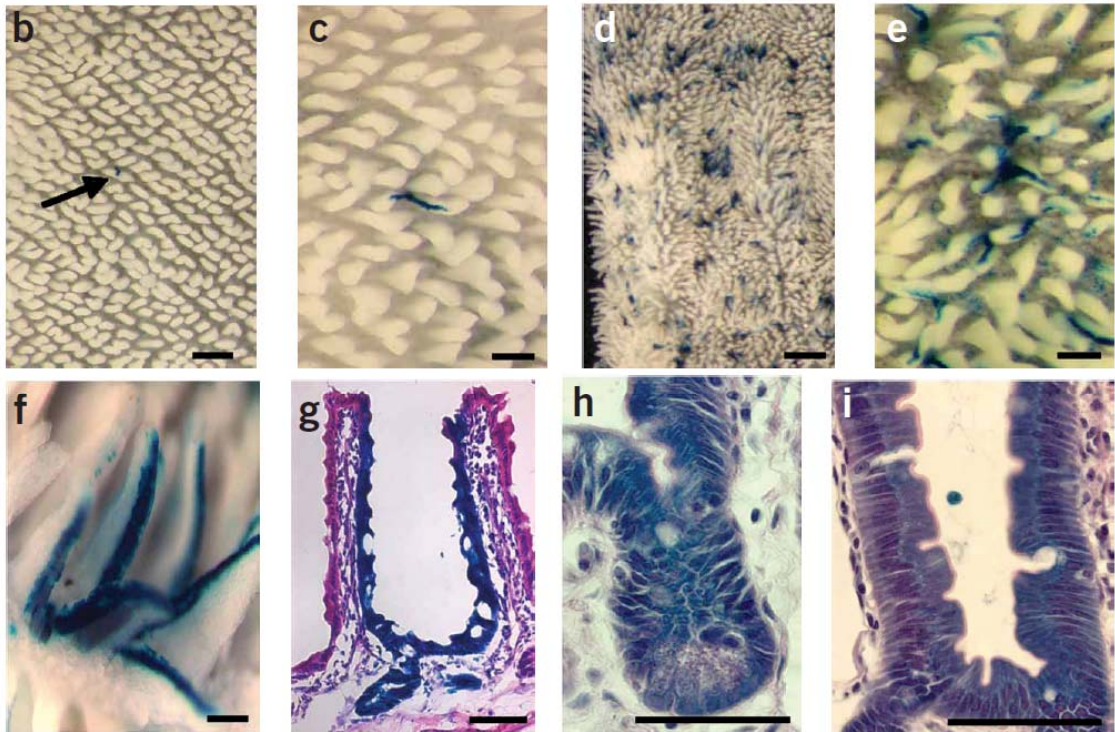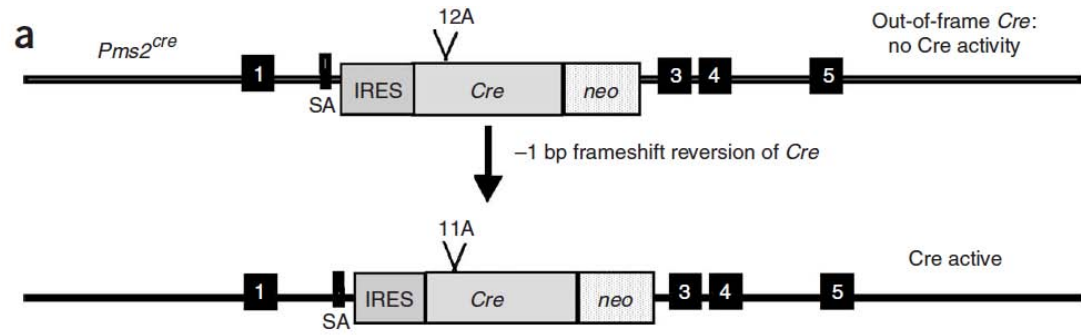
Figure 2.1. Generation and characterization of *Pms2^{cre}* mice. (**a**) A schematic of the *Pms2^{cre}* allele activation by frameshift mutation. b-f) ß-gal stained whole mount mouse intestinal sections. (**b,c**) *Pms2$^{cre/+}$* small intestine (scale bars .5 mm, .25mm, respectively). Arrow in (**b**) indicates the single ß-gal$^+$ focus in this field. (**d,e,f**) *Pms2$^{cre/cre}$* small intestine (scale bars 1 mm, 0.25 mm, 0.1mm, respectively). (**g-i**) Hematoxylin/eosin-stained 5μ paraffin sections of *Pms2$^{cre/cre}$* small intestine crypt (scale bars 50 um, 25 um, 25 um, respectively). (**j**) Distribution of average number of ß-gal$^+$ foci in the gastrointestinal tract of age-matched *Pms2$^{cre/cre}$* (n=10) and *Pms2$^{cre/+}$* (n=4) mice.
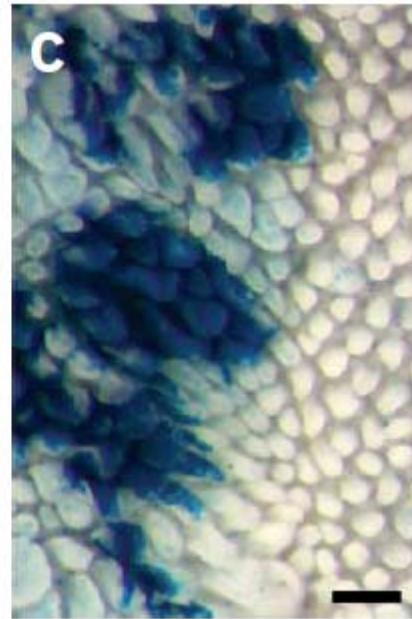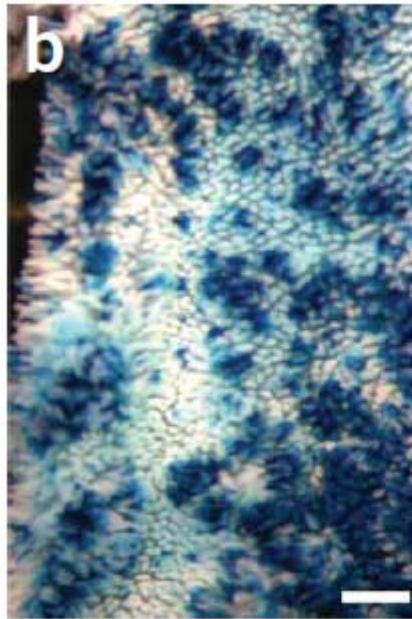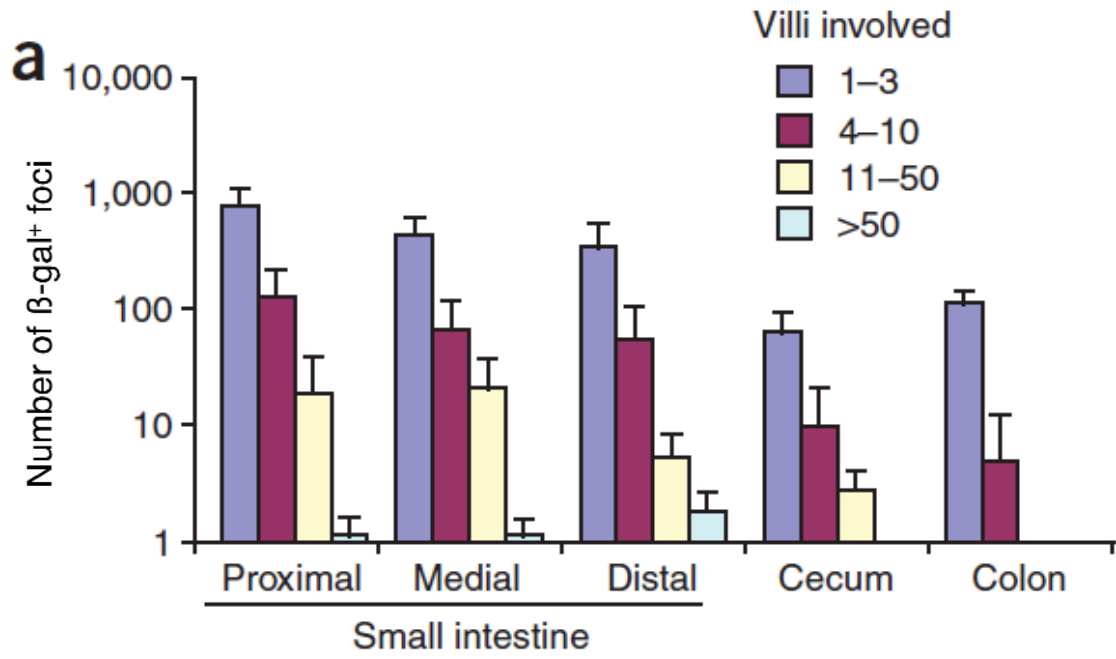
Figure 2.2. Activation of *K-ras* results in larger regions of ß-gal$^+$ foci. (**a**) Distribution of average ß-gal$^+$ foci per region in *Pms2$^{cre/cre}$,LSL-K-ras^{G12D}* animals (n=5). The size of ß-gal$^+$ foci per area increases compared to *Pms2$^{cre/cre}$, Rosa26r* animals. (**b, c**) Whole mount x-gal stained small intestine from *Pms2$^{cre/cre}$,LSL-K-ras^{G12D}* animals show expanded (large) regions of staining (scale bars 1 mm, 0.5 mm, respectively).

a

b

Micro-dissected villi

Blue Blue White Blue Blue White Blue Blue White
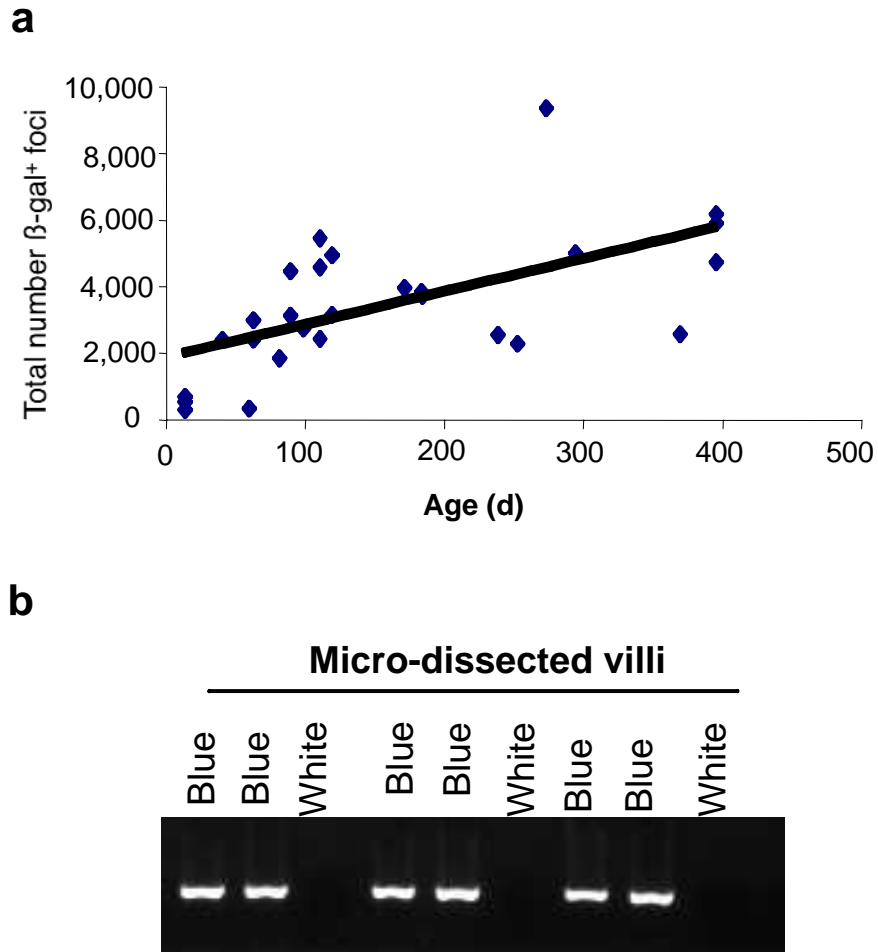
Figure 2.3. Characterization of Cre activation in *Pms2^cre* mice. (**a**) Distribution of total number of ß-gal$^+$ foci per intestine as a function of age in *Pms2^cre/cre^, Rosa26r* mice (n=27). (**b**) Post-Cre recombination PCR amplification products at the *Rosa26r* locus of individual micro-dissected villi. Blue = ß-gal$^+$; White = ß-gal$^-$.

Chapter 3

Isolated disruption of *TgfβrII* with *Pms2^{cre}*

Mosaic disruption of *TgfßrII* reveals cell competition in the mouse intestinal crypt/villus axis.

Ashleigh J. Miller[1], Sandra Dudley[1], Darryl Shibata[2], and R. Michael Liskay[1*].

1 Molecular and Medical Genetics, L103, OHSU, 3181 Sam Jackson Park Rd., Portland, OR, 97239.

 2 Department of Pathology, USC Keck School of Medicine, Los Angeles, CA 90033.

*Corresponding author: R. Michael Liskay

Dept. of Molecular and Medical Genetics

Oregon Health & Science University, L103

3181 SW Sam Jackson Park Rd.

Portland, OR   97239-3098

Phone: (503) 494-3475

FAX: (503) 494-6886

Email: liskaym@ohsu.edu

I. ABSTRACT:

TgfßrII is essential for mouse embryogenesis. However, the role of *TgfßrII* in maintaining adult intestinal homeostasis is not well understood. Using a stochastic Cre-*lox* system, we investigated the effects of conditional mosaic disruption of *TgfßrII* on homeostasis within the intestinal crypt/villus axis. Our findings suggest that reduction of *TgfßrII* expression in isolated in stem and/or long-lived progenitor cells compromises the ability of these cells to normally populate the differentiated cell lineages within the crypt/villus axis. Furthermore, reducing *TgfßrII* places cells in the villus at a competitive disadvantage with neighboring normal cells. Disrupting *TgfßrII* expression did not appear to significantly alter either the cell number or number of actively dividing cells in the crypt. However, we observed increased apoptosis within crypts with reduced *TgfßrII*. Furthermore, our results support a form of haploinsufficiency for *TgfßrII* in maintaining proper intestinal homeostasis. Our findings contrast with other reports in which tissue-wide disruption of *TgfßrII* suggests it is largely dispensable for maintenance of adult intestinal epithelia. Finally, our findings suggest that *TgfßrII* would not be advantageous as a first hit in intestinal tumorigenesis.

II. INTRODUCTION:

Tgfß signaling has critical roles in cellular differentiation, cell motility, cell cycle and apoptosis (Massague et al., 2000). A key component of Tgfß signaling is the Tgfß type II receptor (TGFßRII), a membrane bound receptor tyrosine kinase, which after binding ligand dimerizes with and activates TgfßRI (Massague, 1998; Piek et al., 1999). The activated receptor complex phosphorylates and activates Smad2 and 3, which in turn bind to Smad4, forming a transcriptional complex that translocates to the nucleus and regulates target genes (Kurisaki et al., 2001; Massague and Chen, 2000). Somatic mutation of *TGFßRII* is associated with several types of human cancers, including colorectal cancer (Akhurst, 2004). *TGFßRII* is mutated in 9-15% of microsatellite-stable colorectal cancers and in 90% of colon cancers with microsatellite instability, suggesting it as a common target for inactivation in tumor progression (Grady et al., 1999; Markowitz et al., 1995; Sjoblom et al., 2006; Takayama et al., 2006). Additionally, mutations within the Tgfß signaling pathway are found within most colorectal cancers (Chittenden et al., 2008). Paradoxically, increased levels of Tgfß signaling in human tumors have been correlated with more advanced tumors, including metastatic cancers (Xu and Pasche, 2007). Furthermore, colorectal cancers with intact TGFßRII are often more aggressive and refractive to treatment (Oft et al., 1998; Picon et al., 1998). Therefore, TgfßrII appears to have dual roles as both a tumor suppressor and promoter.

Because complete loss of *TgfßrII* function in mice is embryonic lethal (Oshima et al., 1996), experiments to discern *TgfßrII* function in adult tissues have been limited.

48

More recent experiments have investigated *TgfßrII* function by conditional disruption of a *loxP*-marked allele in a tissue-specific manner (Chytil et al., 2002). Deletion of *TgfßrII* alone in the intestinal epithelia affects tumorigenesis only when combined with other initiating events. For example, loss of *TgfßrII* in the intestinal epithelia increases the adenoma number and accelerates progression of adenomas induced with the colon carcinogen AOM or the *APC[1638N]* mutation (Biswas et al., 2004; Munoz et al., 2006). In these studies, ablation of *TgfßrII* was tissue-wide, whereas in sporadic human tumorigenesis, *TGFßRII* mutation occurs in a single cell surrounded by otherwise normal tissue. Therefore, we sought to investigate the consequence of *TgfßrII* disruption in isolated cells within the mouse intestinal tract as a potentially more accurate model of how human cancers arise.

To investigate the role of *TgfßrII*–dependent signaling in the mouse intestinal tract, we used the *Pms2[cre]* system to stochastically disrupt one or both copies of *TgfßrII* (Miller et al., 2008). A central feature of the stochastic system is *Pms2[cre]*, a *Pms2* null allele, which contains a +1 missense mutation in *cre* targeted to *Pms2*. *Pms2* is a mismatch repair gene that is expressed in many cell types, including intestinal stem cells (Narayanan et al., 1997). In this system, Cre becomes functional following spontaneous reversion, the rate of which is modulated by DNA mismatch repair status. To mark cell lineages with Cre reversion, the system employs the *LSL-Rosa26[r]* Cre-inducible ß-gal allele (Soriano, 1999). By using the *Pms2[cre]* system, floxed *TgfßrII* alleles can be stochastically inactivated in isolated stem cell or long-lived progenitor cells within

intestinal crypts, more closely modeling how early mutations arise in sporadic human cancer.

We found that isolated loss of either one or both *TgfßrII* alleles in intestinal crypts did not lead to development of tumors but rather to a competitive disadvantage of cells in the crypt/villus axis manifested in part by increased apoptosis relative to wild type cells. The increased apoptosis and competitive disadvantage findings suggest that normal *TgfßrII* levels are important for crypt/villus homeostasis. Our findings contrast with the conclusions from a previous investigation involving intestinal epithelium-wide loss of *TgfßrII* (Biswas et al., 2004), which inherently could not see such competition between cells. Therefore, the results presented here illustrate the value of a stochastic system for studying the effect of isolated gene disruption, where mutant cells are in the midst of wild type cells along the crypt/villus axis. Additionally, the results support a form of haploinsufficiency for *TgfßrII* in maintaining normal homeostasis within the mouse intestinal tract. Finally, the observed competitive disadvantage of *TgfßrII* mutant cells within intestinal crypts suggests that mutation of *TgfßrII* would not be a productive initiating event in cancer development, consistent with studies placing *TGFßRII* mutation as a later event during human colorectal cancer development (Grady et al., 1998; Jones et al., 2008).

III. RESULTS

We used the stochastic Cre-*lox Pms2^{cre}* system (Miller et al., 2008) to determine the consequences of *TgfßrII* disruption in isolated crypts within the mouse small intestine. Briefly, the *Pms2^{cre}* allele is comprised of a +1 missense *cre* gene that contains a mutable 12 bp mononucleotide A-run targeted to the *Pms2*; a DNA mismatch repair gene expressed in multiple cell types including intestinal stem cells and or long-lived progenitors (Narayanan et al., 1997). Targeting of the out-of-frame *cre* cassette resulted in a *Pms2* null allele by deletion of exon 2. Whereas *Pms2$^{cre/+}$* animals are DNA mismatch-repair (MMR) proficient, *Pms2$^{cre/cre}$* animal are MMR-deficient and show a 50-100 fold increased frequency of *Cre* reversion (Miller et al., 2008). A critical feature of the *Pms2^{cre}* system is use of the Cre-inducible *LSL-Rosa26^r* ß-gal allele (Soriano, 1999), which facilitates detection of ß-gal$^+$ cell lineages that have experienced Cre reversion. Recently, a similarly versatile system was described that also featured frameshift reversion as the mode for stochastic expression of Cre (Akyol et al., 2008).

Effect of isolated *TgfßrII* disruption on tumorigenesis and lifespan.

Initially, we asked if isolated loss or reduction of *TgfßrII* expression would contribute to a tumor phenotype. We utilized a *loxP*-marked *TgfßrII* allele in which exon 2 is removed upon Cre-mediated recombination, resulting in a *TgfßrII* null allele (Chytil et al., 2002). We followed cohorts of *Pms2$^{cre/cre}$;TgfßrII$^{+/+}$*, *Pms2$^{cre/cre}$;TgfßrII$^{fx/+}$*, and *Pms2$^{cre/cre}$;TgfßrII$^{fx/fx}$* (hereafter designated *TrII$^{+/+}$*, *TrII$^{fx/+}$* and *TrII$^{fx/fx}$*) mice and sacrificed upon evidence of morbidity. Tumor predispositions were similar between the

51

three cohorts, consisting solely of lymphomas attributable to the MMR-deficiency of the

Pms2$^{cre/cre}$ background (Prolla et al., 1998), with 50% of mice presenting at 200 days age

(Figure 3.1). The lack of an intestinal tumor phenotype in either *TrII$^{fx/+}$* or *TrII$^{fx/fx}$* mice is

in agreement with previous reports showing that *TgfßrII* loss in intestinal epithelia is not

sufficient to induce tumors (Biswas et al., 2004; Munoz et al., 2006).

Isolated loss of *TgfßrII* expression impacts homeostasis within the intestinal

crypt/villus axis.

Next, we examined the effect of isolated *TgfßrII* disruption on cell fates within

intestinal crypts by scoring the number and staining patterns of ß-gal$^+$ foci. We observed

a comparable overall number and distribution of ß-gal$^+$ foci in the *TrII$^{+/+}$* and *TrII$^{fx/fx}$*

mice in each intestinal region (Figure 3.2). However, we found that the blue staining

patterns representing ß-gal$^+$ foci in *TrII$^{fx/fx}$* mice were strikingly altered (Figure 3.3). In

TrII$^{+/+}$ mice, staining of the entire crypt and associated ribbon-like, or striped-villus

staining pattern was predominantly observed (Figure 3.3A). Furthermore, as reported

previously (Miller et al., 2008) all four differentiated cell types of the crypt/villi stained

positive for ß-gal. This staining pattern is consistent with *Cre* reversion and concomitant

ß-gal activation having occurred in a stem or long-lived progenitor cell. In contrast, a

much greater fraction of ß-gal$^+$ foci in *TrII$^{fx/fx}$* displayed a discontinuous, or "speckled"

villus staining pattern, with ß-gal$^+$ cells intermingled with ß-gal$^-$ cells (Figure 3.3B). In

addition, we observed a more extreme phenotype in *TrII$^{fx/fx}$* mice, characterized by ß-gal$^+$

blue-staining restricted to cells within the crypt, which we term crypt-restricted staining

(Figure 3.3C). Furthermore, in histological sections from *TrII*$^{fx/fx}$ mice, we noted that

23% of ß-gal$^+$ crypts showed an absence of stained Paneth cells, a pattern observed in

only 2% of ß-gal$^+$ crypts in *TrII*$^{+/+}$ mice (Figure 3.3D). As shown in Table 1 and Figure

2A, the percentages of speckled and crypt-restricted staining were significantly increased

in the duodenum and jejunum of *TrII*$^{fx/fx}$ mice as compared to wild-type (p < 0.001), with

a corresponding decrease in striped staining. We verified Cre recombination at the

TgfßrII locus using a post Cre recombination PCR assay of ß-gal$^+$ micro-dissected villi

and found that 23/24 amplified as positive for Cre recombination (Data Not Shown).

Within this ß-gal$^+$ group, we noted positive PCR signal at the *TgfßrII* locus in both striped

and speckled micro-dissected villi, suggesting that the striped stained villi were not

simply a consequence of inefficient Cre recombination. The speckled, crypt-restricted

and Paneth cell-negative staining patterns suggest that loss of *TgfßrII* alters the

developmental fate within the crypt, including placing cells that reach the villus at a

competitive disadvantage relative to adjacent *TrII*$^{+/+}$ cells.

Loss of a single copy of *TgfßrII* impacts crypt/villus homeostasis.

Interestingly, increased speckled and crypt-restricted staining was also observed

in the *TrII*$^{fx/+}$ intestines suggesting that even a reduction in *TgfßrII* has consequences. In

TrII$^{fx/+}$ intestines we observed a shift in ß-gal staining pattern similar to the *TrII*$^{fx/fx}$

intestines, with a significantly higher proportion of speckled or crypt-restricted staining

patterns and a corresponding decrease in striped-stained villi (Table 3.1, Figure 3.4A).

Although we did not directly measure TgfßrII protein levels in ß-gal$^+$ foci, other studies

of heterozygous knockout mice noted a decrease in both mRNA and protein in *TgfßrII$^{ko/+}$*

cells (Im et al., 2001). The altered staining patterns we observed in the *TrII$^{fx/+}$* mice

imply a form of *TgfßrII* haploinsufficiency, suggesting that the fate of cells with reduced

levels of *TgfßrII* is altered, resulting in a competitive disadvantage when bordered with

cells expressing normal levels of *TgfßrII*.

Altered ß-gal expression patterns associated with *TgfßrII* disruption are

independent of DNA mismatch repair status.

The initial observations of increased speckled and crypt-restricted ß-gal

expression patterns associated with reduction or loss of *TgfßrII* expression were made in

Pms2$^{cre/cre}$ animals, which are DNA mismatch repair deficient. To determine whether

mismatch repair deficiency contributed to these aberrant staining patterns, we scored ß-

gal expression patterns from *Pms2$^{cre/+}$;TgfßrII$^{+/+}$, Pms2$^{cre/+}$;TgfßrII$^{fx/+}$*, and

Pms2$^{cre/+}$;TgfßrII$^{fx/fx}$ intestines (Table 2, Figure 3.4B). We observed similar increased

speckled and crypt-restricted staining in the duodenum and jejunum of the

Pms2$^{cre/+}$;TgfßrII$^{fx/+}$ and *Pms2$^{cre/+}$;TgfßrII$^{fx/fx}$* mice, indicating that DNA mismatch repair

deficiency is not a contributing factor in the altered ß-gal expression patterns.

Loss of *TgfßrII* does not detectably alter the number of S-phase cells in intestinal

crypts.

We speculated that the altered staining patterns observed in *TrII*$^{fx/+}$ and *TrII*$^{fx/fx}$ villi might be due to effects on cellular division rates. To explore this possibility, we administered a BrDU pulse-label followed two hours later by sacrificing the mice and completing immunohistochemistry on histological sections (Figure 3.5A). ß-gal$^+$ *TrII*$^{fx/fx}$ crypts contained an average of 3 BrDU positive cells per hemi-crypt, similar to ß-gal$^-$ crypts. In addition, we observed similar numbers of S-phase cells within ß-gal$^+$ and ß-gal$^-$ crypts of *TrII*$^{fx/fx}$ and *TrII*$^{+/+}$ mice (Figure 3.5B). Thus, the loss of *TgfßrII* in intestinal crypts did not alter, detectably, the number of cells in S-phase. Next, we estimated the cell number within the crypts of the duodenum of *TrII*$^{fx/fx}$ mice, and observed similar numbers in ß-gal$^+$ and ß-gal$^-$ crypts. In *TrII*$^{fx/fx}$ mice, ß-gal$^+$ crypts contained an average of 19.8 cells, (confidence interval: 18.6 - 20.9), as compared to an average of 19.9 cells ß-gal$^-$crypts, (confidence interval: 19.1 - 20.9). Taken together, these results suggested that loss of *TgfßrII* did not alter either the number of S-phase cells or the cell number within the intestinal crypts.

Isolated *TgfßrII* disruption is associated with increased apoptosis within intestinal crypts.

We reasoned that the impact of *TgfßrII* disruption on cell fate associated within the crypt/villus axis, including the apparent competitive disadvantage, might be manifested by an increase in apoptosis. To investigate apoptosis within crypts, we performed TUNEL staining on histological sections of *TrII*$^{+/+}$, *TrII*$^{fx/+}$, and *TrII*$^{fx/fx}$ intestines (Figure 3.6, Table 3.3). In *TrII*$^{+/+}$ crypts, we observed no significant difference

between ß-gal$^+$ and ß-gal$^-$ crypts harboring apoptotic cells, either in the duodenum or jujenum (p = > 0.77 and 1.0, respectively). A significantly higher number of ß-gal$^+$ *TrII$^{fx/+}$* crypts in the duodenum contained apoptotic cells as compared to ß-gal$^-$ crypts within the same intestines (10.6% vs. 1.7%, respectively, p = < 0.03). We observed a similar increase in the jejunum, namely 11.1% and 2.9%, for ß-gal$^+$ and ß-gal$^-$ crypts, respectively (p = < 0.02). A significant difference in apoptosis was also observed between ß-gal$^+$ and ß-gal$^-$ *TrII$^{fx/fx}$* crypts. In the duodenum, 14.8% of ß-gal$^+$ crypts harbored apoptotic cells versus 3.8% in ß-gal$^-$ crypts (p= < 0.001) and 20% of ß-gal$^+$ jejunal crypts versus 4.3% in ß-gal$^-$ crypts (p= < 0.03). Furthermore, a majority (79%) of apoptotic cells in the ß-gal$^+$ *TgfßrII*-disrupted crypts were found in the region populated mainly with transient amplifying cells. The remaining apoptotic cells were in or near the crypt base. Apoptotic cells in the villi were restricted to villus tips. These data suggested that either reduction or loss of *TgfßrII* increased apoptosis levels within intestinal crypts. Again, we note that the increase in apoptosis within the ß-gal$^+$ crypts of *TrII$^{fx/+}$* mice supported a form of *TgfßrII* haploinsufficiency.

IV. DISCUSSION

Using a stochastic Cre-*lox* system, we investigated the effects of mosaic *TgfßrII* disruption on homeostasis within the intestinal crypt/villus axis. Our findings suggest that reduction of *TgfßrII* expression in isolated stem and/or long-lived progenitor cells compromised the ability of cells to normally populate the differentiated cell lineages within the crypt/villus axis and apparently placed cells at a competitive disadvantage once reaching the villus proper. BrDU labeling revealed no difference in cycling cells between crypts with normal versus disrupted *TgfßrII* expression. However, we did observe significantly increased levels of apoptosis cells in crypts suffering loss of either one or both copy of *TgfßrII*. Furthermore, we note that our results support a form of haploinsufficiency for *TgfßrII* in maintaining proper intestinal homeostasis. Finally, our findings suggest that mutation of *TgfßrII* would not be advantageous as a first hit in intestinal tumorigenesis.

The altered ß-gal expression patterns, reflecting cell lineages experiencing Cre reversion and *TgfßrII* disruption, suggested that reduced *TgfßrII* alters the developmental fate of crypt cells, impacting the ability to populate the differentiated regions of the intestinal epithelia. The different ß-gal expression patterns seen in the *TgfßrII$^{fx/fx}$* and *TgfßrII$^{fx/+}$* animals may reflect Cre reversion and hence reduced *TgfßrII* expression occurring within different crypt cell populations: The most severe phenotypes, crypt-restricted and Paneth cell negative ß-gal expression, may result from reduced *TgfßrII* expression in a stem cell or early proliferating progenitor cell. In turn, we suggest that

the speckled and striped ß-gal expression patterns may result from reduced *TgfßrII* in various stage transient amplifying cells that have already undergone partial cell fate specification. One approach to test these possibilities would be to place a stochastically expressing *cre* cassette under a stem cell versus transient amplifying cell promoter, such as *Lgr5* (Barker et al., 2007) and *Hes1* (Riccio et al., 2008), respectively.

The altered ß-gal expression patterns of both the *TgfßrII$^{fx/+}$* and *TgfßrII$^{fx/fx}$* mice support a role for *TgfßrII*-dependent signaling in intestinal epithelial homeostasis, and are remarkable given other reports. Heterozygosity for a germline *TgfßrII* null mutation had no reported consequence on mouse intestinal homeostasis (Oshima et al., 1996). Additionally, complete loss of *TgfßrII* restricted to the epithelia of the small intestine did not alter villus length (Munoz et al., 2006). Furthermore, as determined by proliferation assays and histology, colonic epithelia-wide disruption of *TgfßrII* did not appear to impact homeostasis (Biswas et al., 2004). In these studies, *TgfßrII* disruption occurred throughout the tissue. In contrast, our findings likely reflect the consequence of different relative levels of *TgfßrII* in adjacent crypt/villus units, suggesting that a balance of *TgfßrII* levels within the crypt/villi is important. Further, our data support haploinsufficiency for *TgfßrII*, further enforcing the notion that the relative levels of *TgfßrII* within a tissue are important for normal intestinal homeostasis. Previous studies with *D. melanogaster* suggested that the *TgfßrII* homologue, *punt*, showed haploinsufficiency, and was a dosage-sensitive component of the Tgfß signaling pathway (Simin et al., 1998).

The results presented here, which allow for competition between wild-type and mutant cells, are reminiscent of the developmental phenomenon of cell competition first reported in studies of mosaic *D. melanogaster*. Cell competition was defined as neighboring cells influencing the growth rate of an adjacent population of cells (Morata and Ripoll, 1975). In the *D. melanogaster* studies, cells of the imaginal discs heterozygous for *Minute* mutations in ribosomal genes, *Myc* or *Tgfß* signaling components, were eliminated through cell competition (Burke and Basler, 1996; de la Cova et al., 2004; Morata and Ripoll, 1975; Tyler et al., 2007). Thus, the adult flies are disproportionately composed of wild-type cells. One mouse *Minute* allele is identified, harboring a mutation in the ribosomal protein L24 (*Rpl24*). Heterozygous mutation of *Rpl24* results in slow-growing animals with skeletal, pigmentation and retinal defects. Chimeric *Rpl24*$^{+/-}$ and *Rpl24*$^{+/+}$ mice phenocopy *D. melanogaster Minute* heterozygotes: chimeric animals have no defects and bear a significantly increased percentage of *Rpl24*$^{+/+}$ cells, suggesting the *Rpl24*$^{+/-}$ cells were less competitive (Oliver et al., 2004). Our data suggest a similar effect, namely, a cell that has reduced levels of *TgfßrII* has reduced survival only when adjacent to a normal *Tgfß*-responding cell. Therefore, the findings presented here illustrate a form of cell competition arising from isolated sporadic disruption of *TgfßrII* within the mouse intestinal epithelia.

Cell competition in heterozygous clones of *Minute*, *Myc*, and the *Tgfß* receptor homologue in *D. melanogaster* occur, at least in part, through a combination of reduced cell division and increased apoptosis. We investigated both these possibilities in *TgfßrII*-disrupted crypt/villus units to account for cell competition. Using a BrDU labeling

protocol, we observed no difference in the number of actively dividing cells within normal and *TgfßrII* disrupted crypts. Furthermore, estimation of cell number within the normal versus *TgfßrII* disrupted crypts revealed no difference. Taken together, these findings are in agreement with a previous report (Munoz et al., 2006) demonstrating that tissue-wide loss of *TgfßrII* in adult intestinal epithelia did not alter cellular proliferation. These data suggested that reduced competitive fitness along the crypt/villi axis in *TgfßrII*-disrupted crypts was not associated with altered cellular division or cell number.

Our studies suggested that *TgfßrII* loss or reduction resulted in a significant increase in crypts harboring apoptotic cells, and thus partly account for the aberrant phenotype. The increased apoptosis appeared to mainly occur in the transient amplifying population. The increased apoptosis may be due in part to a failure of proliferating cells to receive growth inhibitory or differentiation cues from Tgfß. In support of this notion, a recent report demonstrated that blocking Tgfß ligand increased apoptosis of intestinal epithelial cells (Sakuraba et al., 2007). Additionally, experiments in *D. melanogaster* demonstrated that isolated cells heterozygous for *Myc* or *Tgfß* signaling components undergo cell competition and are lost mainly through apoptosis (de la Cova et al., 2004; Tyler et al., 2007). Therefore, our findings suggest a role for balanced Tgfß signaling in regulating apoptosis within intestinal crypts. Whether the increased apoptosis in *TgfßrII*-disrupted cells is the result of autocrine or paracrine signaling will require further investigation.

In agreement with other studies (Bhowmick et al., 2004; Biswas et al., 2004; Hahm et al., 2002), stochastic reduction or elimination of *TgfßrII* apparently was not sufficient to initiate intestinal tumorigenesis. Our results provide one reason why loss of *TgfßrII* is not a productive tumor-initiating lesion (Jones et al., 2008): mosaic reduction of *TgfßrII* actually increased apoptosis within the crypt, a property not generally conducive to tumorigenesis. Additionally, the loss of *TgfßrII*-reduced cells that appeared to occur through cell competition may represent a potentially anti-cancer mechanism to rid tissue of aberrant cells (Moreno, 2008; Tyler et al., 2007). Cell competition can be overcome, as shown in *D. melanogaster* experiments in which *Minute* clones persist when a subset of tumor suppressor genes, mainly in the *Tgfß* pathway, are concurrently mutated (Tyler et al., 2007).

Interestingly, we observe a comparable number of ß-gal$^+$ foci in *TrII*$^{+/+}$, *TrII*$^{fx/+}$ and *TrII*$^{fx/fx}$ intestines, suggesting that sporadic *TgfßrII* loss does not appear to alter the survival of long-lived stem cells. This is in contrast to our studies with Cre-activated *Kras*^{G12D}, in which isolated expression of this oncogenic form of *Kras* appeared to confer a competitive advantage to stem cells, manifested by an increase in the size of ß-gal$^+$ *Kras* mutant foci (Miller et al., 2008). *KRAS* mutations are more frequent than *TGFBRII* mutations in sporadic human colorectal cancer (Jones et al., 2008), consistent with the idea that a mutation that directly causes clonal expansion may more often be selected for during tumorigenesis (Tomlinson and Bodmer, 1999). It is tempting to speculate that in human colon cancer development, cells with mutant *TgfßrII* may persist, setting up for a more aggressive tumor phenotype upon a second, "initiating" mutation (Grady et al.,

1998; Oft et al., 1998). In agreement, gastrointestinal tumors developing from the mutant

APC^{1638N} or induced with the mouse colon carcinogen AOM are more aggressive and

arise earlier in the context of intestinal epithelial *TgfßrII* mutation (Biswas et al., 2004;

Munoz et al., 2006). It will be valuable to examine isolated mutation of *TgfßrII*

concurrently with other conditional *"fx"* alleles, such as those disabling the apoptotic

response or increasing cellular proliferation, to further elucidate the impact of disrupting

Tgfß signaling on intestinal tumorigenesis. Finally, the results illustrate the novel

insights that can be gained using the *Pms2^{cre}* mouse or a similar stochastic Cre-*lox* system

(Akyol et al., 2008).

V. METHODS

Generation of mouse strains. *TgfßrII^{fx/fx}* mice (Chytil et al., 2002) mice were bred to *Pms2^{cre/+};Rosa26^R* (Miller et al., 2008; Soriano, 1999) mice to generate *Pms2^{cre/+};Rosa26^{R/+};TgfßrII^{fx/+}* mice. These mice were interbred to produce *Pms2^{cre/cre};TgfßrII^{+/+}*, *Pms2^{cre/cre};TgfßrII^{fx/+}* and *Pms2^{cre/cre};TgfßrII^{fx/fx}* animals carrying at least one copy of *Rosa26^R*. Experimental animals were identified by genotyping with primers *Pms2^+* and *Pms2^{cre}* primers (Miller et al., 2008), *TgfßrII* primers (Chytil et al., 2002) and *Rosa26^R* primers (Soriano, 1999). All mice were maintained in a specific pathogen free environment in the Animal Care Facility in accordance with the OHSU IACUC institutional guidelines.

Tissue harvest and immunohistochemistry. Animals were injected with BrDU (120 mg/kg) 2 hours before sacrifice. After sacrifice, mouse intestines were harvested as previously described (Wong et al., 1996). Briefly, intestines were divided into five regions, duodenum, jejunum and ileum, caecum, and colon, which were pined onto wax plates and whole-mount stained with x-gal (5-bromo-4-chloro-3-indolyl-beta-D-galactopyranoside). X-gal positive (ß-gal expressing) villi were enumerated as previously described. Striped, speckled, and crypt-restricted staining patterns in *Pms2^{cre/cre};TgfßrII* animals were quantified by examining representative 0.5mm segments at 40x magnification and counting the number of x-gal stained villi of each staining pattern. 3-5 fields were quantified for each mouse in each region of the small intestine. For *Pms2^{+/cre};TgfßrII* mice, villi staining patterns were determined by counting the

entirety of each intestinal region. To determine the number of foci in each region, x-gal stained villi were counted from three 1-cm segments of each intestinal region, averaged and extrapolated for the entire length of the region. Foci size was determined based on number of villi involved: 0 to 3, representing a single crypt, 4 to 10, representing 2-3 crypts. Intestines were mounted in paraffin blocks and sectioned at 8 uM. Tissue sections were subject to standard hematoxalin and eosin staining or nuclear fast red counterstain and were imaged using Leica DMRXA camera and LeicaCam v. 1.5 software.

Post-Cre recombination PCR

Single ß-gal$^+$ and ß-gal$^-$ villi from *TgfßrII$^{fx/fx}$* intestines were microdissected under 40x magnification, washed in dH$_2$O, and digested in proteinaseK (0.1mg/ml) in water at 65°C for 2 hours, followed by heat-inactivation at 95deg for 10 minutes. PCR for post-Cre specific recombination products was performed. Primers were as follows: *Rosa26^r* F: GCAAGGCGATTAAGTTGGGTAACG, R: CAGTAGTCCAGGGTTTCCTTGATG, *TgfßrII^{fx}* F: TAAACAAGGTCCGGAGCCCA, R: AGAGTGAAGCCGTGGTAGGT GAGCTTG (Chytil et al., 2002).

Immunohistochemistry. Tissue sections were cut to 8 uM, deparaffinized, and rehydrated. BrDU immunohistochemistry was performed by incubating sections in 1M HCl at 4°C for 10 min, followed by 2N HCl at 37°C for 20 min. After neutralizing in borate buffer (0.5M Borate pH 8.5) for 15 minutes, sections were blocked with BSA blocking buffer (12% BSA in PBS) for 30 min, then probed with mouse anti-BRDU (Roche) diluted 1:100 in BSA block overnight at 4°C. Secondary detection was

performed using DAKOCytomation EnVision+ System-HRP, according to manufactures direction. BrDU sections were counterstained with nuclear fast red. Proliferation index was determined by counting the number of BrDU+ cells on one hemi-crypt of complete crypts, as defined by having a horseshoe shape and containing Paneth cells. Total number of cells per crypt was determined by counting the column of cells in one hemi-crypt, from base to neck, of a horseshoe-shaped crypt. 80 hemi-crypts were counted per crypt type and averaged. Confidence intervals were determined by Prism software, version 3.0. Apoptotic cells were visualized with the ApopTag kit (Chemicon) used according to manufacture's direction. ApopTag-stained slides were counterstained with methyl green. Apoptosis was determined by examining crypts at 400x magnification.

FIGURES
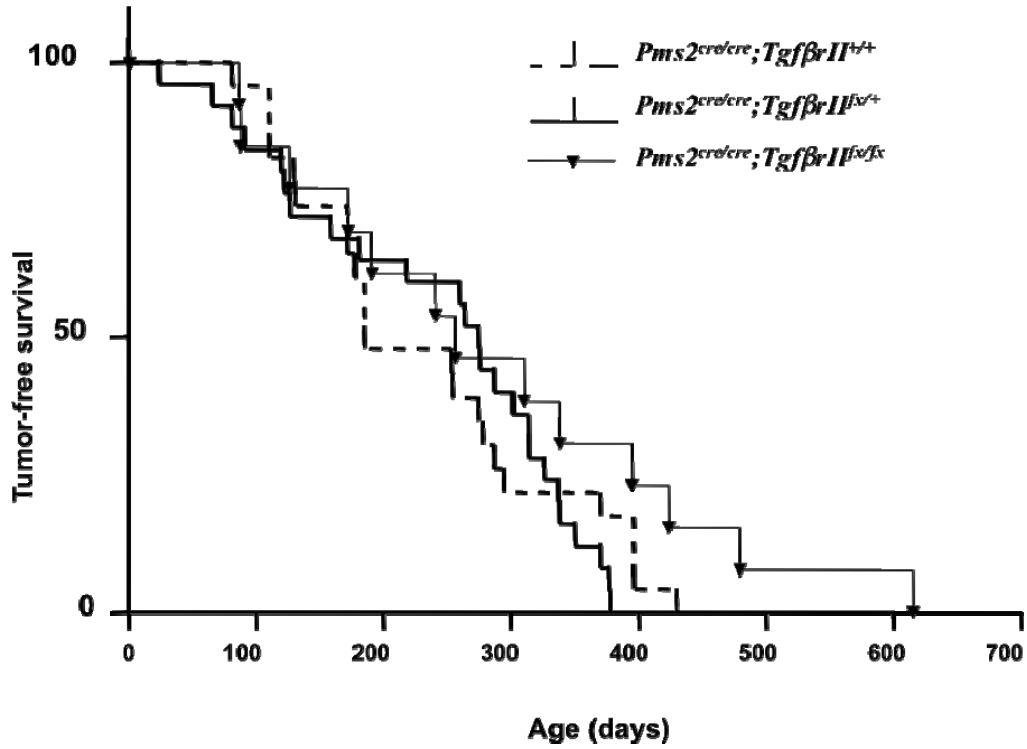
Figure 3.1. Tumor-free survival graph of $Pms2^{cre/cre};Tgf\beta rII^{+/+}$, $Pms2^{cre/cre};Tgf\beta rII^{fx/+}$,
and $Pms2^{cre/cre};Tgf\beta rII^{fx/fx}$ **mice.**
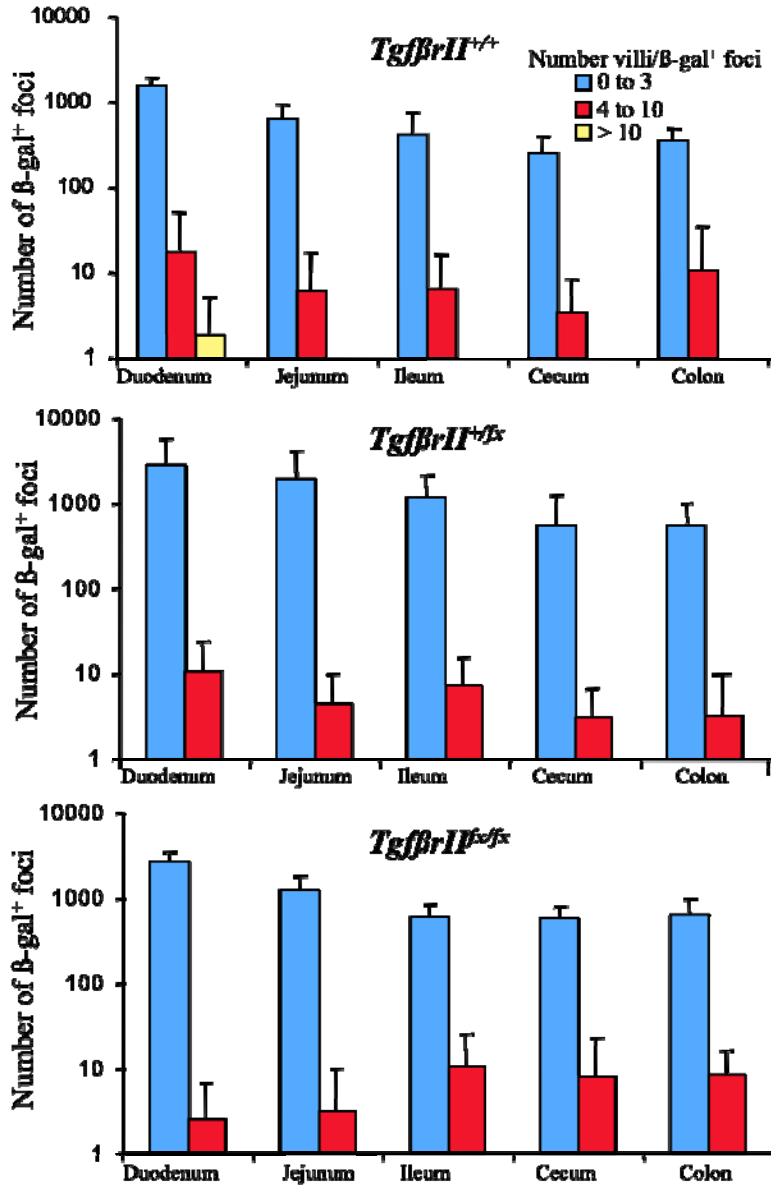
Figure 3.2 Comparison of number of ß-gal⁺ expressing foci in intestines of age-matched *Pms2^{cre/cre};TgfßrII^{+/+}* **(n=6),** *Pms2^{cre/cre};TgfßrII^{fx/+}* **(n=6), and** *Pms2^{cre/cre};TgfßrII^{fx/fx}* **(n=6) mice.** Error bars, s.d.
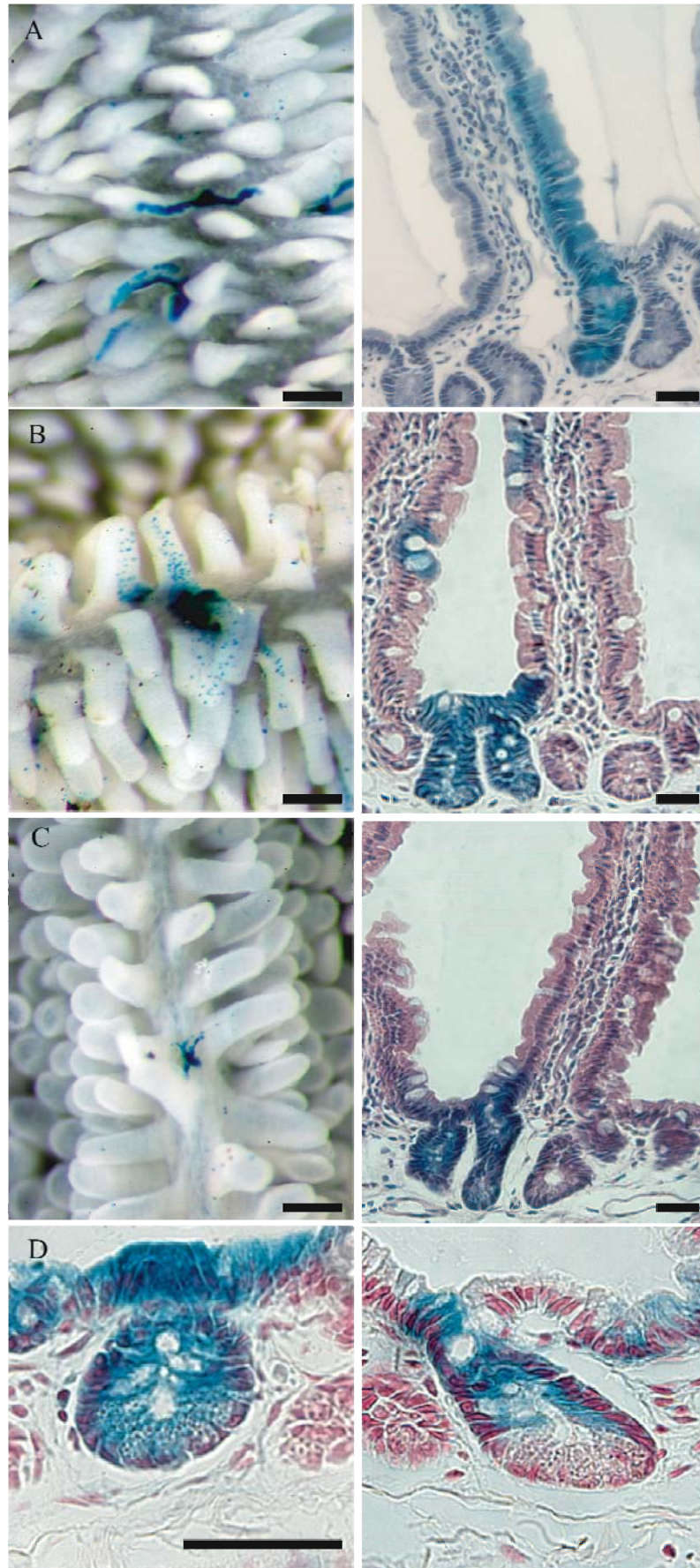
Figure 3.3 Types of ß-gal⁺ foci in intestines of *Pms2$^{cre/cre}$;TgfßrII$^{fx/+}$* and *Pms2$^{cre/cre}$;TgfßrII$^{fx/fx}$* mice. (A-D) Representative whole mount and cross sections of intestinal villi from *Pms2$^{cre/cre}$;TgfßrII$^{fx/fx}$* mice. Typical striped pattern on villi indicating ß-gal expression (A, scale bars 0.25 mM, 25 uM, respectively), speckled villi ß-gal expression (B, scale bars 0.25 mM, 25 uM, respectively), and crypt-restricted ß-gal expression (C scale bars 0.25 mM, 25 uM, respectively). (D) Duodenal crypts showing complete ß-gal expression in Paneth cells and ß-gal negative Paneth cells within a ß-gal expressing crypt (scale bars 25 uM).

Table 3.1 Quantification of ß-galactosidase staining patterns of intestinal villi in *Pms2$^{cre/cre}$;TgfßrII* animals.

		Striped	Speckled	Crypt restricted
Pms2$^{cre/cre}$;TgfßrII$^{+/fx}$ (N=6)	Duodenum	49.8%	43.7%	6.5%
	Jejunum	61.7%	32.2%	6.2%
	Ileum	47.1%	39.9%	13.0%
Pms2$^{cre/cre}$;TgfßrII$^{fx/fx}$ (N=6)	Duodenum	52.5%	40.7%	6.9%
	Jejunum	43.0%	40.1%	16.9%
	Ileum	40.2%	39.5%	20.4%
Pms2$^{cre/cre}$;TgfßrII$^{+/+}$ (N=2)	Duodenum	90.3%	8.9%	0. 5%
	Jejunum	91.2%	5.4%	0.9%
	Ileum	88.1%	7.4%	< 0.3%

P <0.001 for striped vs. non-striped villi in *Pms2$^{cre/cre}$;TgfßrII$^{fx/+}$* and *Pms2$^{cre/cre}$;TgfßrII$^{fx/fx}$* as compared to *Pms2$^{cre/cre}$;TgfßrII$^{+/+}$*

Table 3.2 Quantification of ß-galactosidase staining patterns of intestinal villi in *Pms2$^{cre/+}$;TgfßrII* animals.

		Striped	Speckled	Crypt restricted
Pms2$^{+/cre}$;TgfßRII$^{+/fx}$ (N=3)	Duodenum	28.5%	27.8%	43.7%
	Jejunum	5.2%	36.1%	58.7%
Pms2$^{+/cre}$;TgfßRII$^{fx/fx}$ (N=3)	Duodenum	30.7%	45.9%	23.4%
	Jejunum	34.8%	50.0%	15.2%
Pms2$^{+/cre}$;TgfßRII$^{+/+}$ (N=2)	Duodenum	92.8%	7.2%	0%
	Jejunum	95.7%	4.3%	0%
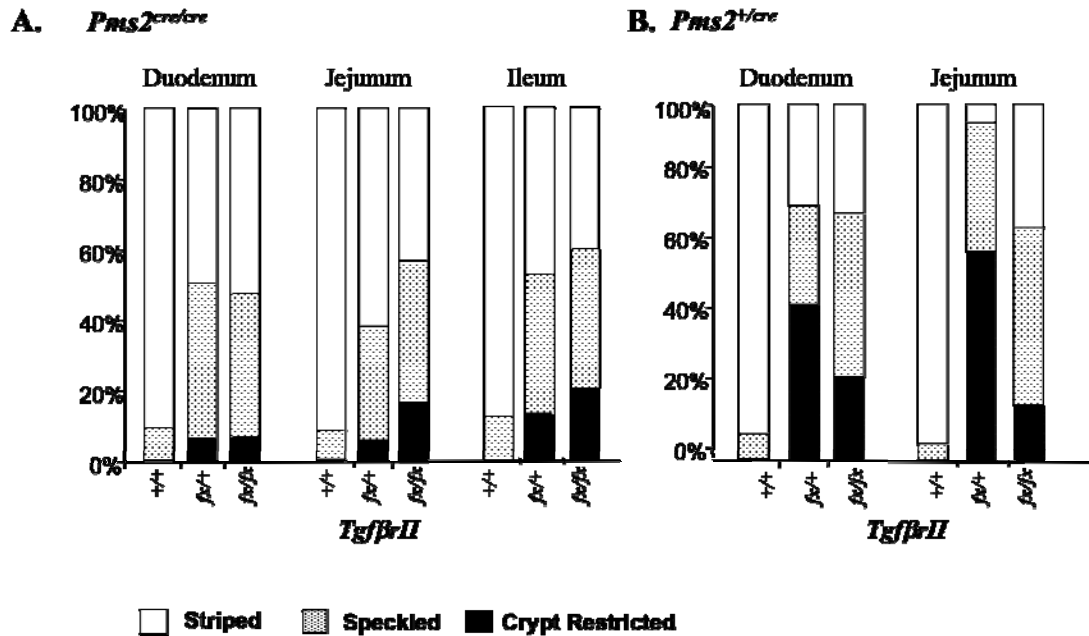
Figure 3.4 Striped, speckled, and crypt-restricted ß-gal expression patterns of
Pms2$^{cre/cre}$;TgfßrII **and** *Pms2$^{+/cre}$;TgfßrII* **mice.** (A) Comparison of percentage of villi
with striped, speckled, or crypt restricted ß-gal+ expression patterns in each region of
Pms2$^{cre/cre}$;TgfßrII animals. Between 500 and 1200 ß-gal$^+$ villi were evaluated per
region, per genotype. (B) Comparison of percentage of villi with striped, speckled, or
crypt restricted ß-gal+ expression patterns in each region of *Pms2$^{+/cre}$;TgfßrII* animals.
Ileum not included as most lacked any ß-gal$^+$ villi. Total number of villi evaluated in
each genotype: *Pms2$^{+/cre}$;TgfßrII$^{fx/fx}$* n=457, *Pms2$^{+/cre}$;TgfßrII$^{+/fx}$* n=659, for
Pms2$^{+/cre}$;TgfßrII$^{+/+}$, n=173.
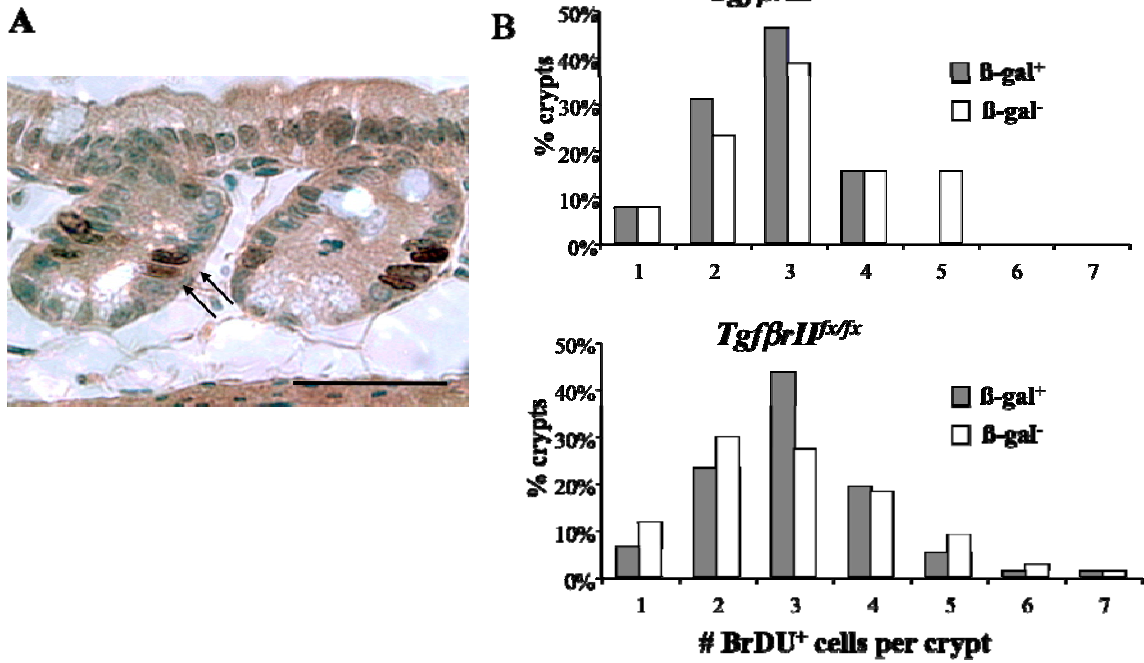
Figure 3.5 Cellular proliferation in *Pms2^{cre/cre};TgfβrII^{+/+}* and *Pms2^{cre/cre};TgfβrII^{fx/fx}*

crypts. (A) Representative immunohistochemistry of BrDU-labeled cells in duodenal

crypt, scale bar, 25 uM. BrDU was administered 2 hours post sacrifice. Black arrows

indicate BrDU$^+$ crypt cells. (B) Histogram representing number of BrDU-positive cells

in ß-gal$^+$ versus ß-gal$^-$ expressing crypts in *Pms2^{cre/cre};TgfβrII^{+/+}* and

Pms2^{cre/cre};TgfβrII^{fx/fx} intestines. N=3 for both genotypes.
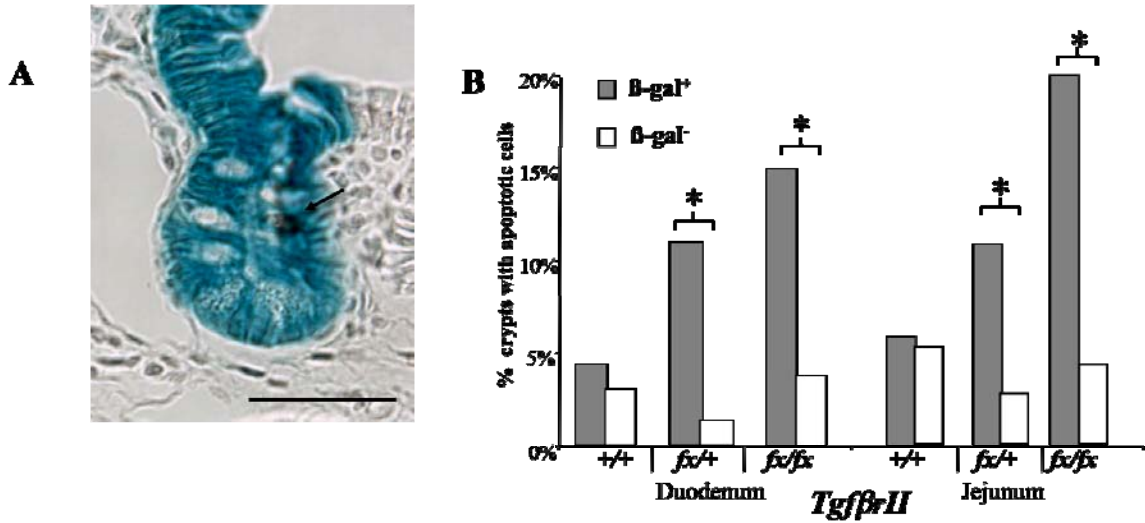
Figure 3.6. Apoptosis in intestinal crypts of *Pms2$^{cre/cre}$;TgfßrII* animals. (A) Representative ApopTag-stained ß-gal expressing crypt, scale bar, 25 uM. Arrow indicates apoptotic cell within a ß-gal$^+$ crypt. (B) Percentage of duodenal and jejunal crypts harboring apoptotic cells in *Pms2$^{cre/cre}$;TgfßrII$^{+/+}$*, *Pms2$^{cre/cre}$;TgfßrII$^{+/fx}$*, *Pms2$^{cre/cre}$;TgfßrII$^{fx/fx}$*. * indicates statistically significant P values, as calculated via Fischers Exact test by comparing number of ß-gal$^+$ crypts with apoptosis to ß-gal$^-$ crypts with apoptosis within the same genotype. *Pms2$^{cre/cre}$;TgfβRII$^{fx/+}$* duodenum p= 0.003, jejunum p=<0.001. *Pms2$^{cre/cre}$;TgfβRII$^{fx/fx}$* duodenum p= 0.02, jejunum p=0.003.

Table 3.3 Apoptosis-positive crypts in *Pms2^{cre/cre};TgfβrII* mice.

	ß-gal$^+$ crypts	ß-gal$^-$ crypts	P value*
Duodenum			
Pms2^{cre/cre};TgfβRII^{+/+} (N=4)	7/159 (4.4%)	5/155 (3.2%)	0.77
Pms2^{cre/cre};TgfβRII^{fx/+} (N=4)	10/188 (10.6%)	3/182 (1.7%)	**0.003**
Pms2^{cre/cre};TgfβRII^{fx/fx} (N=4)	42/283 (14.8%)	10/267 (3.8%)	**< 0.001**
Jejunum			
Pms2^{cre/cre};TgfβRII^{+/+} (N=4)	7/105 (6.7%)	6/105 (5.7%)	1.00
Pms2^{cre/cre};TgfβRII^{fx/+} (N=4)	13/117 (11.1%)	3/104 (2.9%)	**0.02**
Pms2^{cre/cre};TgfβRII^{fx/fx} (N=4)	17/85 (20%)	3/70 (4.3%)	**0.003**

* P values calculated with Fischer's exact test.

Chapter 4

Consequences of *Smad4* inactivation and *c-Myc* stabilization

Stabilized *c-Myc* accelerates *Smad4*-dependent gastrointestinal tumorigenesis.

Ashleigh J. Miller[1], Rosalie Sears[1], Darryl Shibata[2], and R. Michael Liskay[1*].

1 Molecular and Medical Genetics, L103, OHSU, 3181 Sam Jackson Park Rd., Portland, OR, 97239.

2 Department of Pathology, USC Keck School of Medicine, Los Angeles, CA 90033.

*Corresponding author: R. Michael Liskay

Dept. of Molecular and Medical Genetics

Oregon Health & Science University, L103

3181 SW Sam Jackson Park Rd.

Portland, OR   97239-3098

Phone: (503) 494-3475

FAX: (503) 494-6886

Email: liskaym@ohsu.edu

I. Abstract

SMAD4 inactivation is implicated in human gastric cancers and the familial cancer disorder Juvenile Polyposis Syndrome. To further our understanding of additional genetic contributions to these cancers, we applied a novel stochastic Cre/*lox* system to study the gastrointestinal (GI) tumor consequence of isolated mutations to *Smad4* and *c-Myc*, alone and in combination, in mice. Whereas we found no GI tumors in *c-Myc* mice, a moderate number of *Smad4* mice developed gastric/duodenal adenomas. The *Smad4/c-Myc* combination resulted in a complete GI tumor phenotype with adenomas found both in the gastric/duodenal region and in the small intestine. *Smad4/c-Myc* gastric/duodenal adenomas developed at an accelerated rate as compared to those in *Smad4*-only mice, and displayed a more invasive phenotype. The tumor-initiating cell type appears to be within the stroma and may be from a CD45^{+} bone-marrow-derived lineage. These data suggest that stabilized *c-Myc* accelerates *Smad4*-dependent gastric tumors in mice.

II. Introduction

Juvenile Polyposis Syndrome (JPS) is a hereditary form of colon cancer associated with mutation in the gene *SMAD4* (Houlston et al., 1998; Howe et al., 1998). SMAD4 is a tumor suppressor gene, whose protein product is a central component of the TGFβ and BMP signaling pathways, which both regulate cellular differentiation, migration, cell cycle, and apoptosis. SMAD4 is part of the Smad transcriptional complex; it is the co-Smad that binds to activated r-SMADs (Massague and Chen, 2000; Piek et al., 1999). *SMAD4* mutations is strongly implicated as a tumor-promoting lesion and is found in many human epithelial cancers, including esophageal (Barrett et al., 1996), colorectal (Koyama et al., 1999; Salovaara et al., 2002; Thiagalingam et al., 1996), and prostate (MacGrogan et al., 1997) cancers. Additionally, inactivation of *SMAD4* is frequently found in human gastric carcinomas (Powell et al., 1997), and more recently, inactivation of *SMAD4* has been linked to gastric cancer progression (Shun, Human Cancer Biology 2007; (Wang et al., 2007a).

Mice that are heterozygous for *Smad4* develop gastric-type tumors entering into the duodenum, with 100% penetrance between 8 and 15 months age (Hohenstein et al., 2003; Takaku et al., 1999; Xu et al., 2000). These gastric/duodenal tumors contain a high degree of eosinophil infiltration with only the more advanced tumors having loss of heterozygosity for *Smad4*. The relatively long time of onset of these tumors suggest mutations in additional genes contribute to the tumor formation. However, the gastric/duodenal adenomas were not found to contain mutations in the candidate genes *kRas*, *cMet*, *p31*, *p53*, *C-ERB2* and *APC* (Xu et al., 2000).

More recently, a conditional allele of *Smad4* was constructed in which exon 8 was flanked by *loxP* sites, allowing inactivation of both *Smad4* alleles upon expression of Cre recombinase (Yang et al., 2002). Interestingly, conditional deletion of *Smad4* within the T-cell population resulted in gastric adenoma development similar to adenomas observed with other models, causing duodenal occlusion, and displaying a serrated appearance with moderate amount of stromal cell infiltration (Kim et al., 2006). These experiments suggest inactivation of *Smad4* is sufficient to initiate gastric carcinogenesis. However, additional mutations contributing to *Smad4*-dependent gastric/duodenal adenoma development and progression remain largely unidentified.

c-Myc is a transcription factor essential to regulation of cell growth, cell proliferation, and survival (Coller et al., 2000). c-Myc levels are elevated in 70% of human gastrointestinal tumors (Erisman et al., 1988). Yet mutations in *c-Myc* are rarely found in these cancers (Erisman et al., 1985), suggesting increased c-Myc protein levels are a consequence of upregulated gene expression or reduced protein degradation. *c-Myc* is transcriptionally activated by Wnt signaling (He et al., 1998), a pathway often activated in colon cancers. *c-Myc* appears to be the critical tumor-promoting target of Wnt signaling, since *c-Myc* deletion in the small intestine—in conjunction with deletion of *Apc*, the negative regulator of Wnt signaling—reduces *Apc*-dependent adenoma formation (Sansom et al., 2007).

Myc protein stability is regulated, in part, by a sequence of phosphorylations within the evolutionarily conserved Myc box 1 region (Yeh et al., 2004). Phosphorylation of residue Thr58 is one modification that governs c-Myc protein stability (Sears et al., 2000) and is a site frequently mutated in human lymphomas (Bahram et al., 2000). Additionally, abnormal phosphorylation patterns at Thr58 and another critical residue, Ser62, are observed in leukemias, suggesting alterations upstream in the Myc regulatory pathway contribute to the oncogenic capacity of Myc (Malempati et al., 2006).

To investigate the consequence of stabilized *c-Myc* and inactivated *Smad4^{fx}* on gastrointestinal tumor development in mice, we used the *Pms2^{cre}* system (Miller et al., 2008) to stochastically alter these target genes alone and in combination. In this study, we used a mouse harboring a Cre-activated stabilized *c-Myc^{T58A}* allele targeted to the *Rosa26* locus. We found that, in a *Pms2^{cre/cre}* background, *c-Myc^{T58A}* expression did not result in a gastrointestinal phenotype. However, inactivation of *Smad4^{fx}* led to gastric/duodenal adenomas with a moderate frequency. Mice harboring both the *Smad4^{fx}* and *c-Myc^{T58A}* alleles developed gastric/duodenal adenomas at an increased frequency, with a more rapid onset. The *Smad4^{fx}/c-Myc^{T58A}* gastric/duodenal adenomas displayed a more aggressive phenotype with evidence of local invasion. *Smad4^{fx}/c-Myc^{T58A}* mice also developed, at a later age of onset, adenomas in the small intestine. Additionally, *Smad4^{fx}/c-Myc^{T58A}* harboring two *c-Myc^{T58A}* alleles developed gastric/duodenal adenomas at an even more accelerated rate, suggesting a dose-dependence of c-Myc in tumor formation, a finding similar to other studies (Murphy et al., 2008). Both *Smad4^{fx}/c-*

81

Myc^{T58A} gastric/duodenal adenomas and small intestinal adenomas contained an expanded

stromal cell population, largely composed of bone marrow derived cells, that was

possibly the tumor-initiating cell type. In contrast, the tumor initiating cell type in

Smad4fx-only gastric/duodenal adenomas appeared to be in the epithelia. Our findings

suggest stabilized *c-Myc* in combination with inactivated *Smad4* is sufficient to initiate

gastrointestinal adenomas in mice.

III. Results

The goal of this study was to investigate the effects of isolated stabilized *c-Myc* and inactivated *Smad4*, alone and in combination, on gastrointestinal tumorigenesis. We selected *Smad4* because it is implicated in gastric/duodenal adenoma development in humans and mice (Powell et al., 1997; Takaku et al., 1999). We utilized the *loxP*-marked *Smad4^{fx}* allele, harboring *loxP* sites flanking exon 8. Cre-mediated recombination at the *loxP* sites removes exon 8, creating a null allele (Yang et al., 2002). *c-Myc* was selected because it is a downstream transcriptional target of Wnt signaling (Grandori et al., 2000), a pathway activated in 85% of human gastrointestinal tumors (Sjoblom et al., 2006). Additionally, *c-Myc* is a transcriptional target of *Smad4* and is down-regulated by *Tgfß* signaling (Yagi et al., 2002). We used a form of *c-Myc* containing a point mutation in codon 58, which alters a phosphorylated residue in the c-Myc protein critical to its stability; the c-Myc^{T58A} protein exhibits an increased protein half-life due to its failure to be targeted for ubiquitin-mediated destruction (Yeh et al., 2004). Expression of the *c-Myc^{T58A}* allele, targeted to the ubiquitously expressed *Rosa26* locus, is conditionally activated upon Cre-mediated removal of a lox-stop-lox sequence upstream of the gene (Sears, unpublished).

Tumor type and onset differs between *Smad4^{fx}*, and *Smad4^{fx}/c-Myc^{T58A}* mice.

Initially, we investigated the consequence of isolated *Smad4* inactivation or stabilized *c-Myc* expression on tumor-free survival (Figure 4.1). *Pms2$^{cre/cre}$;Smad4$^{fx/fx}$* (hereafter, *Smad4^{fx}*) and *Pms2$^{cre/cre}$;RFS-c-Myc^{T58A}* (hereafter, *c-Myc^{T58A}*) mice had

similar tumor-free survival compared with *Pms2$^{cre/cre}$* mice. However,

Pms2$^{cre/cre}$;Smad4$^{fx/fx}$;RFS-c-Myc^{T58A} (hereafter *Smad4^{fx}/c-Myc^{T58A}*) mice had a greatly

reduced tumor-free survival time, with an average age of tumor onset at approximately

120 days. The five *Pms2$^{cre/cre}$;Smad4$^{fx/fx}$;(2x)RFS-c-Myc^{T58A}* mice obtained, which

harbored two copies of *c-Myc^{T58A}*, had a more pronounced reduction in tumor-free

survival, with an average age of tumor detection at 75 days. Thus, the combination of

Smad4^{fx}/c-Myc^{T58A} accelerated tumor onset as compared to *Smad4*-only initiated tumors.

Next, we compared mortality from gastric/duodenal adenomas in each cohort of

mice. As shown in Table 4.1, neither the *Pms2$^{cre/cre}$* nor the *c-Myc^{T58A}* mice developed

gastric/duodenal adenomas. The *c-Myc^{T58A}* mice displayed a nearly indistinguishable

tumor phenotype from *Pms2$^{cre/cre}$*, with a majority of mice developing thymic and

mesenteric lymphomas. Approximately 30% of *Smad4^{fx}* mice developed

gastric/duodenal adenomas, with an average age of onset of 270 days. Additionally, the

Smad4^{fx} mice developed lymphomas at an earlier age and skin lesions at more advanced

ages (data not shown). Interestingly, 80% of *Smad4^{fx}/c-Myc^{T58A}* mice developed

gastric/duodenal adenomas at an earlier age than the *Smad4^{fx}* mice, with an average age

of onset at 124 days. Three *Smad4^{fx}/c-Myc^{T58A}* mice were sacrificed due to a high

number of adenomas (>20) in the small intestine, with an average age of onset of 220

days. Interestingly, 100% of *Pms2$^{cre/cre}$;Smad4$^{fx/fx}$;(2x)RFS-c-Myc^{T58A}* developed

gastric/duodenal adenomas at an even earlier average age, 75 days. Thus, mice harboring

Smad4^{fx} alleles developed gastric/duodenal adenomas, and including stabilized *c-Myc^{T58A}*

increased the frequency of the tumors, reducing the average age of onset in a dose-dependent manner.

Intestinal adenomas in *Smad4^{fx}/c-Myc^{T58A}* mice.

Intestinal adenomas in the $Smad4^{fx}/c\text{-}Myc^{T58A}$ mice developed in all regions of the small intestine, with an average of 14 in the proximal, 30 in the medial, and 6 in the distal region. To evaluate where Cre activation occurred, and thus where $Smad4^{fx}$ and $c\text{-}Myc^{T58A}$ underwent recombination, a Cre-responsive β-galactosidase allele was included in the background. Whole mount and histological section staining for β-gal expression revealed mainly stromal ß-gal$^+$ cells in intestinal adenomas (Figure 4.2 A, B). Interestingly, the villi surrounding the lesion appeared to have a normal morphology, a phenotype distinct from mutant Apc-driven adenomas (Oshima et al., 1995). Additionally, several villi not associated with adenomas had an abnormal phenotype, having bulbous tips and mid-villi invaginations (Figure 4.2 C-E), and on whole-mount staining appeared to contain β-gal$^+$ cells within the stroma (Figure 4.2 C, black arrows). In contrast, villi that contained β-gal$^+$ cells in the epithelial layer appeared normal, both on whole-mount and histological examination (Figure 4.2 C, white arrow).

The stromal β-gal expression in adenomas and abnormal villi in $Smad4^{fx}/c\text{-}Myc^{T58A}$ mice prompted us to identify the stromal cell sub-type in the intestinal adenomas. Immunofluorescence for CD45, a pan-leukocyte marker, and smooth muscle actin (SMA), a myofibroblast marker, revealed increased CD45$^+$ cells at the apical portion of

the adenomas (Figure 4.3), the same region in which β-gal$^+$ cells were observed on histological section (Figure 4.2 B).

Smad4 and *c-Myc* modification in intestinal epithelia has neutral consequence.

Epithelial ß-gal$^+$ villi of *Smad4^{fx}/c-Myc^{T58A}* mice appeared normal (Figure 4.2 C, white arrow). To examine the overall effect epithelial modification of these genes, we compared, by whole-mount inspection of villi, the number of ß-gal$^+$ foci. All genotypes had a similar number and distribution of ß-gal$^+$ foci, and were comparable to *Pms2$^{cre/cre}$*-only mice (Figure 4.4 A, 2.1 J). We tested for Cre recombination by post-Cre recombination PCR on ß-gal$^+$ and ß-gal$^-$ microdissected villi for *Smad4^{fx}* and *Rosa26-LSL*, where both *c-Myc^{T58A}* and the β-galactosidase reporter gene were targeted. We detected positive recombination for *Smad4^{fx}* in 86% of villi and in 93% of villi for *Rosa26-LSL* (Figure 4.4B). In contrast, ß-gal$^-$ microdissected villi rarely showed positive PCR signal for post-Cre recombination (<1% for *Smad4*, 15% for *Rosa26-LSL*). The PCR results confirm ß-gal expression is a valid indication of where Cre recombination has occurred. Taken together, these findings suggest Cre-mediated recombination of *Smad4* and *c-Myc^{T58A}*, alone and in combination, had little impact when disrupted within the crypt/villi epithelia.

Gastric/duodenal adenomas in *Smad4* and *Smad4/c-Myc* mice

Gastric/duodenal adenomas from *Smad4^{fx}* mice and *Smad4^{fx}/c-Myc^{T58A}* mice were examined both on whole mount and in histological section (Figure 4.5). *Smad4^{fx}* gastric/duodenal adenomas were similar to those reported in other *Smad4* models (Hohenstein et al., 2003; Kim et al., 2006; Takaku et al., 1999). Typically, a single lobe of tumor epithelia occluded the gastric/duodenal junction (Figure 4.5 A, B), leading to tumor-associated anemia. Histological examination of *Smad4^{fx}* gastric/duodenal adenomas revealed hyperplastic epithelial growth with minimal stromal involvement (Figure 4.5B, C). Additionally, β-gal expression was frequently observed in *Smad4^{fx}* tumor epithelia and only rarely in the stroma (Figure 4.5C). *Smad4^{fx}/c-Myc^{T58A}* gastric/duodenal adenomas formed as a single large lobe with irregular appearance at the gastric/duodenal junction (Figure 4.5D, E). Histologically, the *Smad4^{fx}/c-Myc^{T58A}* gastric/duodenal adenomas displayed increased stromal infiltration as compared to *Smad4^{fx}* adenomas (Figure 4.5E, F). *Smad4^{fx}/c-Myc^{T58A}* adenomas consistently contained ß-gal^{+} cells mainly in the stroma (Figure 4.5F). Additionally, the *Smad4^{fx}/c-Myc^{T58A}* gastric/duodenal adenomas showed invasion into the underlying basement membrane, classifying the tumors as adenocarcinomas (Figure 4.5G).

To further investigate the composition of increased stromal cells within *Smad4^{fx}/c-Myc^{T58A}* tumors, we again performed immunofluorescence on histological tumor sections using anti-CD45 and anti-SMA. As shown in Figure 4.6, the expanded stromal component in the gastric/duodenal tumors mainly consisted of CD45^{+} cells. Interestingly, when compared to the β-gal expression pattern (Figure 4.5E,F), the CD45^{+} cells appear to be the same population exhibiting strong β-gal expression.

IV. Discussion

Using a stochastic Cre/*lox* system, we investigated the effects of isolated inactivation of *Smad4* and activation of stabilized *c-Myc*[T58A] alone, or in combination, in mice. Our findings suggest that stochastic inactivation of *Smad4* leads to gastric/duodenal adenomas in approximately 30% of the mice. Interestingly, approximately 80% of *Smad4*[fx]/*c-Myc*[T58A] developed gastric/duodenal adenocarcinomas, and the tumors developed at an earlier age with a more aggressive phenotype. Additionally, all *Smad4*[fx]/*c-Myc*[T58A] mice developed gastrointestinal tumors, either presenting as gastric/duodenal adenocarcinomas or intestinal adenomas. *Smad4*[fx]/*c-Myc*[T58A] gastric/duodenal adenocarcinomas contained an expanded stroma, consisting mainly of bone-marrow derived stromal cells. Finally, reporter staining suggest the cell population in which Cre was activated was different between *Smad4*[fx] and *Smad4*[fx]/*c-Myc*[T58A] mice – mainly epithelial cells in *Smad4*[fx] versus stromal cells in *Smad4*[fx]/*c-Myc*[T58A] - suggesting different tumor-initiating cell types for each tumor model.

Smad4[fx] mice developed gastric/duodenal adenomas similar to those tumors found with other *Smad4* mouse models (Xu et al., 2000); (Takaku et al., 1999); (Kim et al., 2006). *Smad4*[fx] mice also developed lymphomas, similar to those arising in *Pms2*[cre/cre]– only mice, and skin tumors at advanced age. The skin tumor phenotype is not surprising considering other reports of *Smad4* inactivation involvement in skin tumor development (Qiao et al., 2006; Yang et al., 2005). Each tumor type arose at distinct ages and likely is a consequence of the stochastic nature of *Pms2*[cre], hence *Smad4* inactivation, occurring in

multiple cell types at different ages. Overall, the multiple tumor types found in *Smad4^fx^*

mice suggest loss of *Smad4* is sufficient to initiate tumorigenesis in multiple tissue types.

The combination of *Smad4^fx^* and *c-Myc^T58A^* in mice led specifically to

gastrointestinal adenomas; most animals developed gastric/duodenal adenocarcinomas

while a smaller percentage, at a later age, developed intestinal adenomas. The few

*Smad4^fx^;c-Myc^T58A^* mice that did not develop gastric/duodenal adenocarcinomas likely did

not have Cre activated in the cell type necessary to initiate those tumors. Interestingly,

*Smad4^fx^*;(2x)*c-Myc^T58A^* mice harboring two copies of the stabilized *c-Myc* allele developed

gastric/duodenal tumors at an even earlier age than those with only one *c-Myc^T58A^*,

suggesting a dose-dependent effect of *c-Myc* on tumorigenesis, and is consistent with

findings from other labs (Murphy et al., 2008). These observations suggest that *c-Myc^T58A^*

accelerates *Smad4*-dependent gastrointestinal tumorigenesis in mice.

In addition to the gastrointestinal tumors observed in the *Smad4^fx^/c-Myc^T58A^* mice,

a number of villi exhibited aberrant morphology. Dysmorphic villi included hyperplasia

at the villus tip and bifrucated villi. The abnormal villi possibly represent very early stage

adenomas and would be an expected outcome of recent Cre activation, and subsequent

changes to *c-Myc* and *Smad4*, in the *Pms2^cre^* background. Much like the adenomas, the

abnormal villi contained β-gal^+ expressing cells within the stroma, suggesting genetic

changes within underlying stroma influences dysmorphic villi growth.

We observed ß-gal$^+$ epithelial cells in the *Smad4^{fx}* gastric/duodenal adenomas, as well as some ß-gal$^+$ stromal cells. In contrast, we consistently observed ß-gal$^+$ stromal cells in the *Smad4^{fx};c-Myc^{T58A}* adenocarcinomas, with only occasional regions of ß-gal$^+$ epithelial cells. Additionally, intestinal adenomas and hyperplastic villi in *Smad4^{fx};c-Myc^{T58A}* mice showed only stromal ß-gal$^+$ cells. Taken together, these data suggest the tumor initiating cell type in epithelial gastrointestinal adenomas of *Smad4^{fx};c-Myc^{T58A}* mice is within the stromal cell population. In support of this, the Litterio lab reported conditional inactivation of *Smad4* specifically within a T-cell population led to development of similar gastric/duodenal adenomas in mice (Kim et al., 2006). It would be interesting to more directly test the cell type driving the gastrointestinal adenomas in *Smad4^{fx};c-Myc^{T58A}* mice by placing the stochastically activated *Cre* under a stromal-specific and gastrointestinal epithelia-specific promoter and compare resulting tumor development.

Smad4^{fx};c-Myc^{T58A} gastrointestinal adenomas contained increased numbers of stromal cells. Immunofluorescence on both *Smad4^{fx};c-Myc^{T58A}* intestinal adenomas and gastric/duodenal adenocarcinoma sections for the stromal-specific markers SMA and CD45 revealed an expansion of CD45$^+$ cells in the apical regions of the tumors. This suggests the expanded cells within the stroma are bone-marrow derived cells (BMDC). This phenotype is reminiscent of human colon cancers in which refractoriness to Tgfß is associated with increased numbers of tumor-infiltrating lymphocytes (Baker et al., 2006). Interestingly, comparing the sections stained for ß-gal expression to the CD45-stained sections shows a high degree of overlap between the two staining patterns. These staining

patterns suggest the cell type in which Cre was activated was BMDC, and thus these are the tumor-initiating cells.

Interestingly, ß-gal+ cells were observed both within the stromal and epithelial compartments in *Smad4/c-Myc* tumors, whereas mainly epithelial ß-gal+ cells were observed in the *Smad4*-only tumors. An alternative possibility to BMDC being the tumor initiating cell type is the tumor initiating cell was epithelial cells that, in the *Smad4/c-Myc* tumors, underwent epithelial-to-mesencymal transition (EMT). immunohistochemistry for the epithelial marker E-cadherin. Two of five *Smad4/c-Myc* tumors examined showed evidence of EMT by stromally-localized expression of the epithelial cell marker E-cadherin, with the adjacent epithelia showing weaker staining than in other tumor sections (Data not shown). The mis-localized E-cadherin expression is one hallmark of EMT, and suggests in these two tumors EMT was occurring. Of three *Smad4*-only tumors, no mis-expression of E-cadherin was observed, suggesting no EMT had occurred. Increased *Myc* expression in epithelial cells is associated with reduced E-cadherin expression, changes in cell morphology, and anchorage independent growth, all hallmarks of EMT (Cowling and Cole, 2007; Cowling et al., 2007).   The preliminary E-cadherin findings warrant follow-up with additional markers, including the stromal markers vimentin and fibronectin, and the transcription factors slug, snail, and twist (Chen et al., 2008), to determine more definitively if EMT occurred in the *Smad4/c-Myc* tumors.

In human gastric/duodenal tumors, the tumor-initiating epithelial cell is thought to be cells within the junction between stomach and intestine (Kushima et al., 2006). Within

91

this region, epithelial cells are subject to a high degree of cross-talk, as differentiation

signals are received from both stomach and intestine epithelia and stroma. Cell

differentiation and development is largely regulated by growth factor gradients (Hanahan

and Weinberg, 2000), and mounting evidence suggests the tumorigenic potential of

epithelial cells is a direct result of the growth factor signals they receive in a premalignant

state (Potter, 2007). Human epithelial tumors frequently arise at similar junctions: breast

cancers often arise at the junction between duct and gland; lung tumors arise between

alveoli and bronchi (Kim et al., 2005; NCI; Wellings et al., 1975). Our results illustrate

that the gastric/duodenal junction region is particularly sensitive to perturbations in

Smad4-dependent signaling pathways and c-Myc levels. Our data support a role for

stabilized *c-Myc* accelerating the onset and aggressiveness of *Smad4*-dependent

gastric/duodenal adenomas in mice. We show evidence that the tumor-initiating cell type

in *Smad4^{fx}/c-Myc^{T58A}* adenomas is bone-marrow-derived. Finally, our data demonstrate

the advantage of using a system that permits isolated disruption of target genes without

bias to a particular tissue type.

V. Methods

Generation of mouse strains. The cohorts of mice were obtained by interbreeding $Pms2^{cre/+};Rosa26^R$ (Miller et al., 2008; Soriano, 1999), $Smad4^{fx/fx}$ (Yang et al., 2002) and $RFS-c-Myc^{T58A}$ (Sears, unpublished) mice. Experimental animals were identified by genotyping with primers $Pms2^+$ and $Pms2^{cre}$ primers (Miller et al., 2008), $Smad4$ primers (Yang et al., 2002), $RFS-c-Myc^{T58A}$ primers (F - TGCAGGATCTGAGCGC CGCCGCCT; R - GCTGTGGCCTCCAGCAGAAGGTG) and $Rosa26^R$ primers (Soriano, 1999). Animals were harvested at presentation of tumors. Lymphomas were detected as labored breathing or through palpation. Gastric/duodenal tumors and intestinal adenomas presented as frank anemia, and occasionally blood in stools.   All mice were maintained in a specific pathogen-free environment in the Animal Care Facility in accordance with the OHSU IACUC guidelines.

Tissue harvest and histology. Animals were sacrificed and mouse intestines were harvested as previously described (Wong et al., 1996). Briefly, intestines were divided into five regions, duodenum, jejunum and ileum, caecum, and colon, which were pined onto wax plates and whole-mount stained with x-gal. X-gal positive villi were enumerated as previously described (Miller et al., 2008). Briefly, intestines were divided up into five regions, proximal, medial and distal small intestine, cecum and colon.   The number of x-gal positive foci was estimated for each region by averaging counts from 3 fields at 20x magnification and multiplying by the length of the region. For histology, tumors and intestines were mounted in paraffin blocks and sectioned at 8um. Tissue sections were subject to standard hematoxalin and eosin stain, or nuclear fast red

counterstain, and were imaged using a Leica DMRXA camera and LeicaCam v. 1.5

software.

Micro-dissection and post-Cre recombination PCR. Individual blue-stained and

unstained villi from *Pms2$^{cre/cre}$;Smad4$^{fx/fx}$;RFS-c-Myc^{T58A}* intestines were microdissected

at 40x magnification. DNA was extracted and subject to PCR to detect recombination at

each locus. The primers were as follows: Rosa26r F -

,GCAAGGCGATTAAGTTGGGTAACG, R - CAGTAGTCCAGGGTTTCCTTGATG,

Smad4 F - GACCCAAAGCTCACCTTCAC, R – CCTTAGTTGAAGCTTATAACTT

CG.

Immunofluorescence. Tumors and intestines subject to immunofluorescence were fixed

briefly in 2% paraformaldahyde in PBS for 1 hour, and equilibrated in 30% sucrose/PBS

at 4 degrees overnight. Tissue was frozen in OCT and sectioned at 12 uM. After briefly

rinsing in PBS, sections were blocked in blocking buffer (12% BSA in PBS) for 1 hour

and probed with primary antibody diluted in blocking buffer overnight at 4 degrees.

Fluorescent-conjugated secondary antibody was applied in blocking buffer for one hour.

Sections were rinsed, mounted in Crystal mount, and viewed with a Zeiss microscope.

Images were acquired with Open lab software, version 5.0. Antibodies used: mouse-anti-

Smooth Muscle Actin (1:50), conjugated to Alexa 488 (Molecular Probes), rat-anti-CD45

(1:200), detected with goat-anti-rat Cy5 (1:200).

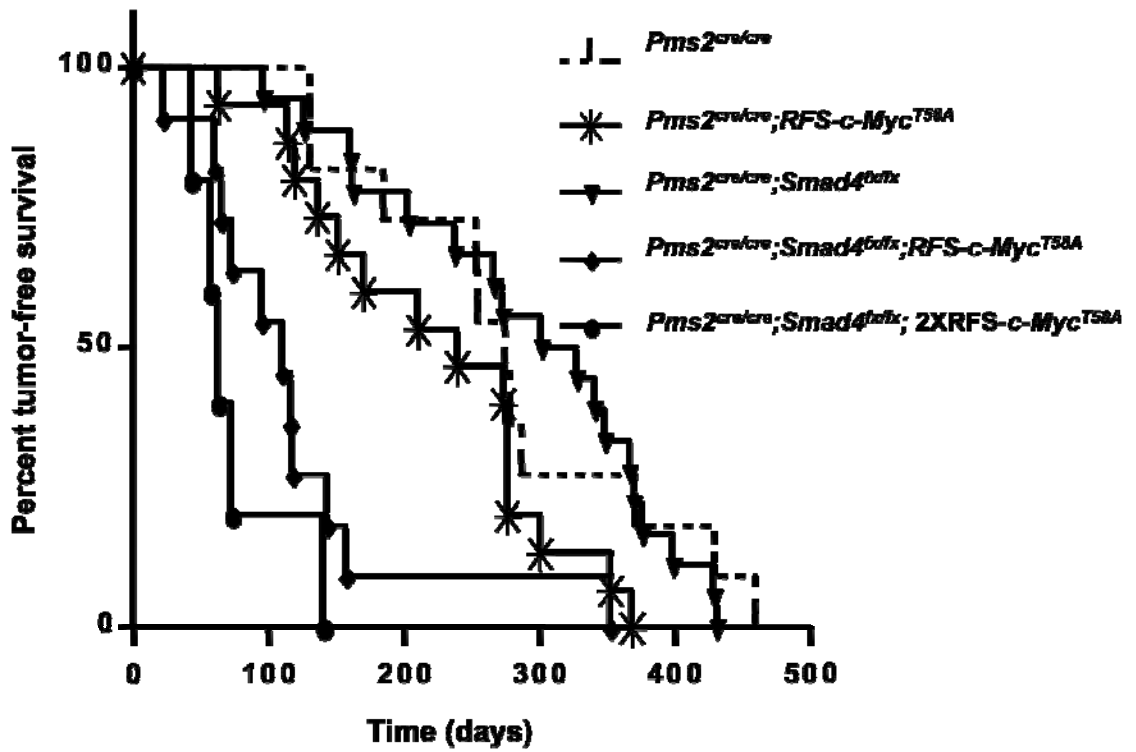**Figure 4.1. Tumor-free survival of** *Pms2$^{cre/cre}$*, *Pms2$^{cre/cre}$;Smad4$^{fx/fx}$*, *Pms2$^{cre/cre}$;RFS-c-Myc^{T58A}*, *Pms2$^{cre/cre}$;Smad4$^{fx/fx}$;RFS-c-Myc^{T58A}*, **and** *Pms2$^{cre/cre}$;Smad4$^{fx/fx}$;(2x)RFS-c-Myc^{T58A}* **mice.**

Table 4.1. Gastric/duodenal adenomas in *Smad4* and *c-Myc*[T58A] mice

Genotype	# animals with GD adenoma/ # animal	Age (age range)
Pms2[cre/cre]	0/10	N/A
Pms2[cre/cre];*RFS-cMyc*[T58A]	0/15	N/A
Pms2[cre/cre];*Smad4*[fx/fx]	6/19	270 (126-398)
Pms2[cre/cre];*Smad4*[fx/fx]; *RFS-cMyc*[T58A]	11/14	124 (91-352)
Pms2[cre/cre];*Smad4*[fx/fx]; 2x*RFS- cMyc*[T58A]	5/5	75 (43-140)
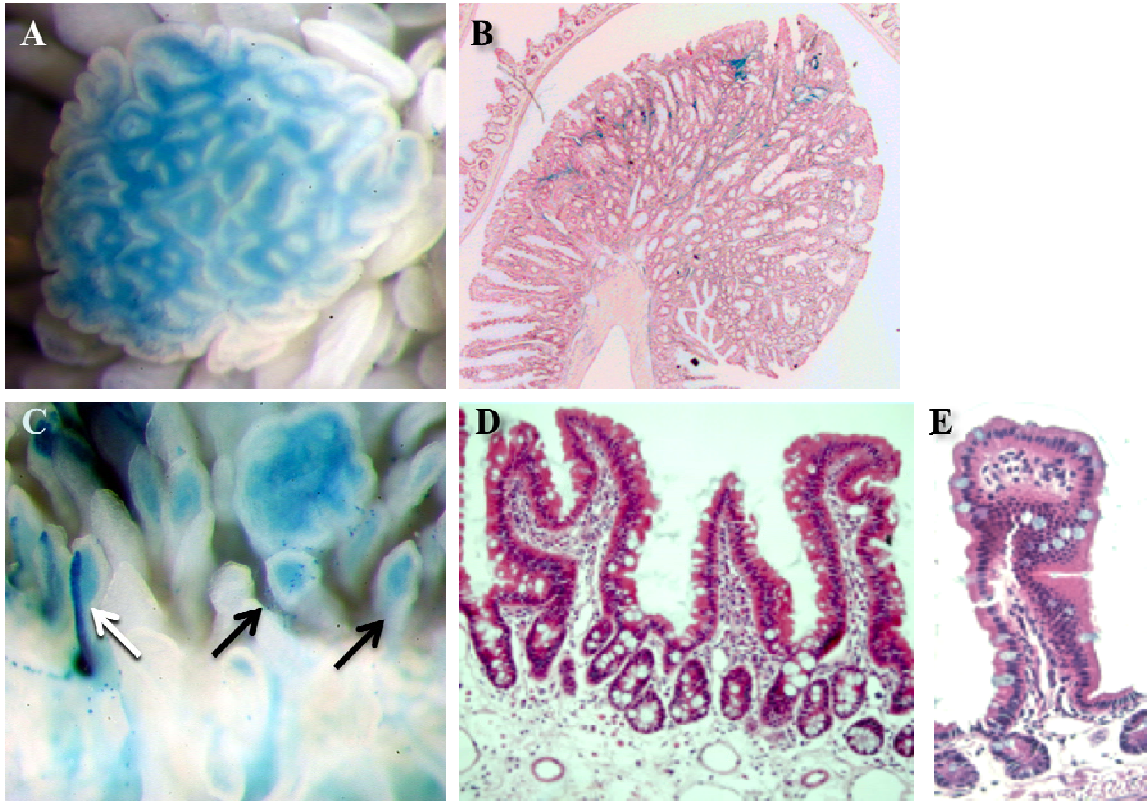
Figure 4.2. β-Galactosidase staining of *Pms2^{cre/cre};Smad4^{fx/fx};RFS-c-Myc^{T58A}*

intestinal adenomas. Whole mount (**A**) and histological section (**B**) of

Pms2^{cre/cre};Smad4^{fx/fx};RFS-c-Myc^{T58A} intestinal adenoma stained on whole-mount. Whole

mount (**C**, black arrows) and histological section (**D,E**) of bulbous, abnormal villi.

Arrows indicate stromal staining (black) and epithelial staining (white). Magnifications

as follows: A, 20x; B, 50x; C, 40x, D,E, 200x.

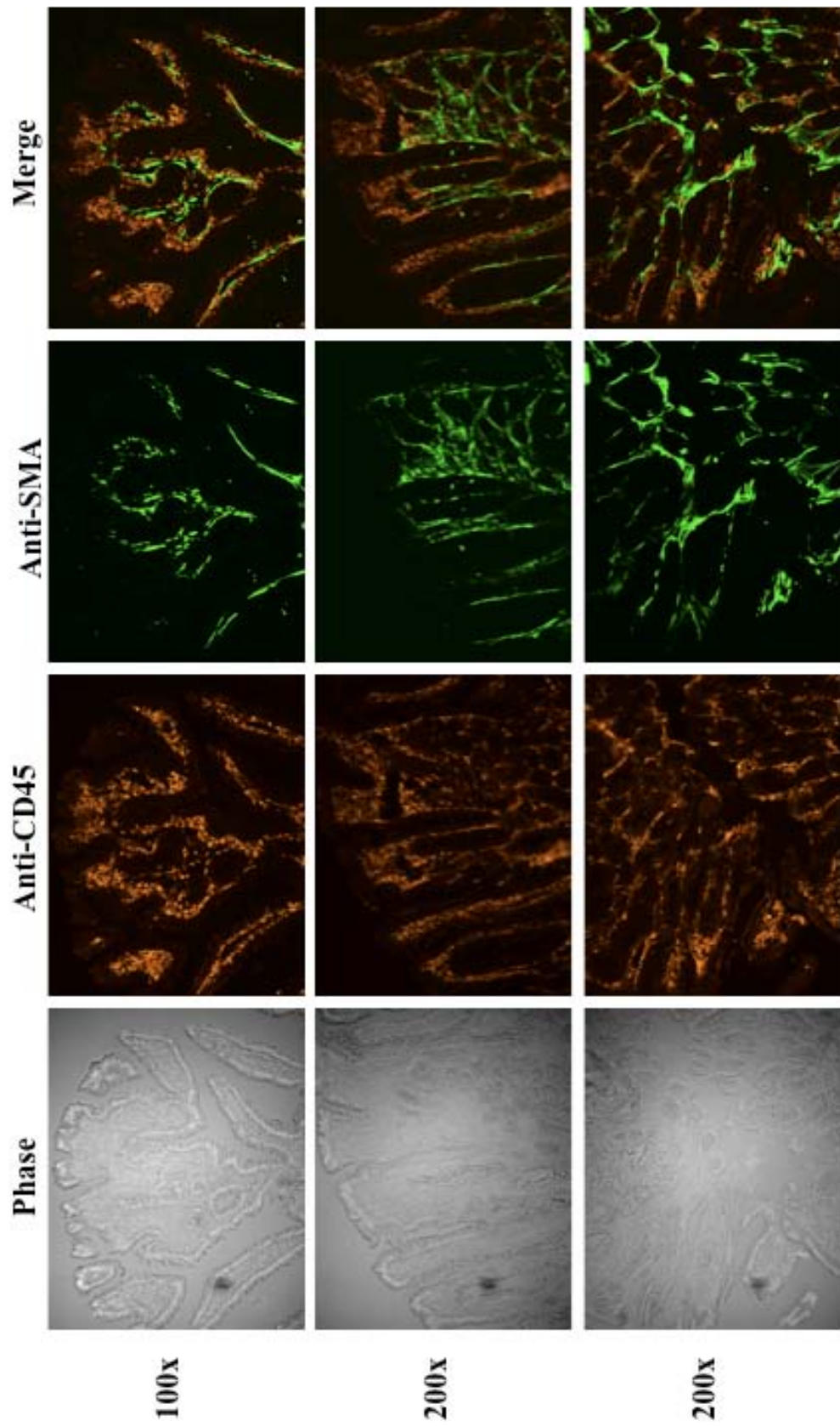Phase   Anti-CD45   Anti-SMA   Merge

100x

200x

200x

98

Figure 4.3. Immunofluorescence of stromal cell subtypes in *Pms2$^{cre/cre}$;Smad4$^{fx/fx}$; RFS-c-Myc^{T58A}* intestinal adenomas. Co-Immunofluorescence of anti-SMA and anti-CD45 on three frozen sections of *Pms2$^{cre/cre}$;Smad4$^{fx/fx}$;RFS-c-Myc^{T58A}* adenomas in the medial small intestine (Jejunum). Image magnifications noted.
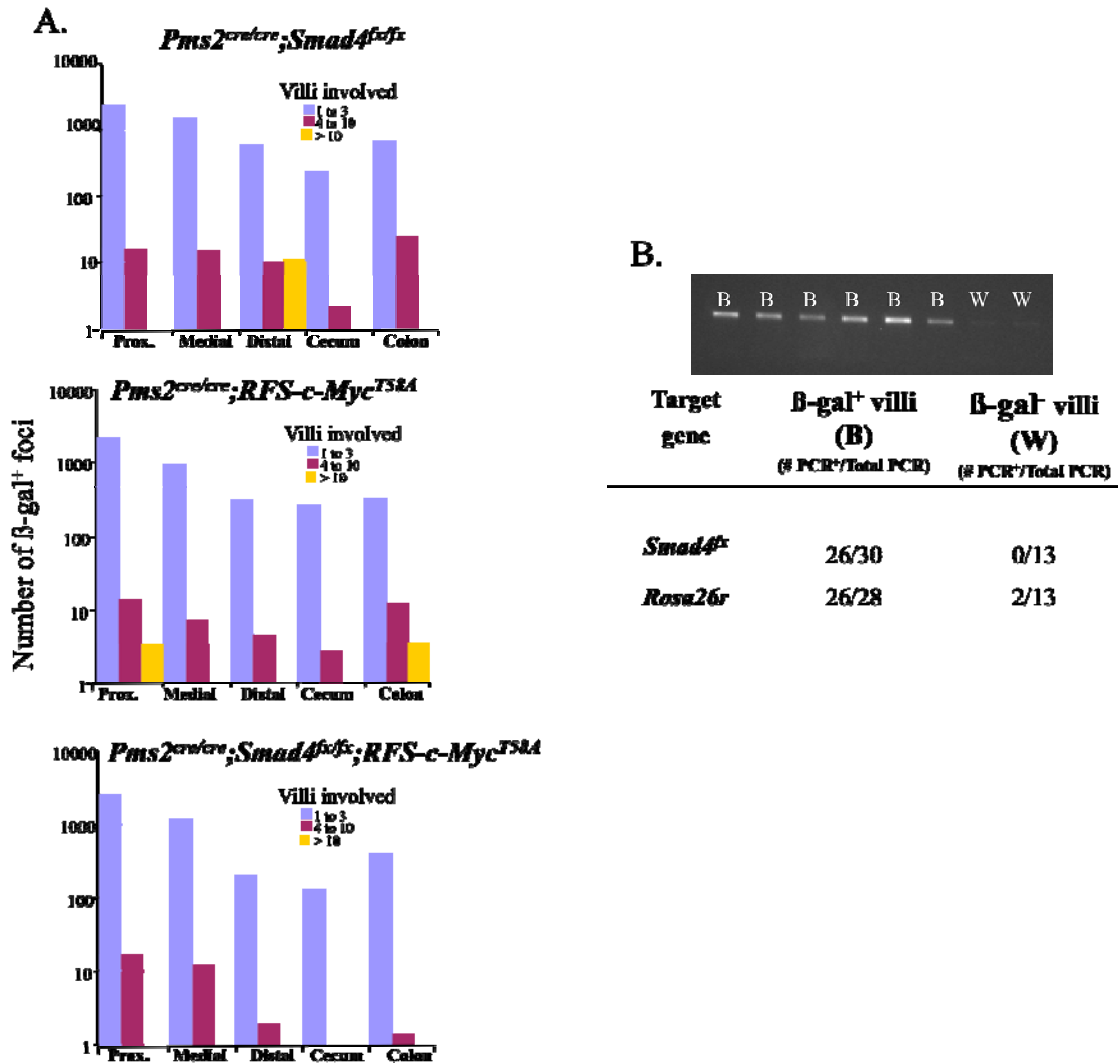
Figure 4.4. Distribution and verification of Cre recombination in intestines of mice. (**A**) Comparison of ß-gal$^+$ foci in each region of intestine in $Pms2^{cre/cre}$;$Smad4^{fx/fx}$, $Pms2^{cre/cre}$;RFS-c-Myc^{T58A}, and $Pms2^{cre/cre}$;$Smad4^{fx/fx}$;RFS-c-Myc^{T58A} mice. Relative size of foci is indicated by number of villi involved. (**B**) Post-Cre recombination PCR of micro-dissected $Pms2^{cre/cre}$;$Smad4^{fx/fx}$;RFS-c-Myc^{T58A} villi. B designates ß-gal$^+$ villi, W designates ß-gal$^-$ villi.
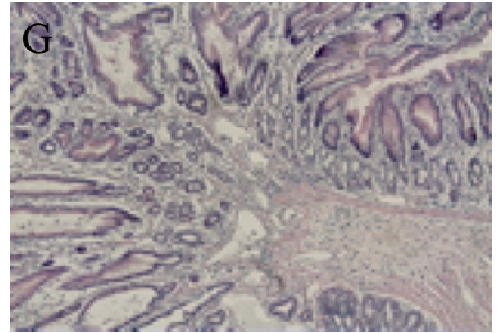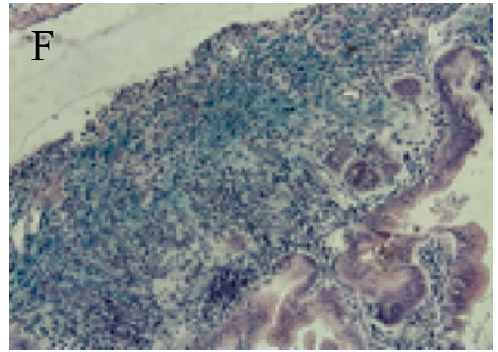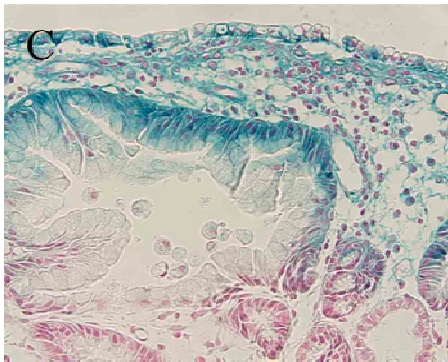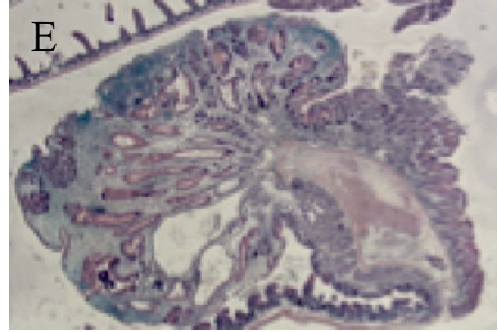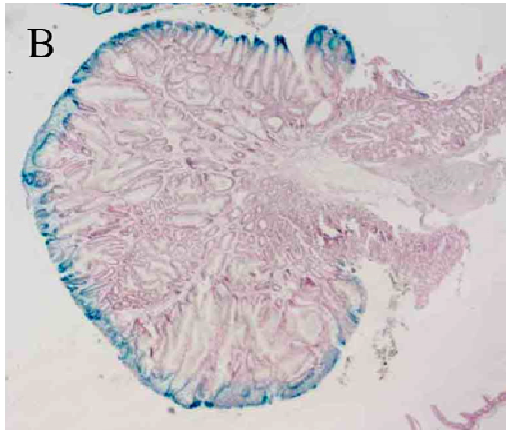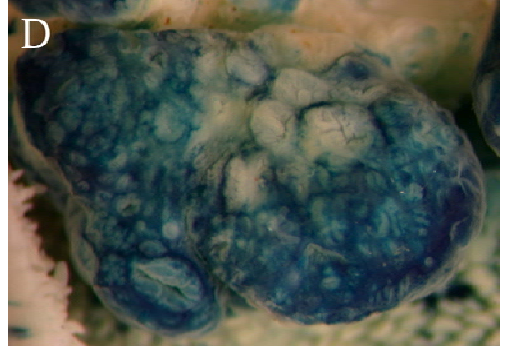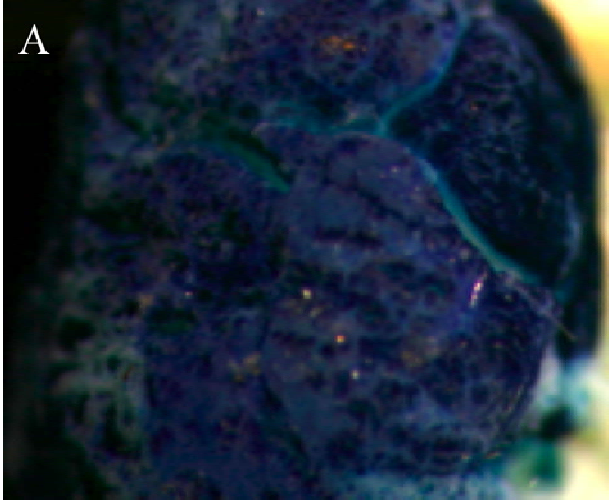
Figure 4.5. Gastric/duodenal adenomas in $Pms2^{cre/cre}$;$Smad4^{fx/fx}$ and $Pms2^{cre/cre}$; $Smad4^{fx/fx}$;RFS-c-Myc^{T58A} mice. Whole mount (**A**) and histological section (**B-C**) of $Pms2^{cre/cre}$;$Smad4^{fx/fx}$ gastric/duodenal adenomas stained with ß-gal on whole mount, nuclear fast red on histological section. Whole mount (**D**) and histological section (**E-G**) of $Pms2^{cre/cre}$;$Smad4^{fx/fx}$;RFS-c-Myc^{T58A} gastric/duodenal adenomas stained with ß-gal on whole mount, hematoxalin and eosin on histological section. Image magnifications as follows: A, D 10x; B, E, 50x; C, F, G, 200x.
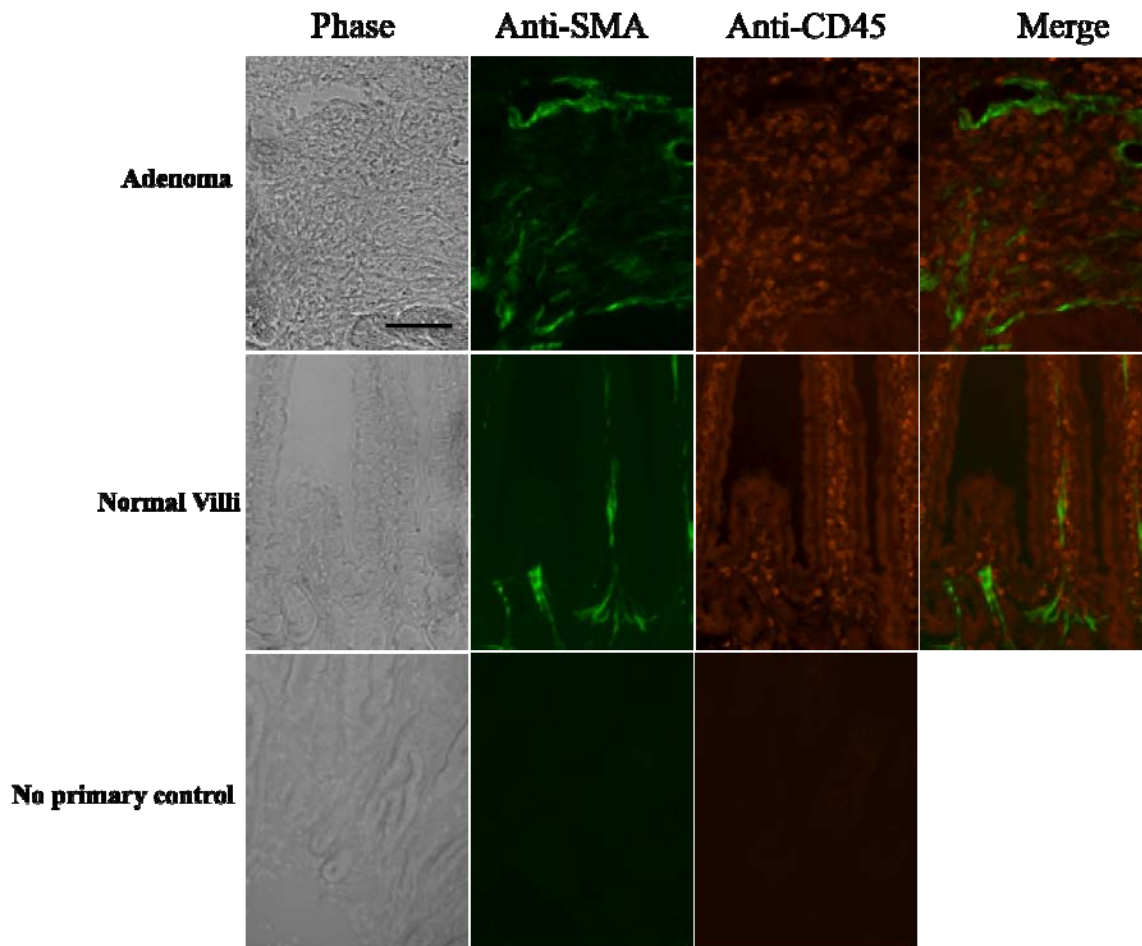
Figure 4.6. Immunofluorescence of stromal cell subtypes in *Pms2$^{cre/cre}$;Smad4$^{fx/fx}$; RFS-c-Myc^{T58A}* gastric/duodenal adenomas and normal villi. Co-Immunofluorescence of anti-SMA and anti-CD45 on frozen sections of gastric/duodenal adenomas and normal villi of *Pms2$^{cre/cre}$;Smad4$^{fx/fx}$;RFS-c-Myc^{T58A}* small intestine. Image magnifications at 100x, scale bar 70 uM.

Chapter 5

Discussion and Future Directions

Discussion and Future Directions

Mouse models have provided vast insight into normal human development and disease processes, particularly the underlying biology of human cancers. The advent of Cre/*lox* technology has greatly facilitated these investigations by restricting expression of mutant tumor suppressors or oncogenes to a particular tissue or at a specific point in time. However, human cancers initially arise from mutations occurring in isolated cells, a manner difficult to recapitulate with standard mouse models. In attempts to create a more accurate model of human tumor initiation, we developed the *Pms2*^{cre} system to facilitate stochastic activation of Cre throughout the life of a mouse. In this thesis I describe and validate the *Pms2*^{cre} system. I subsequently apply *Pms2*^{cre} to investigate the consequence of isolated single target gene disruptions. Finally, I describe a combination of two target genes that resulted in a mouse model of advanced gastric cancer.

The *Pms2*^{cre} system allows random, isolated Cre activation throughout the lifetime of the mouse. Targeting Cre to *Pms2* results in two main advantages. 1) *Pms2* is knocked out, which permits Cre activation to be modulated by MMR status. 2) Cre is under the *Pms2* promoter and can be expressed in most tissues. I characterized Cre activation in the mouse gastrointestinal tract by incorporating a Cre-responsive ß-galactosidase gene. The number of ß-gal$^+$ foci, representing where Cre activation occurred, revealed a gradient of foci, with more in the proximal and fewer in the distal regions of the gastrointestinal tract. The difference in Cre activation may be a consequence of regional differences in stem cell or transient amplifying cell proliferation;

however these possibilities remain to be examined. Additionally, the number of ß-gal$^+$

foci increased with age. Ribbon-like staining was observed on whole-mount and

histological sections of blue-stained crypts from *Pms2$^{cre/cre}$* intestines, a pattern consistent

with Cre activation occurring within the stem cell or long-lived progenitor population.

Quantification of blue-stained foci revealed a 100-fold increase in MMR-deficient

Pms2$^{cre/cre}$ animals compared with MMR-proficient *Pms2$^{cre/+}$* (Figure 2.1J).

I validated our *Pms2^{cre}* system by including a single *loxP*-marked gene. In the

first experiment, we found that including the Cre-activated oncogenic *K-ras^{G12D}* allele

resulted in hyperplasia in the colon, enlarged villi and lung tumors. Interestingly, I

observed large regions of ß-gal$^+$ crypt/villi, suggesting clonal expansion of crypts in

which *K-ras^{G12D}* was expressed (Figure 2.2). The simplest explanation for the larger

regions of staining is that the oncogenic *K-ras^{G12D}* caused increased cellular proliferation

within the crypt and increased crypt fission, resulting in expanded clusters of *K-ras^{G12D}*-

expressing crypts. None of these animals developed any lesions beyond hyperplasia,

suggesting this oncogenic form of *K-ras* is not sufficient to lead to intestinal adenomas.

The Jacks lab performed a similar experiment, limiting *K-ras^{G12D}* expression to the

gastrointestinal epithelia, and observed hyperplasia but no adenomas (Tuveson et al.,

2004), suggesting *K-ras^{G12D}* will only contribute to adenoma formation in cooperation

with other genetic lesions. The ability of oncogenic *K-ras* to act in concert with other

genetic lesions was recently described: activated ß-catenin signaling from loss of *Apc*

requires *K-ras*-dependent proliferation (Phelps et al., 2009).

Pms2^{cre/cre};*LSL-K-ras*^{G12D} — rendering properly:

$Pms2^{cre/cre}$;*LSL-K-ras*^{G12D} mice succumbed to lung tumors at an average age of 5

weeks, suggesting that the oncogenic form of *K-ras* has tissue-specific potency, a similar

result observed with the *K-ras* latent allele (Johnson et al., 2001). The lung-specific

phenotype limits the ability to study this allele in the context of gastrointestinal tumor

formation. However, mutations in *K-ras* are commonly observed in human colon cancers

(Oliveira et al., 2004). Thus, the oncogenic *K-ras* would be instructive when combined

with a stochastic model system. To investigate *K-ras* in combination with other target

alleles, the lung phenotype must be restricted or minimized. Engineering our 12A-*cre* to

a promoter specifically expressed within intestinal-epithelia, such as *Villin* (Madison et

al., 2002), will permit exploration of oncogenic *K-ras* solely within a gastrointestinal

setting. Ultimately, onocgenic *K-ras* could be combined with other target genes to

identify a genetic pathway leading to *K-ras*-dependent adenoma formation.

I next examined the consequence in the intestinal epithelia of isolated disruption

of the tumor suppressor gene *TgfβrII*. In contrast the large stained regions seen with

activated *K-ras*, disrupting *TgfβrII* in isolated crypts resulted in a modified ß-

galactosidase expression pattern, with a reduced number of ß-gal$^+$ cells in villi and Paneth

cell regions. The altered staining pattern suggested reducing *TgfβrII* placed cells at a

competitive disadvantage, and thus *TgfβrII* contributed to homeostasis within the adult

intestine epithelia. The competitive disadvantage is strikingly similar to the cell

competition phenomena described in *Drosophila melanogaster* where heterozygous

clones of *Minute*, *Myc*, and *Tgfβr* are selectively lost (Tyler et al., 2007). I also observed

increased apoptosis within the *TgfβrII*-disrupted crypts, which may partially account for

the lack of competitive advantage. Additionally, I noted haploinsufficiency for *TgfβrII* with both the altered staining patterns and increased apoptosis. These data agree with other mouse experiments and with human colon cancer studies and suggest that mutation at *TgfβrII* is not a productive first hit for tumorigenesis (Grady et al., 1998; Jones et al., 2008). Finally, the *TgfβrII* results demonstrate a novel example of cell competition in mammals.

When *TgfβrII* was disrupted, crypts harboring apoptotic cells were increased, suggesting that *Tgfβ* signaling is involved in regulation of apoptosis within the crypt. Apoptosis occurs in two locations along the crypt/villus axis: within the crypt, in a caspase-3 dependent manner (Marshman et al., 2001), and at the tip of the villi as cells are extruded into the lumen (Hall et al., 1994; Potten, 1998). Signals regulating apoptosis within the crypt are largely unknown (Watson and Pritchard, 2000). Colon crypts of *Bcl2*$^{-/-}$ mice show increased basal levels of apoptosis, although the morphology of the colon is normal (Merritt et al., 1995). Acute loss of *Chk1* within the crypt results in a dramatic increase in apoptosis in transient amplifying cells (Greenow et al., 2009). My results add Tgfß signaling to those pathways regulating apoptosis within the intestinal crypt.

The increased apoptosis seen within the transient amplifying cell population may also suggest why mutation of *TgfβrII* is not a productive first hit in tumor initiation; *TgfβrII*-disrupted cells are lost before they can accumulate additional mutations needed to become tumors. Counteracting the increased apoptosis of *TgfβrII*^{fx} by combining a

disruption to anti-apoptosis target genes, such as $Tp53^{fx}$ (Jonkers et al., 2001), could potentially bypass the apoptotic blockade and permit tumor initiation. Recently, a similar experiment showed suppression of apoptosis in an Apc^{1638N} mouse model led to increased tumor multiplicity and aggressiveness (Leung et al., 2008). It should be noted, however, that loss of *TgfβrII* in human CRC development is found to be a late-occuring event (Grady et al., 1998). As such, loss of *TgfβrII* occurs in the context of advanced clonal evolution of the tumor and associated tumor-initiated fibroblast changes in the surrounding stroma; a dissimilar environment from the isolated ablation of *TgfβrII* in normal mouse epithelia in our model. Tumors developing from a $Pms2^{cre/cre};TgfβrII^{fx}$ background therefore may have limited biological parallels with human CRC development, and is a common limitation with mouse models of human cancers.

One possibility yet to be explored is that the reduced staining patterns along the crypt/villi axis indicates reduction of *TgfβrII* alters migration of differentiating cells. Tgfβ signaling regulates migration of intestinal epithelial cells in wound models (Ciacci et al., 1993). Similarly, lowering Tgfß responsiveness by ablation of *Smad2* delayed wound healing in part through cell migration defects (Hosokawa et al., 2005). In a similar experiment, the Clevers lab demonstrated migration defects in the Paneth cell population by generating targeted deletion mouse strains of the *Ephrin* genes *EphB2* and *EphB3*, critical regulators of Paneth cell differentiation (Batlle et al., 2002). One interesting approach to investigate migration defects in isolated *TgfβrII*-disrupted cells would be to create a wound in the intestinal epithelia (Owen et al., 2008) and determine how much of the wound is composed of ß-gal+, *TgfβrII*-disrupted cells.

The final experiment investigated stochastically activated expression of a stabilized form of *c-Myc* and inactivated *Smad4* alone, or in combination. *Pms2$^{cre/cre}$;RFS-c-Myc^{T58A}* mice showed no change in tumor onset or type. In agreement with other model systems, *Pms2$^{cre/cre}$;Smad4$^{fx/fx}$* mice developed gastric/duodenal adenomas at a fairly advanced age. Significantly, combining both target genes within the same mouse, *Pms2$^{cre/cre}$;Smad4$^{fx/fx}$;RFS-c-Myc^{T58A}*, resulted in 100% of mice developing gastrointestinal adenomas at an earlier age, with most presenting with gastric/duodenal adenomas and a smaller number developing adenomas in the small intestine. Further, the gastric/duodenal adenomas of *Pms2$^{cre/cre}$;Smad4$^{fx/fx}$;RFS-c-Myc^{T58A}* mice were more aggressive than those in *Pms2$^{cre/cre}$;Smad4$^{fx/fx}$* mice.

Reporter staining revealed a high degree of Cre activation within stromal cells of *Pms2$^{cre/cre}$;Smad4$^{fx/fx}$;RFS-c-Myc^{T58A}* gastric/duodenal adenomas, suggesting the initiating cell type of the epithelial tumors was within the stroma. Immunofluorescence of *Pms2$^{cre/cre}$;Smad4$^{fx/fx}$;RFS-c-Myc^{T58A}* adenomas indicated an expanded number of bone-marrow-derived CD45$^+$ cells. To specifically determine whether stromal cells were the only cells in which Cre was activated, I isolated stromal and epithelial cells within tumor sections via laser capture micro-dissection followed by PCR specific for Cre recombination at the *Smad4* locus. Results from this experiment were inconclusive, as all laser-captured sample was positive for the recombined *Smad4* allele, regardless of tissue type or reporter staining pattern. The likeliest explanation is a combination of cross-contamination of the laser-captured cells and sensitive PCR conditions. Conclusive

proof of the tumor-initiating cell type could be obtained from placing the 12A-cre under

epithelial- and stromal-cell specific promoters, combining *Smad4^{fx};RFS-c-Myc^{T58A}*, and

comparing resulting tumor development.

Interestingly, I did not observed gastric/duodenal adenomas development in

Smad4^{fx};RFS-c-Myc^{T58A} mice heterozygous for *Smad4*. *Smad4* haploinsufficiency is

seen in JPS patients (Howe et al., 1998). Additionally, *Smad4$^{+/-}$* embryonic mouse

fibroblasts have protein levels reduced by 50% and intermediate transcriptional response

to Tgfß and BMP ligand (Alberici et al., 2008), two concrete indicators of

haploinsufficiency. Several others have reported the gastric adenoma phenotype in mice

heterozygous for *Smad4* (Hohenstein et al., 2003; Takaku et al., 1999). The tumors were

of later onset and showed variable amounts of LOH for *Smad4*, suggesting additional

mechanisms of tumor initiation. In contrast, I did not observe gastric/duodenal adenoma

development in *Pms2$^{cre/cre}$;Smad4$^{fx/+}$* or *Pms2$^{cre/cre}$;Smad4$^{fx/+}$;RFS-c-Myc^{T58A}*. With the

exception of the original *Smad4* deletion mouse, each of the *Smad4* models is a different

truncation mutation. It is assumed no protein product comes from the truncated gene;

however, it is possible that the subtle sequence differences alter transcriptional activity

surrounding the *Smad4* locus, thus resulting in the phenotypic differences.

Finally, the invasive phenotype of *Pms2$^{cre/cre}$;Smad4$^{fx/fx}$;RFS-c-Myc^{T58A}*

gastric/duodenal adenomas suggests that these tumors have metastatic capabilities. One

hallmark of metastasis is epithelial-to-mesenchymal transition (EMT) (Thiery, 2002), a

process known to be driven by changes to Tgfβ signaling (Nawshad et al., 2005; Zavadil

and Bottinger, 2005). I probed for EMT markers with immunohistochemistry and noted in at least one tumor an increase, within the stromal cell population, in E-cadherin (data not shown), an epithelial marker lost during EMT (Peinado et al., 2004) and induced by Smad4 (Muller et al., 2002). I did not find evidence of EMT with other markers, including the stromal cell markers vimentin and fibronectin, and the transcription factors slug, snail and twist (De Craene et al., 2005; Yang et al., 2004). However, expression changes in these proteins may be too subtle to detect through immunohistochemical techniques. An alternative approach would be to examine RNA expression of EMT markers through *in situ* hybridization on tissue sections or RT-PCR on laser-captured sections. The ultimate test of metastatic capacity would be intrasplenic transplantation experiments (Furukawa et al., 1993), where tumor cells harvested from *Pms2$^{cre/cre}$;Smad4$^{fx/fx}$;RFS-c-Myc^{T58A}* mice, injected into the spleen, seed tumors within the liver. I attempted this experiment with the final mouse in the *Pms2$^{cre/cre}$;Smad4$^{fx/fx}$;RFS-c-Myc^{T58A}* cohort, however all transplanted mice died from graft-versus-host disease. It would be valuable to repeat this experiment once we improve transplantation techniques.

Within this thesis I have characterized a stochastic Cre system, and explored the consequence of isolated disruption of targeted tumor suppressor genes and oncogenes alone and in combination. The *Pms2^{cre}* system represents an improved model of human cancer initiation due to the relative ease in which multiple target genes can be combined within the same animal. A central feature of the stochastic *Pms2^{cre}* system is that the frequency of Cre activation can be regulated by DNA mismatch repair (MMR) status;

112

low levels of Cre activation occur in MMR-proficient $Pms2^{cre/+}$ whereas Cre expression increases approximately 100-fold in MMR-deficient $Pms2^{cre/cre}$ mice. Potent combinations of tumor suppressor and oncogenes can be combined in a $Pms2^{cre/+}$ background; then the mice can be interbred to generate $Pms2^{cre/cre}$ mice to facilitate tumor development. The most enlightening experiment with the $Pms2^{cre}$ system to investigate target gene combinations implicated in human colon cancer would be a combination of the main landscaper genes (Wood et al., 2007) *Apc*, *K-ras*, and *Tp53*. This combination would be particularly potent, thus ideally maintaining the final experimental mouse, as Pms2cre/+ would reduce the frequency of Cre activation. Through this and other combinations of target genes, we can thus ask the ultimate question of what combination or combinations of target genes result in advanced adenomas.

Appendix 1: Contributions of Authors to Figures

The contribution of each author to data presented in the figures of this thesis are as follows:

Figure 2.1A: Jen-Lan Tsao created the 12A-Cre cassette. Sandra Dudley created the $Pms2^{cre}$ targeting construct. Chimeric mice were produced by the Transgenic Animal Core facility at OHSU.

Figure 2.1B – I: Mouse breeding, genotyping, sacrificing and x-gal staining was performed by Ashleigh Miller.

Figure 2.1J, 2.2A: The number of ß-gal$^+$ foci was quantified by Ashleigh Miller.

Figure 2.2B: Mouse breeding, genotyping, sacrifice and x-gal staining was performed by Ashleigh Miller.

Figure 2.3A: The total number of ß-gal$^+$ foci as a function of age was calculated by Ashleigh Miller.

Figure 2.3B: Micro-dissection of individual villi and post-cre recombination PCR was performed by Ashleigh Miller.

Figure 3.1: Animal breeding, monitoring, and sacrifice were performed by Ashleigh Miller.

Figure 3.2: X-gal staining and quantification of ß-gal$^+$ foci was performed by Ashleigh Miller.

Figure 3.3A-H: Whole-mount imaging was performed by Ashleigh Miller. Histological sections were cut by OHSU Pathology Core services. H&E staining and all microscopy was performed by Ashleigh Miller.

Table 3.1: Quantificaiton of ß-galactosidase staining patterns was performed by Ashleigh Miller.

Table 3.2: Quantificaiton of ß-galactosidase staining patterns was performed by Ashleigh Miller.

Figure 3.4A,B: Percentages of ß-gal staining patterns were quantified by Ashleigh Miller.

Figure 3.5A: Histological sections were cut by OHSU Pathology Core services. BrDU immunohistochemistryy and counterstain was performed by Ashleigh Miller. Microscopy was performed by Ashleigh Miller.

Figure 3.5B: Quantification of BrDU+ cells was performed by Ashleigh Miller.

Figure 3.6A: Histological sections were cut by OHSU Pathology Core services. ApopTag immunohistochemistry and counterstain was performed by Ashleigh Miller. Microscopy was performed by Ashleigh Miller.

Fiture 3.6B: Quantification of crypts harboring apoptotic cells was performed by Ashleigh Miller.

Table 3.3: Quantification of crypts harboring apoptotic cells was performed by Ashleigh Miller.

Figure 4.1: Animal breeding, monitoring, and sacrifice were performed by Ashleigh Miller.

Table 4.1: Tumor identification was performed by Ashleigh Miller.

Figure 4.2: X-gal staining was performed by Ashleigh Miller. Histological tissue sections were cut by Ashleigh Miller. Images were taken by Ashleigh Miller.

Figure 4.3. Histological sections, immunofluorescence, and microscopy was performed by Ashleigh Miller.

Figure. 4.4A: The number of ß-gal$^+$ foci was quantified by Ashleigh Miller.

Figure 4.4B: Post-cre recombination PCR for *Smad4* was performed by Ashleigh Miller.

Post-cre recombination PCR for *Rosa26r* was performed by Sandra Dudley.

Figure 4.5 – Histological sections were cut by OHSU Pathology Core serviced. X-gal,

H&E, nuclear fast red staining and microscopy was performed by Ashleigh Miller.

Figure 4.6: Histological sections, immunofluorescence, and microscopy was performed

by Ashleigh Miller.

References

Abdollah, S., Macias-Silva, M., Tsukazaki, T., Hayashi, H., Attisano, L., and Wrana, J.L. (1997). TbetaRI phosphorylation of Smad2 on Ser465 and Ser467 is required for Smad2-Smad4 complex formation and signaling. J Biol Chem *272*, 27678-27685.

Abremski, K., Hoess, R., and Sternberg, N. (1983). Studies on the properties of P1 site-specific recombination: evidence for topologically unlinked products following recombination. Cell *32*, 1301-1311.

Adrouny, A.R. (2002). Understanding Colon Cnacer, Illustrated edn (University Press of Mississippi).

Akhurst, R.J. (2004). TGF beta signaling in health and disease. Nat Genet *36*, 790-792.

Akyol, A., Hinoi, T., Feng, Y., Bommer, G.T., Glaser, T.M., and Fearon, E.R. (2008). Generating somatic mosaicism with a Cre recombinase-microsatellite sequence transgene. Nat Methods *5*, 231-233.

Alberici, P., Gaspar, C., Franken, P., Gorski, M.M., de Vries, I., Scott, R.J., Ristimaki, A., Aaltonen, L.A., and Fodde, R. (2008). Smad4 haploinsufficiency: a matter of dosage. Pathogenetics *1*, 2.

Alitalo, K., Schwab, M., Lin, C.C., Varmus, H.E., and Bishop, J.M. (1983).
Homogeneously staining chromosomal regions contain amplified copies of an abundantly
expressed cellular oncogene (c-myc) in malignant neuroendocrine cells from a human
colon carcinoma. Proc Natl Acad Sci U S A *80*, 1707-1711.

Almoguera, C., Shibata, D., Forrester, K., Martin, J., Arnheim, N., and Perucho, M.
(1988). Most human carcinomas of the exocrine pancreas contain mutant c-K-ras genes.
Cell *53*, 549-554.

Andreyev, H.J., Norman, A.R., Cunningham, D., Oates, J.R., and Clarke, P.A. (1998).
Kirsten ras mutations in patients with colorectal cancer: the multicenter "RASCAL"
study. J Natl Cancer Inst *90*, 675-684.

Avery, A., Paraskeva, C., Hall, P., Flanders, K.C., Sporn, M., and Moorghen, M. (1993).
TGF-beta expression in the human colon: differential immunostaining along crypt
epithelium. Br J Cancer *68*, 137-139.

Bahram, F., von der Lehr, N., Cetinkaya, C., and Larsson, L.G. (2000). c-Myc hot spot
mutations in lymphomas result in inefficient ubiquitination and decreased proteasome-
mediated turnover. Blood *95*, 2104-2110.

Baker, K., Chong, G., Foulkes, W.D., and Jass, J.R. (2006). Transforming growth factor-
beta pathway disruption and infiltration of colorectal cancers by intraepithelial
lymphocytes. Histopathology *49*, 371-380.

Baker, S.M., Bronner, C.E., Zhang, L., Plug, A.W., Robatzek, M., Warren, G., Elliott, E.A., Yu, J., Ashley, T., Arnheim, N.*, et al.* (1995). Male mice defective in the DNA mismatch repair gene PMS2 exhibit abnormal chromosome synapsis in meiosis. Cell *82*, 309-319.

Baker, S.M., Plug, A.W., Prolla, T.A., Bronner, C.E., Harris, A.C., Yao, X., Christie, D.M., Monell, C., Arnheim, N., Bradley, A.*, et al.* (1996). Involvement of mouse Mlh1 in DNA mismatch repair and meiotic crossing over. Nat Genet *13*, 336-342.

Barker, N., Ridgway, R.A., van Es, J.H., van de Wetering, M., Begthel, H., van den Born, M., Danenberg, E., Clarke, A.R., Sansom, O.J., and Clevers, H. (2009). Crypt stem cells as the cells-of-origin of intestinal cancer. Nature *457*, 608-611.

Barker, N., van Es, J.H., Kuipers, J., Kujala, P., van den Born, M., Cozijnsen, M., Haegebarth, A., Korving, J., Begthel, H., Peters, P.J.*, et al.* (2007). Identification of stem cells in small intestine and colon by marker gene Lgr5. Nature *449*, 1003-1007.

Barnes, T., Kim, W.C., Mantha, A.K., Kim, S.E., Izumi, T., Mitra, S., and Lee, C.H. (2009). Identification of Apurinic/apyrimidinic endonuclease 1 (APE1) as the endoribonuclease that cleaves c-myc mRNA. Nucleic Acids Res.

Barrett, M.T., Schutte, M., Kern, S.E., and Reid, B.J. (1996). Allelic loss and mutational analysis of the DPC4 gene in esophageal adenocarcinoma. Cancer Res *56*, 4351-4353.

Batlle, E., Henderson, J.T., Beghtel, H., van den Born, M.M., Sancho, E., Huls, G., Meeldijk, J., Robertson, J., van de Wetering, M., Pawson, T., *et al.* (2002). Beta-catenin and TCF mediate cell positioning in the intestinal epithelium by controlling the expression of EphB/ephrinB. Cell *111*, 251-263.

Bhowmick, N.A., Chytil, A., Plieth, D., Gorska, A.E., Dumont, N., Shappell, S., Washington, M.K., Neilson, E.G., and Moses, H.L. (2004). TGF-beta signaling in fibroblasts modulates the oncogenic potential of adjacent epithelia. Science *303*, 848-851.

Biswas, S., Chytil, A., Washington, K., Romero-Gallo, J., Gorska, A.E., Wirth, P.S., Gautam, S., Moses, H.L., and Grady, W.M. (2004). Transforming growth factor beta receptor type II inactivation promotes the establishment and progression of colon cancer. Cancer Res *64*, 4687-4692.

Bjerknes, M., and Cheng, H. (1999). Clonal analysis of mouse intestinal epithelial progenitors. Gastroenterology *116*, 7-14.

Bjerknes, M., and Cheng, H. (2005). Gastrointestinal stem cells. II. Intestinal stem cells. Am J Physiol Gastrointest Liver Physiol *289*, G381-387.

Blackwood, E.M., and Eisenman, R.N. (1991). Max: a helix-loop-helix zipper protein that forms a sequence-specific DNA-binding complex with Myc. Science *251*, 1211-1217.

Blumenthal, G.M., and Dennis, P.A. (2008). PTEN hamartoma tumor syndromes. Eur J Hum Genet *16*, 1289-1300.

Boguski, M.S., and McCormick, F. (1993). Proteins regulating Ras and its relatives. Nature *366*, 643-654.

Bos, J.L. (1989). ras oncogenes in human cancer: a review. Cancer Res *49*, 4682-4689.

Bronner, C.E., Baker, S.M., Morrison, P.T., Warren, G., Smith, L.G., Lescoe, M.K., Kane, M., Earabino, C., Lipford, J., Lindblom, A.*, et al.* (1994). Mutation in the DNA mismatch repair gene homologue hMLH1 is associated with hereditary non-polyposis colon cancer. Nature *368*, 258-261.

Burke, R., and Basler, K. (1996). Dpp receptors are autonomously required for cell proliferation in the entire developing Drosophila wing. Development *122*, 2261-2269.

Cairnie, A.B., Lamerton, L.F., and Steel, G.G. (1965a). Cell proliferation studies in the intestinal epithelium of the rat. I. Determination of the kinetic parameters. Exp Cell Res *39*, 528-538.

Cairnie, A.B., Lamerton, L.F., and Steel, G.G. (1965b). Cell proliferation studies in the intestinal epithelium of the rat. II. Theoretical aspects. Exp Cell Res *39*, 539-553.

Calabrese, P., Tavare, S., and Shibata, D. (2004). Pretumor progression: clonal evolution of human stem cell populations. Am J Pathol *164*, 1337-1346.

Calvert, R., and Pothier, P. (1990). Migration of fetal intestinal intervillous cells in neonatal mice. Anat Rec *227*, 199-206.

Chang, E.H., Gonda, M.A., Ellis, R.W., Scolnick, E.M., and Lowy, D.R. (1982). Human genome contains four genes homologous to transforming genes of Harvey and Kirsten murine sarcoma viruses. Proc Natl Acad Sci U S A *79*, 4848-4852.

Chen, X., Halberg, R.B., Burch, R.P., and Dove, W.F. (2008). Intestinal adenomagenesis involves core molecular signatures of the epithelial-mesenchymal transition. J Mol Histol *39*, 283-294.

Cheng, H., and Bjerknes, M. (1985). Whole population cell kinetics and postnatal development of the mouse intestinal epithelium. Anat Rec *211*, 420-426.

Cheng, H., and Leblond, C.P. (1974a). Origin, differentiation and renewal of the four main epithelial cell types in the mouse small intestine. I. Columnar cell. Am J Anat *141*, 461-479.

Cheng, H., and Leblond, C.P. (1974b). Origin, differentiation and renewal of the four main epithelial cell types in the mouse small intestine. III. Entero-endocrine cells. Am J Anat *141*, 503-519.

Cheng, H., and Leblond, C.P. (1974c). Origin, differentiation and renewal of the four main epithelial cell types in the mouse small intestine. V. Unitarian Theory of the origin of the four epithelial cell types. Am J Anat *141*, 537-561.

Chittenden, T.W., Howe, E.A., Culhane, A.C., Sultana, R., Taylor, J.M., Holmes, C., and Quackenbush, J. (2008). Functional classification analysis of somatically mutated genes in human breast and colorectal cancers. Genomics *91*, 508-511.

Chytil, A., Magnuson, M.A., Wright, C.V., and Moses, H.L. (2002). Conditional inactivation of the TGF-beta type II receptor using Cre:Lox. Genesis *32*, 73-75.

Ciacci, C., Lind, S.E., and Podolsky, D.K. (1993). Transforming growth factor beta regulation of migration in wounded rat intestinal epithelial monolayers. Gastroenterology *105*, 93-101.

Clarke, A.R. (2007). Cancer genetics: mouse models of intestinal cancer. Biochem Soc Trans *35*, 1338-1341.

Clevers, H. (2006). Wnt/beta-catenin signaling in development and disease. Cell *127*, 469-480.

Colicelli, J. (2004). Human RAS superfamily proteins and related GTPases. Sci STKE *2004*, RE13.

Coller, H.A., Grandori, C., Tamayo, P., Colbert, T., Lander, E.S., Eisenman, R.N., and Golub, T.R. (2000). Expression analysis with oligonucleotide microarrays reveals that MYC regulates genes involved in growth, cell cycle, signaling, and adhesion. Proc Natl Acad Sci U S A *97*, 3260-3265.

Collins, S., and Groudine, M. (1982). Amplification of endogenous myc-related DNA sequences in a human myeloid leukaemia cell line. Nature *298*, 679-681.

Cowling, V.H., and Cole, M.D. (2007). E-cadherin repression contributes to c-Myc-induced epithelial cell transformation. Oncogene *26*, 3582-3586.

Cowling, V.H., D'Cruz, C.M., Chodosh, L.A., and Cole, M.D. (2007). c-Myc transforms human mammary epithelial cells through repression of the Wnt inhibitors DKK1 and SFRP1. Mol Cell Biol *27*, 5135-5146.

Crosnier, C., Stamataki, D., and Lewis, J. (2006). Organizing cell renewal in the intestine: stem cells, signals and combinatorial control. Nat Rev Genet *7*, 349-359.

Dalla-Favera, R., Bregni, M., Erikson, J., Patterson, D., Gallo, R.C., and Croce, C.M. (1982). Human c-myc onc gene is located on the region of chromosome 8 that is translocated in Burkitt lymphoma cells. Proc Natl Acad Sci U S A *79*, 7824-7827.

Dang, C.V., O'Donnell, K.A., Zeller, K.I., Nguyen, T., Osthus, R.C., and Li, F. (2006). The c-Myc target gene network. Semin Cancer Biol *16*, 253-264.

Day, D.W., and Morson, B.C. (1978). The adenoma-carcinoma sequence. Major Probl Pathol *10*, 58-71.

de Caestecker, M. (2004). The transforming growth factor-beta superfamily of receptors. Cytokine Growth Factor Rev *15*, 1-11.

De Craene, B., Gilbert, B., Stove, C., Bruyneel, E., van Roy, F., and Berx, G. (2005). The transcription factor snail induces tumor cell invasion through modulation of the epithelial cell differentiation program. Cancer Res *65*, 6237-6244.

de la Cova, C., Abril, M., Bellosta, P., Gallant, P., and Johnston, L.A. (2004). Drosophila myc regulates organ size by inducing cell competition. Cell *117*, 107-116.

de Silva, D.C., and Fernando, R. (1998). Familial adenomatous polyposis. Ceylon Med J *43*, 99-105.

Der, C.J., Krontiris, T.G., and Cooper, G.M. (1982). Transforming genes of human bladder and lung carcinoma cell lines are homologous to the ras genes of Harvey and Kirsten sarcoma viruses. Proc Natl Acad Sci U S A *79*, 3637-3640.

Desch, C.E., Benson, A.B., 3rd, Somerfield, M.R., Flynn, P.J., Krause, C., Loprinzi, C.L., Minsky, B.D., Pfister, D.G., Virgo, K.S., and Petrelli, N.J. (2005). Colorectal cancer surveillance: 2005 update of an American Society of Clinical Oncology practice guideline. J Clin Oncol *23*, 8512-8519.

Edelmann, W., Yang, K., Umar, A., Heyer, J., Lau, K., Fan, K., Liedtke, W., Cohen, P.E., Kane, M.F., Lipford, J.R.*, et al.* (1997). Mutation in the mismatch repair gene Msh6 causes cancer susceptibility. Cell *91*, 467-477.

Erisman, M.D., Rothberg, P.G., Diehl, R.E., Morse, C.C., Spandorfer, J.M., and Astrin, S.M. (1985). Deregulation of c-myc gene expression in human colon carcinoma is not accompanied by amplification or rearrangement of the gene. Mol Cell Biol *5*, 1969-1976.

Erisman, M.D., Scott, J.K., Watt, R.A., and Astrin, S.M. (1988). The c-myc protein is constitutively expressed at elevated levels in colorectal carcinoma cell lines. Oncogene *2*, 367-378.

Fearon, E.R., and Vogelstein, B. (1990). A genetic model for colorectal tumorigenesis. Cell *61*, 759-767.

Feng, X.H., and Derynck, R. (2005). Specificity and versatility in tgf-beta signaling through Smads. Annu Rev Cell Dev Biol *21*, 659-693.

Fernandez, P.C., Frank, S.R., Wang, L., Schroeder, M., Liu, S., Greene, J., Cocito, A., and Amati, B. (2003). Genomic targets of the human c-Myc protein. Genes Dev *17*, 1115-1129.

Fishel, R., Lescoe, M.K., Rao, M.R., Copeland, N.G., Jenkins, N.A., Garber, J., Kane, M., and Kolodner, R. (1993). The human mutator gene homolog MSH2 and its association with hereditary nonpolyposis colon cancer. Cell *75*, 1027-1038.

Fodde, R., Edelmann, W., Yang, K., van Leeuwen, C., Carlson, C., Renault, B., Breukel, C., Alt, E., Lipkin, M., Khan, P.M.*, et al.* (1994). A targeted chain-termination mutation in the mouse Apc gene results in multiple intestinal tumors. Proc Natl Acad Sci U S A *91*, 8969-8973.

Fodde, R., and Khan, P.M. (1995). Genotype-phenotype correlations at the adenomatous polyposis coli (APC) gene. Crit Rev Oncog *6*, 291-303.

Furukawa, T., Kubota, T., Watanabe, M., Nishibori, H., Kuo, T.H., Saikawa, Y., Kase, S., Tanino, H., Teramoto, T., Ishibiki, K.*, et al.* (1993). A suitable model for experimental liver metastasis of human colon cancer xenografts using mice with severe combined immunodeficiency. J Surg Oncol *52*, 64-67.

Giardiello, F.M., Brensinger, J.D., and Petersen, G.M. (2001). AGA technical review on hereditary colorectal cancer and genetic testing. Gastroenterology *121*, 198-213.

Grady, W.M., Myeroff, L.L., Swinler, S.E., Rajput, A., Thiagalingam, S., Lutterbaugh, J.D., Neumann, A., Brattain, M.G., Chang, J., Kim, S.J.*, et al.* (1999). Mutational inactivation of transforming growth factor beta receptor type II in microsatellite stable colon cancers. Cancer Res *59*, 320-324.

Grady, W.M., Rajput, A., Myeroff, L., Liu, D.F., Kwon, K., Willis, J., and Markowitz, S. (1998). Mutation of the type II transforming growth factor-beta receptor is coincident with the transformation of human colon adenomas to malignant carcinomas. Cancer Res *58*, 3101-3104.

Grandori, C., Cowley, S.M., James, L.P., and Eisenman, R.N. (2000). The Myc/Max/Mad network and the transcriptional control of cell behavior. Annu Rev Cell Dev Biol *16*, 653-699.

Greenow, K.R., Clarke, A.R., and Jones, R.H. (2009). Chk1 deficiency in the mouse small intestine results in p53-independent crypt death and subsequent intestinal compensation. Oncogene *28*, 1443-1453.

Gregory, M.A., and Hann, S.R. (2000). c-Myc proteolysis by the ubiquitin-proteasome pathway: stabilization of c-Myc in Burkitt's lymphoma cells. Mol Cell Biol *20*, 2423-2435.

Gregory, M.A., Qi, Y., and Hann, S.R. (2003). Phosphorylation by glycogen synthase kinase-3 controls c-myc proteolysis and subnuclear localization. J Biol Chem *278*, 51606-51612.

Groden, J., Thliveris, A., Samowitz, W., Carlson, M., Gelbert, L., Albertsen, H., Joslyn, G., Stevens, J., Spirio, L., Robertson, M.*, et al.* (1991). Identification and characterization of the familial adenomatous polyposis coli gene. Cell *66*, 589-600.

Hahm, K.B., Lee, K.M., Kim, Y.B., Hong, W.S., Lee, W.H., Han, S.U., Kim, M.W., Ahn, B.O., Oh, T.Y., Lee, M.H.*, et al.* (2002). Conditional loss of TGF-beta signalling leads to increased susceptibility to gastrointestinal carcinogenesis in mice. Aliment Pharmacol Ther *16 Suppl 2*, 115-127.

Hahn, S.A., Schutte, M., Hoque, A.T., Moskaluk, C.A., da Costa, L.T., Rozenblum, E., Weinstein, C.L., Fischer, A., Yeo, C.J., Hruban, R.H.*, et al.* (1996). DPC4, a candidate tumor suppressor gene at human chromosome 18q21.1. Science *271*, 350-353.

Hall, P.A., Coates, P.J., Ansari, B., and Hopwood, D. (1994). Regulation of cell number in the mammalian gastrointestinal tract: the importance of apoptosis. J Cell Sci *107 (Pt 12)*, 3569-3577.

Hanahan, D., and Weinberg, R.A. (2000). The hallmarks of cancer. Cell *100*, 57-70.

Hann, S.R., and Eisenman, R.N. (1984). Proteins encoded by the human c-myc oncogene: differential expression in neoplastic cells. Mol Cell Biol *4*, 2486-2497.

Harfe, B.D., and Jinks-Robertson, S. (2000). DNA mismatch repair and genetic instability. Annu Rev Genet *34*, 359-399.

Hayashi, H., Abdollah, S., Qiu, Y., Cai, J., Xu, Y.Y., Grinnell, B.W., Richardson, M.A., Topper, J.N., Gimbrone, M.A., Jr., Wrana, J.L.*, et al.* (1997). The MAD-related protein

Smad7 associates with the TGFbeta receptor and functions as an antagonist of TGFbeta signaling. Cell *89*, 1165-1173.

He, T.C., Sparks, A.B., Rago, C., Hermeking, H., Zawel, L., da Costa, L.T., Morin, P.J., Vogelstein, B., and Kinzler, K.W. (1998). Identification of c-MYC as a target of the APC pathway. Science *281*, 1509-1512.

Henikoff, S. (1998). Conspiracy of silence among repeated transgenes. Bioessays *20*, 532-535.

Hoess, R., Abremski, K., and Sternberg, N. (1984). The nature of the interaction of the P1 recombinase Cre with the recombining site loxP. Cold Spring Harb Symp Quant Biol *49*, 761-768.

Hohenstein, P., Molenaar, L., Elsinga, J., Morreau, H., van der Klift, H., Struijk, A., Jagmohan-Changur, S., Smits, R., van Kranen, H., van Ommen, G.J.*, et al.* (2003). Serrated adenomas and mixed polyposis caused by a splice acceptor deletion in the mouse Smad4 gene. Genes Chromosomes Cancer *36*, 273-282.

Hosokawa, R., Urata, M.M., Ito, Y., Bringas, P., Jr., and Chai, Y. (2005). Functional significance of Smad2 in regulating basal keratinocyte migration during wound healing. J Invest Dermatol *125*, 1302-1309.

Houlston, R., Bevan, S., Williams, A., Young, J., Dunlop, M., Rozen, P., Eng, C., Markie, D., Woodford-Richens, K., Rodriguez-Bigas, M.A.*, et al.* (1998). Mutations in DPC4 (SMAD4) cause juvenile polyposis syndrome, but only account for a minority of cases. Hum Mol Genet *7*, 1907-1912.

Howe, J.R., Bair, J.L., Sayed, M.G., Anderson, M.E., Mitros, F.A., Petersen, G.M., Velculescu, V.E., Traverso, G., and Vogelstein, B. (2001). Germline mutations of the gene encoding bone morphogenetic protein receptor 1A in juvenile polyposis. Nat Genet *28*, 184-187.

Howe, J.R., Roth, S., Ringold, J.C., Summers, R.W., Jarvinen, H.J., Sistonen, P., Tomlinson, I.P., Houlston, R.S., Bevan, S., Mitros, F.A.*, et al.* (1998). Mutations in the SMAD4/DPC4 gene in juvenile polyposis. Science *280*, 1086-1088.

Howe, J.R., Shellnut, J., Wagner, B., Ringold, J.C., Sayed, M.G., Ahmed, A.F., Lynch, P.M., Amos, C.I., Sistonen, P., and Aaltonen, L.A. (2002). Common deletion of SMAD4 in juvenile polyposis is a mutational hotspot. Am J Hum Genet *70*, 1357-1362.

Hu, S.S., Lai, M.M., and Vogt, P.K. (1979). Genome of avian myelocytomatosis virus MC29: analysis by heteroduplex mapping. Proc Natl Acad Sci U S A *76*, 1265-1268.

Ignatenko, N.A., Holubec, H., Besselsen, D.G., Blohm-Mangone, K.A., Padilla-Torres, J.L., Nagle, R.B., de Alboranc, I.M., Guillen, R.J., and Gerner, E.W. (2006). Role of c-Myc in intestinal tumorigenesis of the ApcMin/+ mouse. Cancer Biol Ther *5*, 1658-1664.

Im, Y.H., Kim, H.T., Kim, I.Y., Factor, V.M., Hahm, K.B., Anzano, M., Jang, J.J., Flanders, K., Haines, D.C., Thorgeirsson, S.S.*, et al.* (2001). Heterozygous mice for the transforming growth factor-beta type II receptor gene have increased susceptibility to hepatocellular carcinogenesis. Cancer Res *61*, 6665-6668.

Imamura, T., Takase, M., Nishihara, A., Oeda, E., Hanai, J., Kawabata, M., and Miyazono, K. (1997). Smad6 inhibits signalling by the TGF-beta superfamily. Nature *389*, 622-626.

Ireland, H., Houghton, C., Howard, L., and Winton, D.J. (2005). Cellular inheritance of a Cre-activated reporter gene to determine Paneth cell longevity in the murine small intestine. Dev Dyn *233*, 1332-1336.

Jackson, E.L., Willis, N., Mercer, K., Bronson, R.T., Crowley, D., Montoya, R., Jacks, T., and Tuveson, D.A. (2001). Analysis of lung tumor initiation and progression using conditional expression of oncogenic K-ras. Genes Dev *15*, 3243-3248.

Johnson, L., Mercer, K., Greenbaum, D., Bronson, R.T., Crowley, D., Tuveson, D.A., and Jacks, T. (2001). Somatic activation of the K-ras oncogene causes early onset lung cancer in mice. Nature *410*, 1111-1116.

Jones, S., Chen, W.D., Parmigiani, G., Diehl, F., Beerenwinkel, N., Antal, T., Traulsen, A., Nowak, M.A., Siegel, C., Velculescu, V.E.*, et al.* (2008). Comparative lesion

sequencing provides insights into tumor evolution. Proc Natl Acad Sci U S A *105*, 4283-4288.

Jones, T.R., and Cole, M.D. (1987). Rapid cytoplasmic turnover of c-myc mRNA: requirement of the 3' untranslated sequences. Mol Cell Biol *7*, 4513-4521.

Jonkers, J., Meuwissen, R., van der Gulden, H., Peterse, H., van der Valk, M., and Berns, A. (2001). Synergistic tumor suppressor activity of BRCA2 and p53 in a conditional mouse model for breast cancer. Nat Genet *29*, 418-425.

Kellendonk, C., Tronche, F., Monaghan, A.P., Angrand, P.O., Stewart, F., and Schutz, G. (1996). Regulation of Cre recombinase activity by the synthetic steroid RU 486. Nucleic Acids Res *24*, 1404-1411.

Kim, B.G., Li, C., Qiao, W., Mamura, M., Kasprzak, B., Anver, M., Wolfraim, L., Hong, S., Mushinski, E., Potter, M.*, et al.* (2006). Smad4 signalling in T cells is required for suppression of gastrointestinal cancer. Nature *441*, 1015-1019.

Kim, C.F., Jackson, E.L., Woolfenden, A.E., Lawrence, S., Babar, I., Vogel, S., Crowley, D., Bronson, R.T., and Jacks, T. (2005). Identification of bronchioalveolar stem cells in normal lung and lung cancer. Cell *121*, 823-835.

Kinzler, K.W., Nilbert, M.C., Su, L.K., Vogelstein, B., Bryan, T.M., Levy, D.B., Smith, K.J., Preisinger, A.C., Hedge, P., McKechnie, D.*, et al.* (1991). Identification of FAP locus genes from chromosome 5q21. Science *253*, 661-665.

Korinek, V., Barker, N., Morin, P.J., van Wichen, D., de Weger, R., Kinzler, K.W., Vogelstein, B., and Clevers, H. (1997). Constitutive transcriptional activation by a beta-catenin-Tcf complex in APC-/- colon carcinoma. Science *275*, 1784-1787.

Koyama, M., Ito, M., Nagai, H., Emi, M., and Moriyama, Y. (1999). Inactivation of both alleles of the DPC4/SMAD4 gene in advanced colorectal cancers: identification of seven novel somatic mutations in tumors from Japanese patients. Mutat Res *406*, 71-77.

Koyama, S.Y., and Podolsky, D.K. (1989). Differential expression of transforming growth factors alpha and beta in rat intestinal epithelial cells. J Clin Invest *83*, 1768-1773.

Kretzschmar, M., Liu, F., Hata, A., Doody, J., and Massague, J. (1997). The TGF-beta family mediator Smad1 is phosphorylated directly and activated functionally by the BMP receptor kinase. Genes Dev *11*, 984-995.

Kurisaki, A., Kose, S., Yoneda, Y., Heldin, C.H., and Moustakas, A. (2001). Transforming growth factor-beta induces nuclear import of Smad3 in an importin-beta1 and Ran-dependent manner. Mol Biol Cell *12*, 1079-1091.

Kushima, R., Vieth, M., Borchard, F., Stolte, M., Mukaisho, K., and Hattori, T. (2006). Gastric-type well-differentiated adenocarcinoma and pyloric gland adenoma of the stomach. Gastric Cancer *9*, 177-184.

Lagna, G., Hata, A., Hemmati-Brivanlou, A., and Massague, J. (1996). Partnership between DPC4 and SMAD proteins in TGF-beta signalling pathways. Nature *383*, 832-836.

Landschulz, W.H., Johnson, P.F., and McKnight, S.L. (1988). The leucine zipper: a hypothetical structure common to a new class of DNA binding proteins. Science *240*, 1759-1764.

Letterio, J.J. (2005). Disruption of the TGF-beta pathway and modeling human cancer in mice. Mutat Res *576*, 120-131.

Leung, N., Turbide, C., Balachandra, B., Marcus, V., and Beauchemin, N. (2008). Intestinal tumor progression is promoted by decreased apoptosis and dysregulated Wnt signaling in Ceacam1-/- mice. Oncogene *27*, 4943-4953.

Lewandoski, M., and Martin, G.R. (1997). Cre-mediated chromosome loss in mice. Nat Genet *17*, 223-225.

Liaw, D., Marsh, D.J., Li, J., Dahia, P.L., Wang, S.I., Zheng, Z., Bose, S., Call, K.M., Tsou, H.C., Peacocke, M.*, et al.* (1997). Germline mutations of the PTEN gene in Cowden disease, an inherited breast and thyroid cancer syndrome. Nat Genet *16*, 64-67.

Lindor, N.M., Rabe, K., Petersen, G.M., Haile, R., Casey, G., Baron, J., Gallinger, S., Bapat, B., Aronson, M., Hopper, J.*, et al.* (2005). Lower cancer incidence in Amsterdam-I criteria families without mismatch repair deficiency: familial colorectal cancer type X. JAMA *293*, 1979-1985.

Liu, P., Jenkins, N.A., and Copeland, N.G. (2002). Efficient Cre-loxP-induced mitotic recombination in mouse embryonic stem cells. Nat Genet *30*, 66-72.

Lu, S.L., Kawabata, M., Imamura, T., Akiyama, Y., Nomizu, T., Miyazono, K., and Yuasa, Y. (1998). HNPCC associated with germline mutation in the TGF-beta type II receptor gene. Nat Genet *19*, 17-18.

Luscher, B., and Eisenman, R.N. (1990). New light on Myc and Myb. Part I. Myc. Genes Dev *4*, 2025-2035.

Lynch, H.T., and de la Chapelle, A. (1999). Genetic susceptibility to non-polyposis colorectal cancer. J Med Genet *36*, 801-818.

Ma, A., Moroy, T., Collum, R., Weintraub, H., Alt, F.W., and Blackwell, T.K. (1993). DNA binding by N- and L-Myc proteins. Oncogene *8*, 1093-1098.

MacGrogan, D., Pegram, M., Slamon, D., and Bookstein, R. (1997). Comparative mutational analysis of DPC4 (Smad4) in prostatic and colorectal carcinomas. Oncogene *15*, 1111-1114.

Madison, B.B., Dunbar, L., Qiao, X.T., Braunstein, K., Braunstein, E., and Gumucio, D.L. (2002). Cis elements of the villin gene control expression in restricted domains of the vertical (crypt) and horizontal (duodenum, cecum) axes of the intestine. J Biol Chem *277*, 33275-33283.

Malempati, S., Tibbitts, D., Cunningham, M., Akkari, Y., Olson, S., Fan, G., and Sears, R.C. (2006). Aberrant stabilization of c-Myc protein in some lymphoblastic leukemias. Leukemia *20*, 1572-1581.

Mansour, S.L., Thomas, K.R., and Capecchi, M.R. (1988). Disruption of the proto-oncogene int-2 in mouse embryo-derived stem cells: a general strategy for targeting mutations to non-selectable genes. Nature *336*, 348-352.

Markowitz, S., Wang, J., Myeroff, L., Parsons, R., Sun, L., Lutterbaugh, J., Fan, R.S., Zborowska, E., Kinzler, K.W., Vogelstein, B.*, et al.* (1995). Inactivation of the type II TGF-beta receptor in colon cancer cells with microsatellite instability. Science *268*, 1336-1338.

Marshman, E., Booth, C., and Potten, C.S. (2002). The intestinal epithelial stem cell. Bioessays *24*, 91-98.

Marshman, E., Ottewell, P.D., Potten, C.S., and Watson, A.J. (2001). Caspase activation during spontaneous and radiation-induced apoptosis in the murine intestine. J Pathol *195*, 285-292.

Marten H. Hofker, J.v.D. (2003). Transgenic mouse: methods and protocols, Vol (Humana Press).

Massague, J. (1996). TGFbeta signaling: receptors, transducers, and Mad proteins. Cell *85*, 947-950.

Massague, J. (1998). TGF-beta signal transduction. Annu Rev Biochem *67*, 753-791.

Massague, J. (2008). TGFbeta in Cancer. Cell *134*, 215-230.

Massague, J., Blain, S.W., and Lo, R.S. (2000). TGFbeta signaling in growth control, cancer, and heritable disorders. Cell *103*, 295-309.

Massague, J., and Chen, Y.G. (2000). Controlling TGF-beta signaling. Genes Dev *14*, 627-644.

McDonald, S.A., Preston, S.L., Greaves, L.C., Leedham, S.J., Lovell, M.A., Jankowski, J.A., Turnbull, D.M., and Wright, N.A. (2006). Clonal expansion in the human gut: mitochondrial DNA mutations show us the way. Cell Cycle *5*, 808-811.

Merritt, A.J., Potten, C.S., Watson, A.J., Loh, D.Y., Nakayama, K., and Hickman, J.A. (1995). Differential expression of bcl-2 in intestinal epithelia. Correlation with attenuation of apoptosis in colonic crypts and the incidence of colonic neoplasia. J Cell Sci *108 (Pt 6)*, 2261-2271.

Meyer, N., and Penn, L.Z. (2008). Reflecting on 25 years with MYC. Nat Rev Cancer *8*, 976-990.

Milburn, M.V., Tong, L., deVos, A.M., Brunger, A., Yamaizumi, Z., Nishimura, S., and Kim, S.H. (1990). Molecular switch for signal transduction: structural differences between active and inactive forms of protooncogenic ras proteins. Science *247*, 939-945.

Miller, A.J., Dudley, S.D., Tsao, J.L., Shibata, D., and Liskay, R.M. (2008). Tractable Cre-lox system for stochastic alteration of genes in mice. Nat Methods *5*, 227-229.

Mitchell, H., Choudhury, A., Pagano, R.E., and Leof, E.B. (2004). Ligand-dependent and -independent transforming growth factor-beta receptor recycling regulated by clathrin-mediated endocytosis and Rab11. Mol Biol Cell *15*, 4166-4178.

Miyaki, M., Konishi, M., Tanaka, K., Kikuchi-Yanoshita, R., Muraoka, M., Yasuno, M., Igari, T., Koike, M., Chiba, M., and Mori, T. (1997). Germline mutation of MSH6 as the cause of hereditary nonpolyposis colorectal cancer. Nat Genet *17*, 271-272.

Morata, G., and Ripoll, P. (1975). Minutes: mutants of drosophila autonomously affecting cell division rate. Dev Biol *42*, 211-221.

Moreno, E. (2008). Is cell competition relevant to cancer? Nat Rev Cancer *8*, 141-147.

Morin, P.J., Sparks, A.B., Korinek, V., Barker, N., Clevers, H., Vogelstein, B., and Kinzler, K.W. (1997). Activation of beta-catenin-Tcf signaling in colon cancer by mutations in beta-catenin or APC. Science *275*, 1787-1790.

Moser, A.R., Pitot, H.C., and Dove, W.F. (1990). A dominant mutation that predisposes to multiple intestinal neoplasia in the mouse. Science *247*, 322-324.

Moustakas, A., Souchelnytskyi, S., and Heldin, C.H. (2001). Smad regulation in TGF-beta signal transduction. J Cell Sci *114*, 4359-4369.

Muller, N., Reinacher-Schick, A., Baldus, S., van Hengel, J., Berx, G., Baar, A., van Roy, F., Schmiegel, W., and Schwarte-Waldhoff, I. (2002). Smad4 induces the tumor suppressor E-cadherin and P-cadherin in colon carcinoma cells. Oncogene *21*, 6049-6058.

Munoz, N.M., Upton, M., Rojas, A., Washington, M.K., Lin, L., Chytil, A., Sozmen, E.G., Madison, B.B., Pozzi, A., Moon, R.T.*, et al.* (2006). Transforming growth factor beta receptor type II inactivation induces the malignant transformation of intestinal neoplasms initiated by Apc mutation. Cancer Res *66*, 9837-9844.

Murphy, D.J., Junttila, M.R., Pouyet, L., Karnezis, A., Shchors, K., Bui, D.A., Brown-Swigart, L., Johnson, L., and Evan, G.I. (2008). Distinct thresholds govern Myc's biological output in vivo. Cancer Cell *14*, 447-457.

Murre, C., McCaw, P.S., and Baltimore, D. (1989). A new DNA binding and dimerization motif in immunoglobulin enhancer binding, daughterless, MyoD, and myc proteins. Cell *56*, 777-783.

Nagase, H., Miyoshi, Y., Horii, A., Aoki, T., Ogawa, M., Utsunomiya, J., Baba, S., Sasazuki, T., and Nakamura, Y. (1992). Correlation between the location of germ-line mutations in the APC gene and the number of colorectal polyps in familial adenomatous polyposis patients. Cancer Res *52*, 4055-4057.

Narayanan, L., Fritzell, J.A., Baker, S.M., Liskay, R.M., and Glazer, P.M. (1997). Elevated levels of mutation in multiple tissues of mice deficient in the DNA mismatch repair gene Pms2. Proc Natl Acad Sci U S A *94*, 3122-3127.

Nawshad, A., Lagamba, D., Polad, A., and Hay, E.D. (2005). Transforming growth factor-beta signaling during epithelial-mesenchymal transformation: implications for embryogenesis and tumor metastasis. Cells Tissues Organs *179*, 11-23.

NCI. National Cancer Institute - Comprehensive Cancer Information.

Nichols, D.B., Cheng, H., and Leblond, C.P. (1974). Variability of the shape and argentaffinity of the granules in the enteroendocrine cells of the mouse duodenum. J Histochem Cytochem *22*, 929-944.

Nicolaides, N.C., Papadopoulos, N., Liu, B., Wei, Y.F., Carter, K.C., Ruben, S.M., Rosen, C.A., Haseltine, W.A., Fleischmann, R.D., Fraser, C.M.*, et al.* (1994). Mutations of two PMS homologues in hereditary nonpolyposis colon cancer. Nature *371*, 75-80.

Nishisho, I., Nakamura, Y., Miyoshi, Y., Miki, Y., Ando, H., Horii, A., Koyama, K., Utsunomiya, J., Baba, S., and Hedge, P. (1991). Mutations of chromosome 5q21 genes in FAP and colorectal cancer patients. Science *253*, 665-669.

Oft, M., Heider, K.H., and Beug, H. (1998). TGFbeta signaling is necessary for carcinoma cell invasiveness and metastasis. Curr Biol *8*, 1243-1252.

Oliveira, C., Westra, J.L., Arango, D., Ollikainen, M., Domingo, E., Ferreira, A., Velho, S., Niessen, R., Lagerstedt, K., Alhopuro, P.*, et al.* (2004). Distinct patterns of KRAS mutations in colorectal carcinomas according to germline mismatch repair defects and hMLH1 methylation status. Hum Mol Genet *13*, 2303-2311.

Oliver, E.R., Saunders, T.L., Tarle, S.A., and Glaser, T. (2004). Ribosomal protein L24 defect in belly spot and tail (Bst), a mouse Minute. Development *131*, 3907-3920.

Orban, P.C., Chui, D., and Marth, J.D. (1992). Tissue- and site-specific DNA recombination in transgenic mice. Proc Natl Acad Sci U S A *89*, 6861-6865.

Oren, M. (2003). Decision making by p53: life, death and cancer. Cell Death Differ *10*, 431-442.

Oshima, M., Oshima, H., Kitagawa, K., Kobayashi, M., Itakura, C., and Taketo, M. (1995). Loss of Apc heterozygosity and abnormal tissue building in nascent intestinal polyps in mice carrying a truncated Apc gene. Proc Natl Acad Sci U S A *92*, 4482-4486.

Oshima, M., Oshima, H., and Taketo, M.M. (1996). TGF-beta receptor type II deficiency results in defects of yolk sac hematopoiesis and vasculogenesis. Dev Biol *179*, 297-302.

Otori, K., Oda, Y., Sugiyama, K., Hasebe, T., Mukai, K., Fujii, T., Tajiri, H., Yoshida, S., Fukushima, S., and Esumi, H. (1997). High frequency of K-ras mutations in human colorectal hyperplastic polyps. Gut *40*, 660-663.

Owen, C.R., Yuan, L., and Basson, M.D. (2008). Smad3 knockout mice exhibit impaired intestinal mucosal healing. Lab Invest *88*, 1101-1109.

Palmiter, R.D., Brinster, R.L., Hammer, R.E., Trumbauer, M.E., Rosenfeld, M.G., Birnberg, N.C., and Evans, R.M. (1982). Dramatic growth of mice that develop from eggs microinjected with metallothionein-growth hormone fusion genes. Nature *300*, 611-615.

Parsons, D.W., Wang, T.L., Samuels, Y., Bardelli, A., Cummins, J.M., DeLong, L., Silliman, N., Ptak, J., Szabo, S., Willson, J.K.*, et al.* (2005). Colorectal cancer: mutations in a signalling pathway. Nature *436*, 792.

Peinado, H., Portillo, F., and Cano, A. (2004). Transcriptional regulation of cadherins during development and carcinogenesis. Int J Dev Biol *48*, 365-375.

Persson, H., and Leder, P. (1984). Nuclear localization and DNA binding properties of a protein expressed by human c-myc oncogene. Science *225*, 718-721.

Phelps, R.A., Chidester, S., Dehghanizadeh, S., Phelps, J., Sandoval, I.T., Rai, K., Broadbent, T., Sarkar, S., Burt, R.W., and Jones, D.A. (2009). A two-step model for colon adenoma initiation and progression caused by APC loss. Cell *137*, 623-634.

Picon, A., Gold, L.I., Wang, J., Cohen, A., and Friedman, E. (1998). A subset of metastatic human colon cancers expresses elevated levels of transforming growth factor beta1. Cancer Epidemiol Biomarkers Prev *7*, 497-504.

Piek, E., Heldin, C.H., and Ten Dijke, P. (1999). Specificity, diversity, and regulation in TGF-beta superfamily signaling. FASEB J *13*, 2105-2124.

Pinto, D., Gregorieff, A., Begthel, H., and Clevers, H. (2003). Canonical Wnt signals are essential for homeostasis of the intestinal epithelium. Genes Dev *17*, 1709-1713.

Potten, C.S. (1998). Stem cells in gastrointestinal epithelium: numbers, characteristics and death. Philos Trans R Soc Lond B Biol Sci *353*, 821-830.

Potter, J.D. (2007). Morphogens, morphostats, microarchitecture and malignancy. Nat Rev Cancer *7*, 464-474.

Powell, S.M., Harper, J.C., Hamilton, S.R., Robinson, C.R., and Cummings, O.W. (1997). Inactivation of Smad4 in gastric carcinomas. Cancer Res *57*, 4221-4224.

Powell, S.M., Zilz, N., Beazer-Barclay, Y., Bryan, T.M., Hamilton, S.R., Thibodeau, S.N., Vogelstein, B., and Kinzler, K.W. (1992). APC mutations occur early during colorectal tumorigenesis. Nature *359*, 235-237.

Prolla, T.A., Baker, S.M., Harris, A.C., Tsao, J.L., Yao, X., Bronner, C.E., Zheng, B., Gordon, M., Reneker, J., Arnheim, N.*, et al.* (1998). Tumour susceptibility and spontaneous mutation in mice deficient in Mlh1, Pms1 and Pms2 DNA mismatch repair. Nat Genet *18*, 276-279.

Pulverer, B.J., Fisher, C., Vousden, K., Littlewood, T., Evan, G., and Woodgett, J.R. (1994). Site-specific modulation of c-Myc cotransformation by residues phosphorylated in vivo. Oncogene *9*, 59-70.

Qiao, W., Li, A.G., Owens, P., Xu, X., Wang, X.J., and Deng, C.X. (2006). Hair follicle defects and squamous cell carcinoma formation in Smad4 conditional knockout mouse skin. Oncogene *25*, 207-217.

Rajagopalan, H., Bardelli, A., Lengauer, C., Kinzler, K.W., Vogelstein, B., and Velculescu, V.E. (2002). Tumorigenesis: RAF/RAS oncogenes and mismatch-repair status. Nature *418*, 934.

Reitmair, A.H., Redston, M., Cai, J.C., Chuang, T.C., Bjerknes, M., Cheng, H., Hay, K., Gallinger, S., Bapat, B., and Mak, T.W. (1996). Spontaneous intestinal carcinomas and skin neoplasms in Msh2-deficient mice. Cancer Res *56*, 3842-3849.

Riccio, O., van Gijn, M.E., Bezdek, A.C., Pellegrinet, L., van Es, J.H., Zimber-Strobl, U., Strobl, L.J., Honjo, T., Clevers, H., and Radtke, F. (2008). Loss of intestinal crypt progenitor cells owing to inactivation of both Notch1 and Notch2 is accompanied by derepression of CDK inhibitors p27Kip1 and p57Kip2. EMBO Rep *9*, 377-383.

Robine, S., Huet, C., Moll, R., Sahuquillo-Merino, C., Coudrier, E., Zweibaum, A., and Louvard, D. (1985). Can villin be used to identify malignant and undifferentiated normal digestive epithelial cells? Proc Natl Acad Sci U S A *82*, 8488-8492.

Rodriguez-Bigas, M.A., Boland, C.R., Hamilton, S.R., Henson, D.E., Jass, J.R., Khan, P.M., Lynch, H., Perucho, M., Smyrk, T., Sobin, L.*, et al.* (1997). A National Cancer

Institute Workshop on Hereditary Nonpolyposis Colorectal Cancer Syndrome: meeting highlights and Bethesda guidelines. J Natl Cancer Inst *89*, 1758-1762.

Rubinfeld, B., Souza, B., Albert, I., Muller, O., Chamberlain, S.H., Masiarz, F.R., Munemitsu, S., and Polakis, P. (1993). Association of the APC gene product with beta-catenin. Science *262*, 1731-1734.

Sakuraba, H., Ishiguro, Y., Yamagata, K., Munakata, A., and Nakane, A. (2007). Blockade of TGF-beta accelerates mucosal destruction through epithelial cell apoptosis. Biochem Biophys Res Commun *359*, 406-412.

Salovaara, R., Roth, S., Loukola, A., Launonen, V., Sistonen, P., Avizienyte, E., Kristo, P., Jarvinen, H., Souchelnytskyi, S., Sarlomo-Rikala, M*., et al.* (2002). Frequent loss of SMAD4/DPC4 protein in colorectal cancers. Gut *51*, 56-59.

Samowitz, W.S., Curtin, K., Neuhausen, S., Schaffer, D., and Slattery, M.L. (2002). Prognostic implications of BAX and TGFBRII mutations in colon cancers with microsatellite instability. Genes Chromosomes Cancer *35*, 368-371.

Sansom, O.J., Meniel, V.S., Muncan, V., Phesse, T.J., Wilkins, J.A., Reed, K.R., Vass, J.K., Athineos, D., Clevers, H., and Clarke, A.R. (2007). Myc deletion rescues Apc deficiency in the small intestine. Nature *446*, 676-679.

Sansom, O.J., Reed, K.R., Hayes, A.J., Ireland, H., Brinkmann, H., Newton, I.P., Batlle, E., Simon-Assmann, P., Clevers, H., Nathke, I.S.*, et al.* (2004). Loss of Apc in vivo immediately perturbs Wnt signaling, differentiation, and migration. Genes Dev *18*, 1385-1390.

Sauer, B., and Henderson, N. (1988). Site-specific DNA recombination in mammalian cells by the Cre recombinase of bacteriophage P1. Proc Natl Acad Sci U S A *85*, 5166-5170.

Schmidt, G.H., Winton, D.J., and Ponder, B.A. (1988). Development of the pattern of cell renewal in the crypt-villus unit of chimaeric mouse small intestine. Development *103*, 785-790.

Sears, R., Nuckolls, F., Haura, E., Taya, Y., Tamai, K., and Nevins, J.R. (2000). Multiple Ras-dependent phosphorylation pathways regulate Myc protein stability. Genes Dev *14*, 2501-2514.

Seshimo, I., Yamamoto, H., Mishima, H., Kurata, A., Suzuki, R., Ezumi, K., Takemasa, I., Ikeda, M., Fukushima, T., Tsujinaka, T.*, et al.* (2006). Expression and mutation of SMAD4 in poorly differentiated carcinoma and signet-ring cell carcinoma of the colorectum. J Exp Clin Cancer Res *25*, 433-442.

Simi, L., Pratesi, N., Vignoli, M., Sestini, R., Cianchi, F., Valanzano, R., Nobili, S., Mini, E., Pazzagli, M., and Orlando, C. (2008). High-resolution melting analysis for rapid

detection of KRAS, BRAF, and PIK3CA gene mutations in colorectal cancer. Am J Clin Pathol *130*, 247-253.

Simin, K., Bates, E.A., Horner, M.A., and Letsou, A. (1998). Genetic analysis of punt, a type II Dpp receptor that functions throughout the Drosophila melanogaster life cycle. Genetics *148*, 801-813.

Simpkins, S.B., Bocker, T., Swisher, E.M., Mutch, D.G., Gersell, D.J., Kovatich, A.J., Palazzo, J.P., Fishel, R., and Goodfellow, P.J. (1999). MLH1 promoter methylation and gene silencing is the primary cause of microsatellite instability in sporadic endometrial cancers. Hum Mol Genet *8*, 661-666.

Sjoblom, T., Jones, S., Wood, L.D., Parsons, D.W., Lin, J., Barber, T.D., Mandelker, D., Leary, R.J., Ptak, J., Silliman, N.*, et al.* (2006). The consensus coding sequences of human breast and colorectal cancers. Science *314*, 268-274.

Soriano, P. (1999). Generalized lacZ expression with the ROSA26 Cre reporter strain. Nat Genet *21*, 70-71.

St Clair, W.H., and Osborne, J.W. (1985). Crypt fission and crypt number in the small and large bowel of postnatal rats. Cell Tissue Kinet *18*, 255-262.

Takaku, K., Miyoshi, H., Matsunaga, A., Oshima, M., Sasaki, N., and Taketo, M.M. (1999). Gastric and duodenal polyps in Smad4 (Dpc4) knockout mice. Cancer Res *59*, 6113-6117.

Takayama, T., Miyanishi, K., Hayashi, T., Sato, Y., and Niitsu, Y. (2006). Colorectal cancer: genetics of development and metastasis. J Gastroenterol *41*, 185-192.

Taketo, M.M., and Edelmann, W. (2009). Mouse models of colon cancer. Gastroenterology *136*, 780-798.

Taketo, M.M., and Takaku, K. (2000). Gastrointestinal tumorigenesis in Smad4 (Dpc4) mutant mice. Hum Cell *13*, 85-95.

Taub, R., Kirsch, I., Morton, C., Lenoir, G., Swan, D., Tronick, S., Aaronson, S., and Leder, P. (1982). Translocation of the c-myc gene into the immunoglobulin heavy chain locus in human Burkitt lymphoma and murine plasmacytoma cells. Proc Natl Acad Sci U S A *79*, 7837-7841.

Thiagalingam, S., Lengauer, C., Leach, F.S., Schutte, M., Hahn, S.A., Overhauser, J., Willson, J.K., Markowitz, S., Hamilton, S.R., Kern, S.E.*, et al.* (1996). Evaluation of candidate tumour suppressor genes on chromosome 18 in colorectal cancers. Nat Genet *13*, 343-346.

Thiery, J.P. (2002). Epithelial-mesenchymal transitions in tumour progression. Nat Rev Cancer *2*, 442-454.

Tomlinson, I., and Bodmer, W. (1999). Selection, the mutation rate and cancer: ensuring that the tail does not wag the dog. Nat Med *5*, 11-12.

Tuveson, D.A., and Jacks, T. (2002). Technologically advanced cancer modeling in mice. Curr Opin Genet Dev *12*, 105-110.

Tuveson, D.A., Shaw, A.T., Willis, N.A., Silver, D.P., Jackson, E.L., Chang, S., Mercer, K.L., Grochow, R., Hock, H., Crowley, D.*, et al.* (2004). Endogenous oncogenic K-ras(G12D) stimulates proliferation and widespread neoplastic and developmental defects. Cancer Cell *5*, 375-387.

Tyler, D.M., Li, W., Zhuo, N., Pellock, B., and Baker, N.E. (2007). Genes affecting cell competition in Drosophila. Genetics *175*, 643-657.

Utomo, A.R., Nikitin, A.Y., and Lee, W.H. (1999). Temporal, spatial, and cell type-specific control of Cre-mediated DNA recombination in transgenic mice. Nat Biotechnol *17*, 1091-1096.

Vasen, H.F. (2007). Review article: The Lynch syndrome (hereditary nonpolyposis colorectal cancer). Aliment Pharmacol Ther *26 Suppl 2*, 113-126.

Vasen, H.F., Watson, P., Mecklin, J.P., and Lynch, H.T. (1999). New clinical criteria for hereditary nonpolyposis colorectal cancer (HNPCC, Lynch syndrome) proposed by the International Collaborative group on HNPCC. Gastroenterology *116*, 1453-1456.

Vennstrom, B., Sheiness, D., Zabielski, J., and Bishop, J.M. (1982). Isolation and characterization of c-myc, a cellular homolog of the oncogene (v-myc) of avian myelocytomatosis virus strain 29. J Virol *42*, 773-779.

Vilar, J.M., Jansen, R., and Sander, C. (2006). Signal processing in the TGF-beta superfamily ligand-receptor network. PLoS Comput Biol *2*, e3.

Vogelstein, B., and Kinzler, K.W. (2004). Cancer genes and the pathways they control. Nat Med *10*, 789-799.

Wang, L.H., Kim, S.H., Lee, J.H., Choi, Y.L., Kim, Y.C., Park, T.S., Hong, Y.C., Wu, C.F., and Shin, Y.K. (2007a). Inactivation of SMAD4 tumor suppressor gene during gastric carcinoma progression. Clin Cancer Res *13*, 102-110.

Wang, W., Warren, M., and Bradley, A. (2007b). Induced mitotic recombination of p53 in vivo. Proc Natl Acad Sci U S A *104*, 4501-4505.

Watson, A.J., and Pritchard, D.M. (2000). Lessons from genetically engineered animal models. VII. Apoptosis in intestinal epithelium: lessons from transgenic and knockout mice. Am J Physiol Gastrointest Liver Physiol *278*, G1-5.

Watson, P., and Riley, B. (2005). The tumor spectrum in the Lynch syndrome. Fam Cancer *4*, 245-248.

Weidensdorfer, D., Stohr, N., Baude, A., Lederer, M., Kohn, M., Schierhorn, A., Buchmeier, S., Wahle, E., and Huttelmaier, S. (2009). Control of c-myc mRNA stability by IGF2BP1-associated cytoplasmic RNPs. RNA *15*, 104-115.

Wellings, S.R., Jensen, H.M., and Marcum, R.G. (1975). An atlas of subgross pathology of the human breast with special reference to possible precancerous lesions. J Natl Cancer Inst *55*, 231-273.

Winston, J.T., Coats, S.R., Wang, Y.Z., and Pledger, W.J. (1996). Regulation of the cell cycle machinery by oncogenic ras. Oncogene *12*, 127-134.

Wong, M.H., Hermiston, M.L., Syder, A.J., and Gordon, J.I. (1996). Forced expression of the tumor suppressor adenomatosis polyposis coli protein induces disordered cell migration in the intestinal epithelium. Proc Natl Acad Sci U S A *93*, 9588-9593.

Wong, M.H., Rubinfeld, B., and Gordon, J.I. (1998). Effects of forced expression of an NH2-terminal truncated beta-Catenin on mouse intestinal epithelial homeostasis. J Cell Biol *141*, 765-777.

Wood, L.D., Parsons, D.W., Jones, S., Lin, J., Sjoblom, T., Leary, R.J., Shen, D., Boca, S.M., Barber, T., Ptak, J.*, et al.* (2007). The genomic landscapes of human breast and colorectal cancers. Science *318*, 1108-1113.

Woodford-Richens, K., Williamson, J., Bevan, S., Young, J., Leggett, B., Frayling, I., Thway, Y., Hodgson, S., Kim, J.C., Iwama, T.*, et al.* (2000). Allelic loss at SMAD4 in polyps from juvenile polyposis patients and use of fluorescence in situ hybridization to demonstrate clonal origin of the epithelium. Cancer Res *60*, 2477-2482.

Woodford-Richens, K.L., Rowan, A.J., Poulsom, R., Bevan, S., Salovaara, R., Aaltonen, L.A., Houlston, R.S., Wright, N.A., and Tomlinson, I.P. (2001). Comprehensive analysis of SMAD4 mutations and protein expression in juvenile polyposis: evidence for a distinct genetic pathway and polyp morphology in SMAD4 mutation carriers. Am J Pathol *159*, 1293-1300.

Xu, X., Brodie, S.G., Yang, X., Im, Y.H., Parks, W.T., Chen, L., Zhou, Y.X., Weinstein, M., Kim, S.J., and Deng, C.X. (2000). Haploid loss of the tumor suppressor Smad4/Dpc4 initiates gastric polyposis and cancer in mice. Oncogene *19*, 1868-1874.

Xu, Y., and Pasche, B. (2007). TGF-beta signaling alterations and susceptibility to colorectal cancer. Hum Mol Genet *16 Spec No 1*, R14-20.

Yagi, K., Furuhashi, M., Aoki, H., Goto, D., Kuwano, H., Sugamura, K., Miyazono, K., and Kato, M. (2002). c-myc is a downstream target of the Smad pathway. J Biol Chem *277*, 854-861.

Yang, J., Mani, S.A., Donaher, J.L., Ramaswamy, S., Itzykson, R.A., Come, C., Savagner, P., Gitelman, I., Richardson, A., and Weinberg, R.A. (2004). Twist, a master regulator of morphogenesis, plays an essential role in tumor metastasis. Cell *117*, 927-939.

Yang, L., Mao, C., Teng, Y., Li, W., Zhang, J., Cheng, X., Li, X., Han, X., Xia, Z., Deng, H.*, et al.* (2005). Targeted disruption of Smad4 in mouse epidermis results in failure of hair follicle cycling and formation of skin tumors. Cancer Res *65*, 8671-8678.

Yang, X., Li, C., Herrera, P.L., and Deng, C.X. (2002). Generation of Smad4/Dpc4 conditional knockout mice. Genesis *32*, 80-81.

Yeh, E., Cunningham, M., Arnold, H., Chasse, D., Monteith, T., Ivaldi, G., Hahn, W.C., Stukenberg, P.T., Shenolikar, S., Uchida, T.*, et al.* (2004). A signalling pathway controlling c-Myc degradation that impacts oncogenic transformation of human cells. Nat Cell Biol *6*, 308-318.

Zavadil, J., and Bottinger, E.P. (2005). TGF-beta and epithelial-to-mesenchymal transitions. Oncogene *24*, 5764-5774.

Zeller, K.I., Jegga, A.G., Aronow, B.J., O'Donnell, K.A., and Dang, C.V. (2003). An integrated database of genes responsive to the Myc oncogenic transcription factor: identification of direct genomic targets. Genome Biol *4*, R69.

Zhu, H., Kavsak, P., Abdollah, S., Wrana, J.L., and Thomsen, G.H. (1999). A SMAD ubiquitin ligase targets the BMP pathway and affects embryonic pattern formation. Nature *400*, 687-693.

Zuber, J., Tchernitsa, O.I., Hinzmann, B., Schmitz, A.C., Grips, M., Hellriegel, M., Sers, C., Rosenthal, A., and Schafer, R. (2000). A genome-wide survey of RAS transformation targets. Nat Genet *24*, 144-152.